

สารออกฤทธิ์ทางชีวภาพจากเถาเมื่อยดูก *Gnetum macrostachyum*, รากปลู้ *Alangium salviifolium* และ เหง้าขมิ้นชัน *Curcuma longa*



นางสาวสุวรรณี สายสิน

ศูนย์วิทยทรัพยากร

จุฬาลงกรณ์มหาวิทยาลัย

วิทยานิพนธ์นี้เป็นส่วนหนึ่งของการศึกษาตามหลักสูตรปริญญาวิทยาศาสตรดุษฎีบัณฑิต

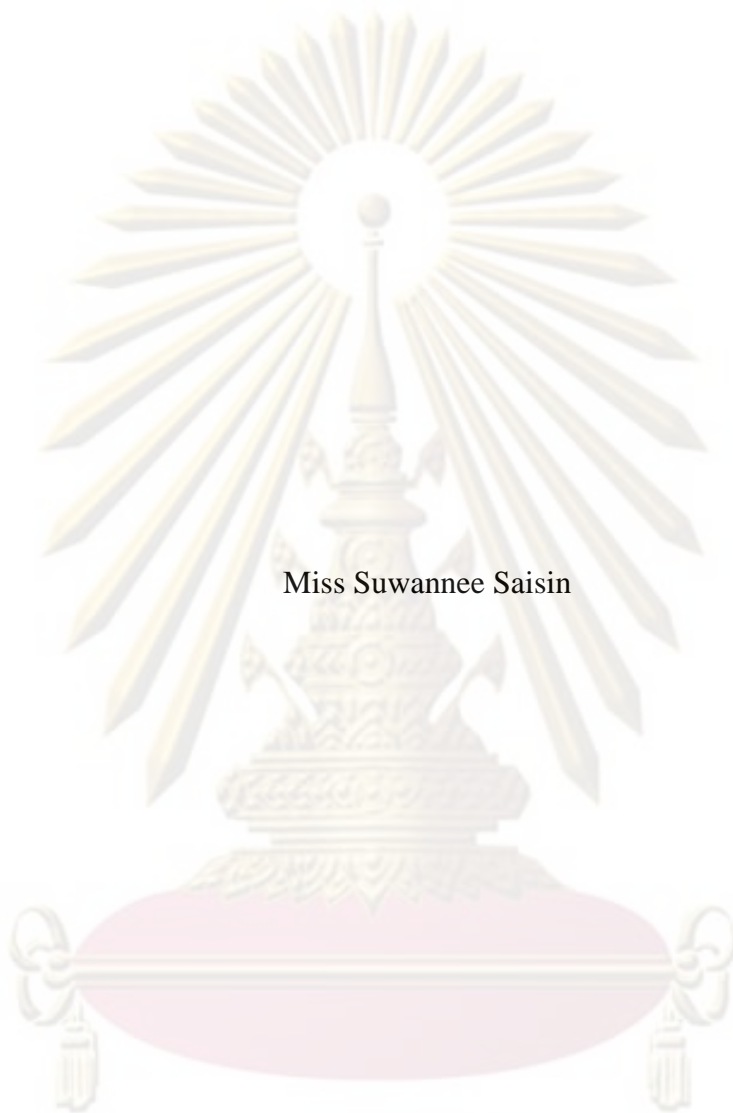
สาขาวิชาเคมี ภาควิชาเคมี

คณะวิทยาศาสตร์ จุฬาลงกรณ์มหาวิทยาลัย

ปีการศึกษา 2552

ลิขสิทธิ์ของจุฬาลงกรณ์มหาวิทยาลัย

BIOACTIVE COMPOUNDS FROM THE LIANAS OF *Gnetum macrostachyum* ,
THE ROOTS OF *Alangium salviifolium* AND THE RHIZOMES OF *Curcuma longa*



Miss Suwannee Saisin

A Thesis Submitted in Partial Fulfillment of the Requirements
for the Degree of Doctor of Science Program in Chemistry


Department of Chemistry
Faculty of Science
Chulalongkorn University

Academic Year 2009


Copyright of Chulalongkorn University

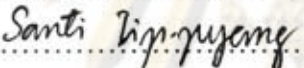
Thesis Title BIOACTIVE COMPOUNDS FROM THE LIANAS OF *Gnetum macrostachyum* , THE ROOTS OF *Alangium salviifolium* AND THE RHIZOMES OF *Curcuma longa*
By Miss Suwannee Saisin
Field of Study Chemistry
Thesis Advisor Associate Professor Santi Tip-pyang, Ph.D.
Thesis Co-advisor Assistant Professor Preecha Phuwapraisirisan, Ph.D.

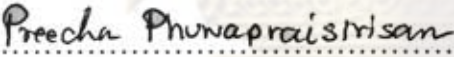
Accepted by the Faculty of Science, Chulalongkorn University in Partial Fulfillment of the Requirements for the Doctoral's Degree


 Dean of the Faculty of Science
(Professor Supot Hannongbua, Dr.rer.nat.)


THESIS COMMITTEE


 Chairman
(Associate Professor Sirirat Kokpol, Ph.D.)

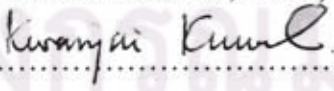
 Thesis Advisor
(Associate Professor Santi Tip-pyang, Ph.D.)

 Thesis Co-advisor
(Assistant Professor Preecha Phuwapraisirisan, Ph.D.)

 Examiner
(Assistant Professor Worawan Bhanthumnavin, Ph.D.)

 Examiner
(Assistant Professor Aroonsiri Shitangkoon, Ph.D.)

 Examiner
(Khanit Suwanborirux, Ph.D.)

 External Examiner
(Associate Professor Kwanjai Kanokmedhakul, Ph.D.)

4873811523: MAJOR CHEMISTRY

KEYWORDS: BIOACTIVE COMPOUNDS, *Gnetum macrostachyum* / STILBENOIDS / RESVERATROL / *Alangium salviifolium* / ALANGICINE / PSYCHOTRINE / *Curcuma longa*

SUWANNEE SAISIN: BIOACTIVE COMPOUNDS FROM THE LIANAS OF *Gnetum macrostachyum*, THE ROOTS OF *Alangium salviifolium* and THE RHIZOMES OF *Curcuma longa*. THESIS ADVISOR: ASSOC. PROF. SANTI TIP-PYANG, Ph.D., THESIS CO-ADVISOR: ASSIST. PROF. PREECHA PHUWAPRAISIRISAN, Ph.D., 125 pp.

In phytochemical investigation for bioactive compounds from Thai medicinal plants, *Gnetum macrostachyum* and *Alangium salviifolium* were selected for isolation, purification and structure elucidation. The chromatographic separation of the acetone extract of *G. macrostachyum* led to the isolation of a new flavonoid, 5,7,2'-trihydroxy-5'-methoxyflavone (1.1) and a new tetramers stilbenoid, (1.10) along with a known flavonoid 5,7,4'-trihydroxy-3'-methoxyflavanone (1.2) and seven known stilbenoids including, resveratrol (1.3), 3-methoxyresveratrol (1.4), shigansu B (1.5), gnetulin (1.6), gnetuhainin C (1.7), parvifolol B (1.8) and pallidol (1.9). Nine isolated compounds (1.1-1.9) were tested for antioxidant activity (DPPH radical scavenging). Compounds 1.3, 1.4, 1.6 and 1.9 showed DPPH radical scavenging activity with IC₅₀ values of 0.40, 0.30, 0.21 and 0.53 mM, respectively.

The chromatographic separation of the butanolic crude extract of *A. salviifolium* led to the isolation of five known alkaloids including, psychotrine (2.1), alangiside (2.2), 3-O-demethyl-2-O-methylalangiside (2.3), alangicine (2.4) and demethylalangiside (2.5). While 1',2'-dehydrotubulosine (2.6) and demethylpsychotrine (2.7) were also yielded from the water crude extract. All isolated alkaloids were evaluated for cytotoxicity against KB and HeLa cells. Compounds 2.1 and 2.4 showed significant cytotoxicity against KB cell with IC₅₀ values of 1.00 and 9.00 µg/mL, respectively. In addition, compound 2.1 also showed the highest cytotoxicity against HeLa cell with IC₅₀ value of 0.70 µg/mL. The structures of all isolated compounds were elucidated by spectroscopic methods as well as comparison with previous literature data.

Curcumin (3.1), demethoxycurcumin (3.2) and bisdemethoxycurcumin (3.3) isolated from the CH₂Cl₂ crude extract from rhizomes of *Curcuma longa* (Zingiberaceae), and their derivatives 3.4-3.14 were evaluated for α-glucosidase inhibitory activity. The results indicated that curcuminoids 3.1-3.3 showed inhibitory activities against α-glucosidase with the IC₅₀ values of 0.81, 0.31 and 0.47 mM, respectively, which were comparable to that of Acarbose® and exhibited more potent inhibitory activity than their derivatives 3.4-3.14. In addition, the derivatives 3.10-3.12, whose C-4 was fully methylated, showed weak α-glucosidase inhibition with the IC₅₀ values of 1.39, 0.89 and 5.27 mM, respectively. On the other hand, the asymmetrical curcuminoids 3.5, 3.8 and 3.11 exhibited more potent inhibitory activity than the symmetrical curcuminoid congeners 3.6, 3.7, 3.9, 3.10 and 3.12-3.14. In conclusion, simple curcumins having at least one hydroxyl group attached to a aromatic moiety possessed enhanced inhibitory effect whereas the introduction of alkyl groups at hydroxyl groups of curcuminoids reduced activities. In addition, the presence of C-4 methylene proton is not associated with blocking enzyme function.

จุฬาลงกรณ์มหาวิทยาลัย

Department:.....Chemistry.....Student's Signature.....Suwannee Saisin
 Field of Study:.....Chemistry.....Advisor's Signature.....Santi Tip-pyang
 Academic Year:.....2009.....Co-advisor's Signature.....Preecha Phuwapraisirisan

ACKNOWLEDGEMENTS

I would like to express my faithful gratitude to my advisor, Associate Professor Dr. Santi Tip-pyang and my co-advisor, Assistant Professor Dr. Preecha Phuwapraisirisan for their assistance and encouragement in conducting this research.

I also gratefully acknowledge the members of my thesis committee, Associate Professor Dr. Sirirat Kokpol, Assistant Professor Dr. Worawan Bhanthumnavin, Assistant Professor Dr. Aroonsiri Shitangkoon, Dr. Khanit Suwanborirux and Associate Professor Dr. Kwanjai Kanokmedakul for their discussion and guidance.

I would like to express my gratitude to Center for Petroleum, Petrochemicals, and Advanced Materials for providing the chemicals and facilities throughout the course of study and thank Professor Dr. H.G. Munro, Professor Dr. John W. Blunt and Department of Chemistry, University of Canterbury, New Zealand for provide some chemicals and laboratory facilities for isolation and purification of *Alangium salviifolium*

The special thank to Ms. Suttira Khumkratok, a botanist at the Walai Rukhavej Botanical Research Institute, Mahasarakham University for plant identification and making the voucher specimen of plant material as well as providing the stems of *Alangium salviifolium* in this study.

My appreciation is also expressed to thank Dr. Pongpan Siripong and the staff of Natural Products Research Section, Research Division, National Cancer Institute for their testing on cytotoxic activity against KB and HeLa cell lines experiment.

I would like to express my gratitude to Huacheiw Chalermprakiet University for financial support in my Doctoral program.

Finally, I would also like to express my appreciation to my family for their great support and encouragement throughout my education.

CONTENTS

	Pages
Abstract (Thai).....	iv
Abstract (English).....	v
Acknowledgements.....	vi
Contents.....	vii
List of Tables.....	x
List of Figures.....	xi
List of Schemes.....	xiv
List of Abbreviations and Symbols.....	xv
CHAPTER I Bioactive compounds from the lianas of <i>Gnetum macrostachyum</i>	
1.1 Introduction.....	1
1.1.1 Stilbenoids constituent from <i>Gnetum</i> species and their biological activities.....	1
1.1.2 Botanical aspect and distribution.....	15
1.2 Results and Discussion.....	18
1.2.1 Extraction and isolation.....	18
1.2.2 Properties and structural elucidation of isolated compounds..	20
1.2.3 Antioxidant activity of isolated compounds.....	27
1.3 Experimental.....	29
1.3.1 Plant material.....	29
1.3.2 General experimental procedures	29
1.3.3 Extraction and purification.....	29
1.3.4 DPPH Radical scavenging activity.....	36
CHAPTER II Bioactive compounds from the roots of <i>Alangium salviifolium</i>	
2.1 Introduction.....	38

	Pages
2.1.1 Chemical constituents from <i>Alangium</i> species and their biological Activities.....	38
2.1.2 Botanical aspect and distribution.....	51
2.2 Results and Discussion.....	53
2.2.1 Structural elucidation of <i>Alangium</i> alkaloids.....	53
2.2.2 Cytotoxic activity against KB and HeLa cell lines of <i>Alangium</i> alkaloids	59
2.3 Experimental.....	61
2.3.1 Plant material.....	61
2.3.2 General experimental procedures	61
2.3.3 Extraction and purification.....	61
2.3.4 The cytotoxic activity against KB and HeLa cell lines by MTT assay	68
CHAPTER III Bioactive compounds from the rhizomes of <i>Curcuma longa</i>	
3.1 Introduction.....	69
3.2 Results and discussion.....	72
3.2.1 Isolation of curcuminoids.....	72
3.2.2 Synthesis of curcuminoids analogues.....	74
3.2.3 α - Glucosidase inhibitory activity of curcuminoids and curcumin analogues.....	83
3.3 Experimental.....	85
3.3.1 General experimental procedures	85
3.3.2 Extraction and isolation.....	85
3.3.3 General procedure for the preparation of curcumin analogues.....	85
3.3.4 α -Glucosidase inhibitory assay	91
CHAPTER IV Conclusion	
4.1 Bioactive compounds from the lianas of <i>Gnetum macrostachyum</i>	94

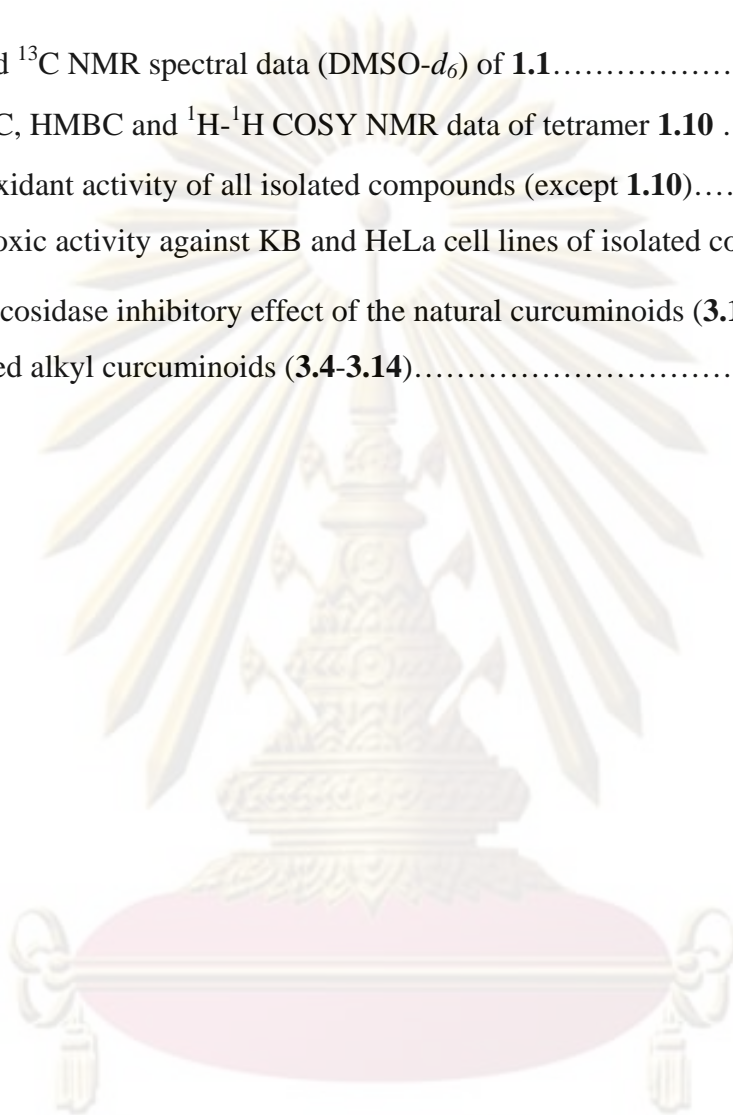
	Pages
4.2 Bioactive compounds from the roots of <i>Alangium</i> <i>salviifolium</i>	96
4.3 Bioactive compounds from the rhizomes of <i>Curcuma longa</i>	98
REFERENCES	101
APPENDIX	110
VITA	125



ศูนย์วิทยทรัพยากร
จุฬาลงกรณ์มหาวิทยาลัย

List of Tables

Tables	Pages
1.1 ^1H and ^{13}C NMR spectral data (DMSO- d_6) of 1.1	22
1.2 ^1H , ^{13}C , HMBC and ^1H - ^1H COSY NMR data of tetramer 1.10	25
1.3 Antioxidant activity of all isolated compounds (except 1.10).....	28
2.1 Cytotoxic activity against KB and HeLa cell lines of isolated compounds.	60
3.1 α -Glucosidase inhibitory effect of the natural curcuminoids (3.1-3.3) and synthesized alkyl curcuminoids (3.4-3.14).....	84



ศูนย์วิจัยทรัพยากร
จุฬาลงกรณ์มหาวิทยาลัย

List of Figures

Figures	Pages
1.1 Stilbene oligomers of group A	3
1.2 Stilbene oligomers of group B	5
1.3 Stilbenoids from <i>G. ula</i> , <i>G. venosum</i> , <i>G. leyboldii</i> and <i>G. schwackeanum</i>	6
1.4 Stilbenoids from <i>G. klossii</i>	7
1.5 Stilbenoids from <i>G. latifolium</i> and <i>G. gnemon</i>	9
1.6 Stilbenoids from <i>G. parvifolium</i>	10
1.7 Stilbenoids from <i>G. cleistostachyum</i> and <i>G. hainanense</i>	11
1.8 Stilbenoids from <i>G. africanum</i>	13
1.9 Stilbenoids from <i>G. montanum</i> and <i>G. montanum</i> f. <i>megalocarpum</i>	14
1.10 Flowers (A), seeds (B) and lianas (C) of <i>G. macrostachyum</i>	17
1.11 Flavonoids and stilbenoids isolated from <i>G. macrostachyum</i> lianas.....	18
1.12 Key HMBC and NOESY correlations of 1.1	22
1.13 Selected HMBC correlations of 1.10	24
1.14 The proposed structure of 1.10	25
1.15 Structures of DPPH and DPPH _n	37
2.1 Propose biosynthesis sequence of the alkaloids and nitrogenous glucosides in <i>Alangium lamarchii</i>	41
2.2 Benzoquinolizidine and indolobanzoquinolizidine alkaloids from the root bark of <i>A. lamarchii</i>	42
2.3 Tetrahydroisoquinoline monoterpene glucosides from the hot methanolic fraction of <i>A. lamarchii</i> fruits	44
2.4 Iridoid glucoside from the water soluble fraction of <i>A. lamarchii</i> fruits .	47
2.5 Iridoid glucoside and flavanoids from <i>A. kurzii</i> leaves	48
2.6 Phenolic glucoside from <i>A. chinense</i>	49
2.7 Banzoquinolizidine from <i>A. longiflorum</i>	50
2.8 Indolobenzoquinolizidine from <i>A. salviifolium</i>	50

Figures	Pages
2.9 Leaves (A) and flowers (B) <i>Alangium salviifolium</i>	52
2.10 Structure of alkaloid 2.1-2.7 from the butanolic and water extract of <i>A. salviifolium</i> roots	53
2.11 The key HMBC correlations of 2.1	54
2.12 The key HMBC correlations of 2.2	55
2.13 The key HMBC correlations of 2.3	56
2.14 The key HMBC correlations of 2.4	57
2.15 The key HMBC correlations of 2.5	57
2.16 The key HMBC correlations of 2.6	58
2.17 The key HMBC correlations of 2.7	59
3.1 The structures of curcuminoids	69
3.2 Hydrolysis of 1,4-glucosidic linkages	70
3.3 Digestion of starch in the small intestine by α -glucosidase enzyme	71
3.4 Structures of α -glucosidase inhibitors	71
3.5 Curcuminoids from the <i>Curcuma longa</i> rhizomes	72
3.6 Key HMBC correlations of 3.4	75
3.7 Key HMBC correlations of 3.5	76
3.8 Key HMBC correlations of 3.6	76
3.9 Key HMBC correlations of 3.9	78
3.10 Key HMBC correlations of 3.12	82
3.11 Hydrolysis of p-nitrophenyl- α -D-glucopyranoside by α -glucosidase ..	92
4.1 The isolated compounds from <i>Gnetum macrostachyum</i> lianas	94
4.2 The isolated compounds from <i>Alangium salviifolium</i> roots	97
4.3 The structure of curcuminoids and curcumin analogues	98
A-1.1 ^1H NMR spectrum (acetone- d_6) of 1.1	111
A-1.2 ^{13}C NMR spectrum (acetone- d_6) of 1.1	111
A-1.3 HSQC spectrum (acetone- d_6) of 1.1	112

Figures	Pages
A-1.4 HMBC spectrum (acetone- <i>d</i> ₆) of 1.1	112
A-1.5 ¹ H NMR spectrum (acetone- <i>d</i> ₆) of 1.10	113
A-1.6 COSY spectrum (acetone- <i>d</i> ₆) of 1.10	113
A-1.7 HMQC spectrum (acetone- <i>d</i> ₆) of 1.10	114
A-1.8 HMBC spectrum (acetone- <i>d</i> ₆) of 1.10	114
A-1.9 ¹ H NMR spectrum (CDCl ₃) of 3.4	115
A-1.10 COSY spectrum (CDCl ₃) of 3.4	115
A-1.11 HMQC spectrum (CDCl ₃) of 3.4	116
A-1.12 HMBC spectrum (CDCl ₃) of 3.4	116
A-1.13 ¹ H NMR spectrum (CDCl ₃) of 3.5	117
A-1.14 HMBC spectrum (CDCl ₃) of 3.5	117
A-1.15 ¹ H NMR spectrum (CDCl ₃) of 3.6	118
A-1.16 ¹³ C spectrum (CDCl ₃) of 3.6	118
A-1.17 COSY spectrum (CDCl ₃) of 3.6	119
A-1.18 HMQC spectrum (CDCl ₃) of 3.6	119
A-1.19 HMBC spectrum (CDCl ₃) of 3.6	120
A-1.20 ¹ H NMR spectrum (CDCl ₃) of 3.9	120
A-1.21 ¹³ C spectrum (CDCl ₃) of 3.9	121
A-1.22 HMBC spectrum (CDCl ₃) of 3.9	121
A-1.23 ¹ H NMR spectrum (CDCl ₃) of 3.12	122
A-1.24 ¹³ C spectrum (CDCl ₃) of 3.12	122
A-1.25 COSY spectrum (CDCl ₃) of 3.12	123
A-1.26 HMQC spectrum (CDCl ₃) of 3.12	123
A-1.27 HMBC spectrum (CDCl ₃) of 3.12	124

List of Schemes

Schemes	Pages
1.1 The extraction procedure of <i>G. macrostachyum</i> lianas	31
1.2 The isolation procedure of the acetone crude extract	32
2.1 Extraction of <i>A. salviifolium</i> roots	63
2.2 Isolation procedure of the butanolic crude extract	64
2.3 Isolation procedure of the water crude extract	65
3.1 The isolation procedure of curcuminoids from <i>Curcuma longa</i> rhizomes	73
3.2 Prenylation of curcuminoids (3.1-3.3)	74
3.3 Acetylation of curcuminoids (3.1-3.3)	77
3.4 Methylation of curcuminoids (3.1-3.3)	79
3.5 Generation of phenoxyl and enolate anions in basic condition	80

ศูนย์วิจัยทรัพยากร
จุฬาลงกรณ์มหาวิทยาลัย

List of Abbreviations and Symbols

acetone- <i>d</i> ₆	deuterated acetone
brs	broad singlet (NMR)
brd	broad doublet (NMR)
BuOH	butanol
calcd	calculated
¹³ C NMR	carbon 13 nuclear magnetic resonance
CC	column chromatography
<i>c</i>	concentration
COSY	correlated spectroscopy
DMSO- <i>d</i> ₆	deuterated dimethyl sulfoxide
CDCl ₃	deuterated chloroform
CD ₃ OD	deuterated methanol
DM	diabetes mellitus
CH ₂ Cl ₂	dichloromethane
DMSO	dimethyl sulfoxide
DPPH	2,2-diphenyl-1-picrylhydrazyl free radical
DPPHn	2,2-diphenyl-1-picrylhydrazine
d	doublet (NMR)
dd	doublet of doublet (NMR)
ESIMS	electrospray ionization mass spectrometry
g	gram (s)
¹ H NMR	proton nuclear magnetic resonance
HMBC	heteronuclear multiple bond correlation experiment
HSQC	heteronuclear single quantum correlation
Hz	hertz
HRESIMS	high resolution electrospray ionization mass spectrometry
HPLC	high performance liquid chromatography
HeLa cell line	human cervical carcinoma

IC ₅₀	concentration that is required for 50% inhibition in vitro
<i>J</i>	coupling constant
KB cell line	human epidermoid carcinoma
K ₂ CO ₃	potassium carbonate
LC-APCIMS	liquid chromatographic atmospheric pressure chemical ionization mass spectrometry
<i>m/z</i>	mass per charge
MHz	megahertz
MeOH	methanol
mg	milligram (s)
min	minute
mL	milliliter (s)
M	molar
m	multiplet (NMR)
MTT	[3-(4,5-dimethylthiazol-2-yl)-2,5-diphenyl tetrazolium bromide]
NMR	nuclear magnetic resonance
NOESY	nuclear overhauser enhancement spectroscopy
s	singlet (NMR)
Na ₂ CO ₃	sodium carbonate
pNPG	<i>p</i> -nitrophenyl α-D-glucopyranoside
pyridine- <i>d</i> ₅	deuterated pyridine
TLC	thin layer chromatography
TMSCHN ₂	trimethylsilyldiazomethane
t	triplet (NMR)
UV	ultraviolet
U	unit
VLC	vacuum liquid chromatography
δ	chemical shift
δ _c	chemical shift of carbon

δ_{H}	chemical shift of proton
ϵ	molar extinction coefficient
λ_{max}	maximum wavelength
μL	microliter (s)
ϵ	molar extinction coefficient



ศูนย์วิทยทรัพยากร
จุฬาลงกรณ์มหาวิทยาลัย

CHAPTER I

BIOACTIVE COMPOUNDS FROM THE LIANAS OF *Gnetum macrostachyum*

1.1 Introduction

The Gnetaceae family has been recognized as a rich source of stilbene oligomers. Natural stilbene oligomers are a group of compounds mostly obtained from nine plant families, namely Dipterocarpaceae [1-2], Vitaceae [3-4], Cyperaceae [5], Gnetaceae [6-10], Leguminosae [11], Iridaceae [12], Celastraceae [13], Paeoniaceae [14] and Moraceae [15]. Many stilbene derivatives have been isolated from various plants and possessed biological activities such as blood sugar reduction [16], induction of apoptosis in colon cancer [17], protein kinase C inhibition [18], antiHIV and cytotoxicity [19], antifungal [20], cyclooxygenase (COX I, COX II) inhibition [21], antiinflammatory and antioxidant activities [22].

Recently, more attention has been focused on naturally occurring oligostilbenes because of their multifunctional bioactivities. Therefore, stilbenoids are regarded as potential lead compounds for the development of new drugs.

1.1.1 Stilbenoid constituents from *Gnetum* species and their biological activities

The genus *Gnetum* is one of the main genera of Gnetaceae, consisting of about 30 species distributed mainly in the tropical region. This genus has been recognized to contain monomer and stilbene oligomers of isorhapontigenins and resveratrols. In 1993, the naturally occurring oligostilbenes were divided into two groups (A and B) [23]. Group A possessed at least one five-membered oxygen heterocyclic rings. The reported heterocyclic rings of group A were generally dihydrobenzofuran types or the *trans*-2-aryl-2,3-dihydrobenzofuran moiety except for anigopreissin A, the first resveratrol dimer with benzofuran system [24]. Group B of stilbene oligomers did not

contain any oxygen heterocyclic rings, including cyclodimeric stilbenes, indanes, indanone and tetralins skeleton [25-26].

However, the stilbene oligomers in this family have a variety of frameworks resulting from different oxidative condensation of nucleus in dihydrofuran ring, benzocyclopentane ring (indanes skeleton), benzocyclohexane (tetralins skeleton), dibenzo[2.1]octadiene system, dibenzobicyclo[3.2.1]octadiene system, dibenzobicyclo[3.3.0]octadiene system, tribenzobicyclo[3.3.2]octatriene system and dibenzobicyclo[5.3.0]decadiene system [27].

The examples of stilbene oligomers belonging to group A were (-)- ϵ -viniferin, gnetin H, anigopreissin A, gnetuhainin G, pauciflorol E and hopeaphenol, while group B were pallidol, isorhaformicols A, pauciflorol F and copalliferol B. All of these structures were summarized in Figures 1.1 and 1.2.

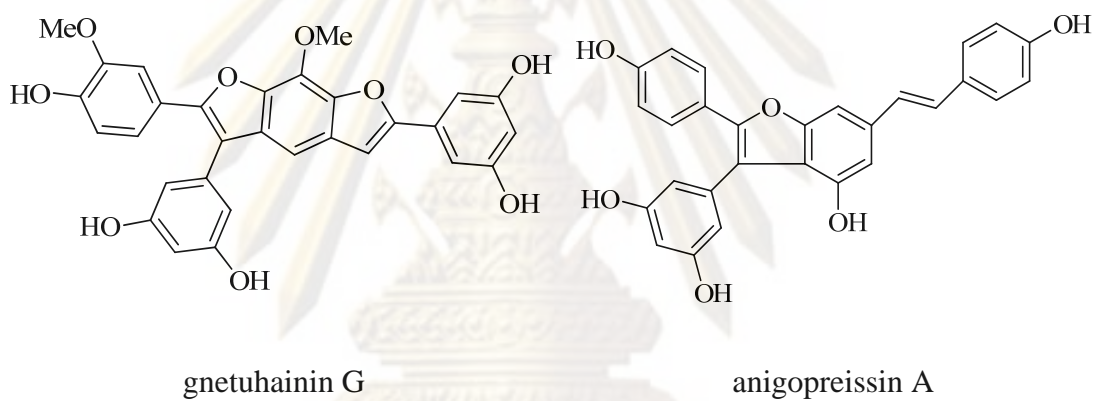
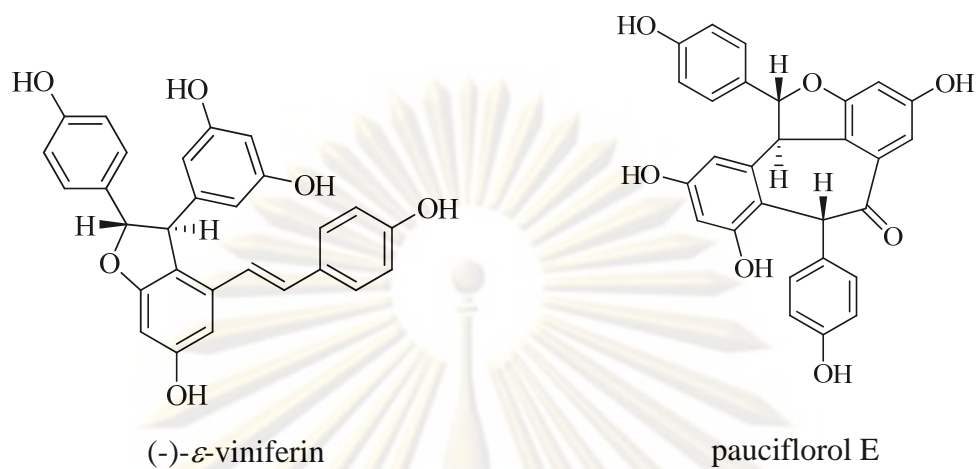
Group A

(-)- ϵ -Viniferin and gnetin H are characterized by coupling of two resveratrols to form a *trans*-2-aryl-2,3-dihydrobenzofuran ring. The anigopreissin A and gnetuhainin G were the resveratrol dimer and the isorhapontigenin dimer, respectively. These two compounds possessed the benzofuran rings, instead of 2,3-dihydrobenzofuran. In addition, hopeaphenol and pauciflorol E were the resveratrol tetramers and dimer, in which their representative skeleton consist of a dihydrobenzofuran ring, dibenzo[2.1]octadiene system and a dihydrobenzofuran ring, dibenzo[2.1]octadienone system, respectively.

ศูนย์วิทยทรัพยากร

จุฬาลงกรณ์มหาวิทยาลัย

Dimer



Trimers

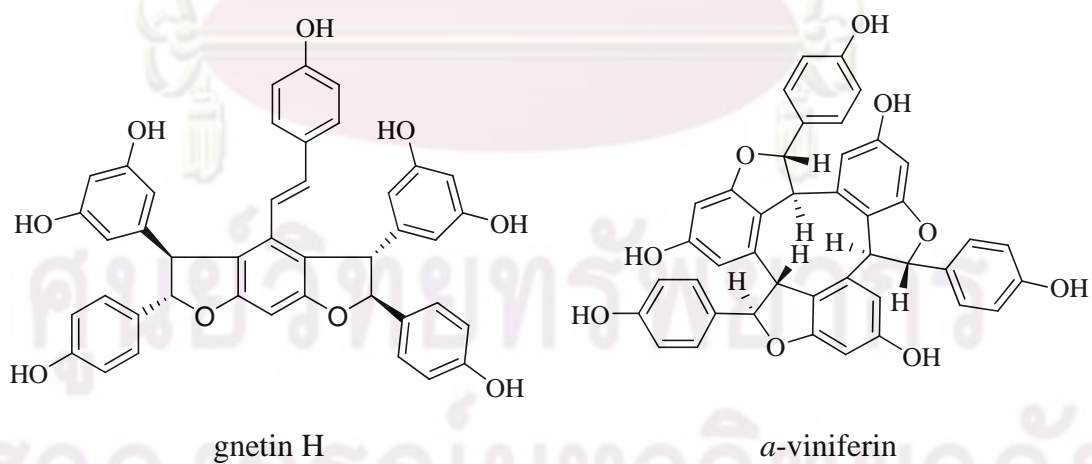


Figure 1.1 Stilbene oligomers of group A

Tetramers

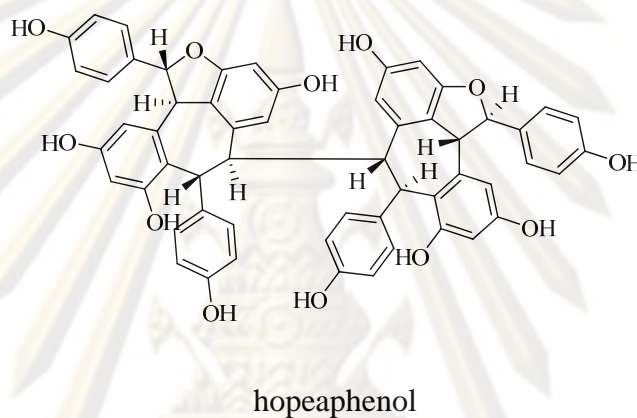
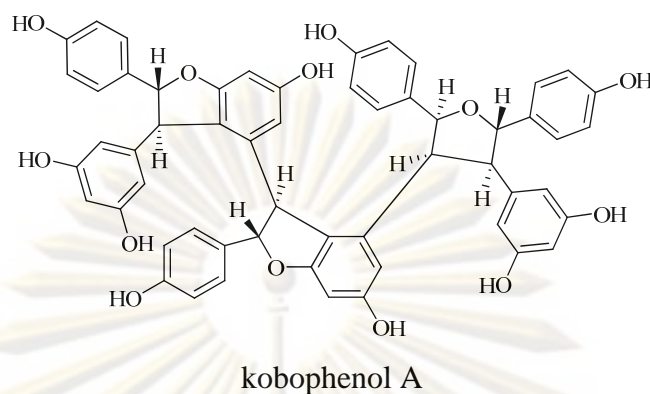


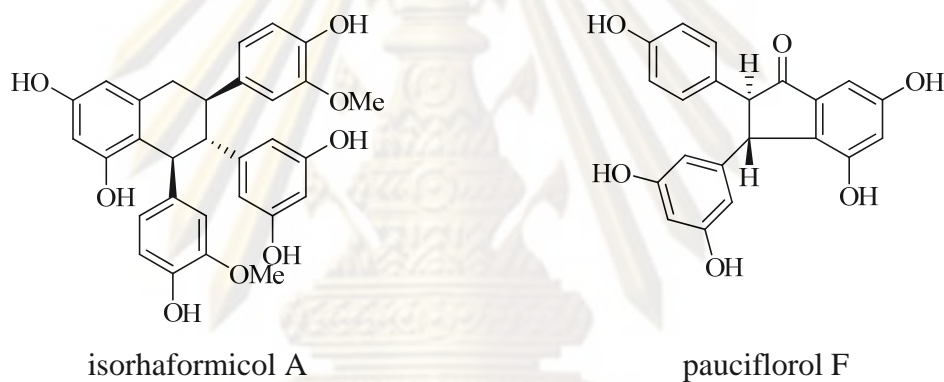
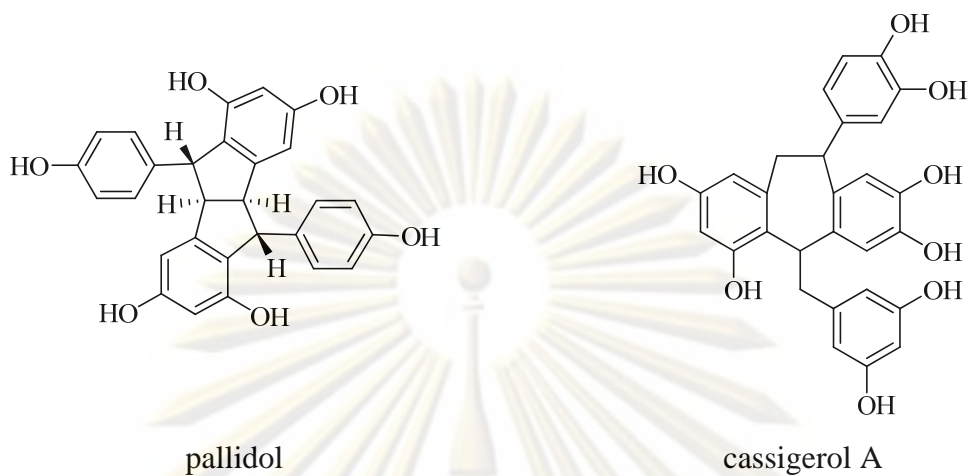
Figure 1.1 Stilbene oligomers of group A (cont.).

Group B

Pallidol is characterized by coupling two resveratrols to form benzocyclopentane rings, while isorhaformicol A is characterized by coupling two isorhapontigenin to form benzocyclohexane rings. In addition, copalliferol B was the resveratrol trimers, which possessed benzocyclopentane ring and benzocycloheptane ring in the structure. Moreover, pauciflorol F had an indanone skeleton, which was different from the other types of the stilbene dimers.

จุฬาลงกรณ์มหาวิทยาลัย

Dimer



Trimers

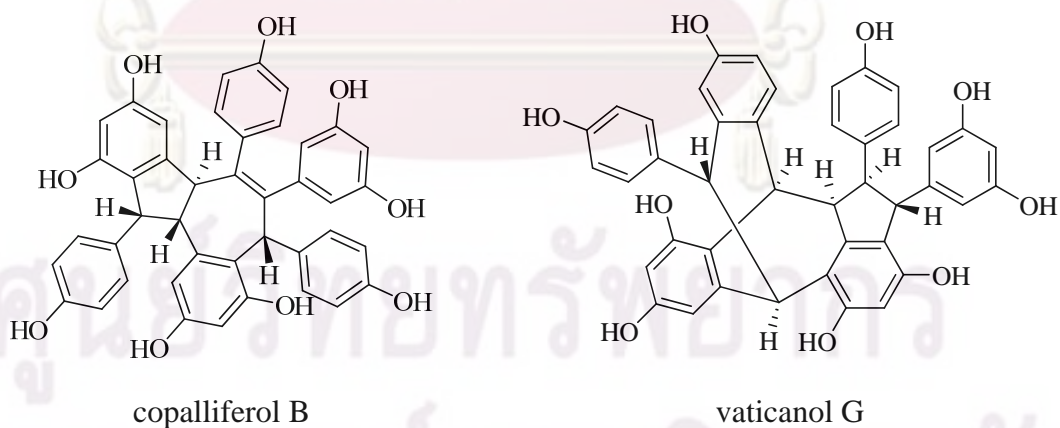


Figure 1.2 Stilbene oligomers of group B

Gnetin, gnetulin and resveratrol were isolated from the wood of *G. ula*, while isorhapontigenin, gnetin C and gnetin E were obtained from the seed of *G. venosum*

[28-29]. Moreover, the gnetins A, B, D were also isolated from the lianas of *G. leyboldii*, while gnetins C and E were yielded from *G. schwackeanum* [6] (Fig 1.3).

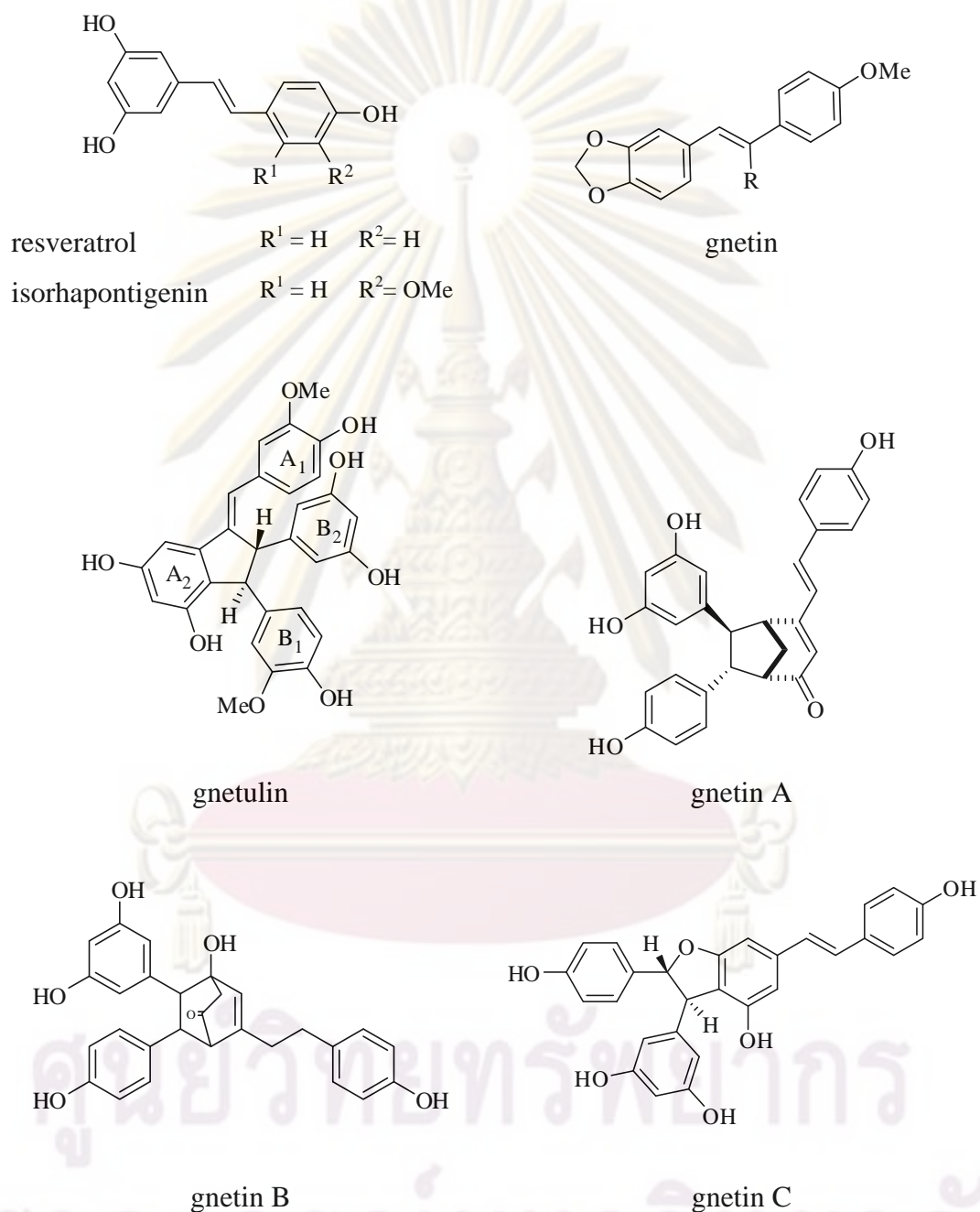


Figure 1.3 Stilbenoids from *G. ula*, *G. venosum*, *G. leyboldii* and *G. schwackeanum*

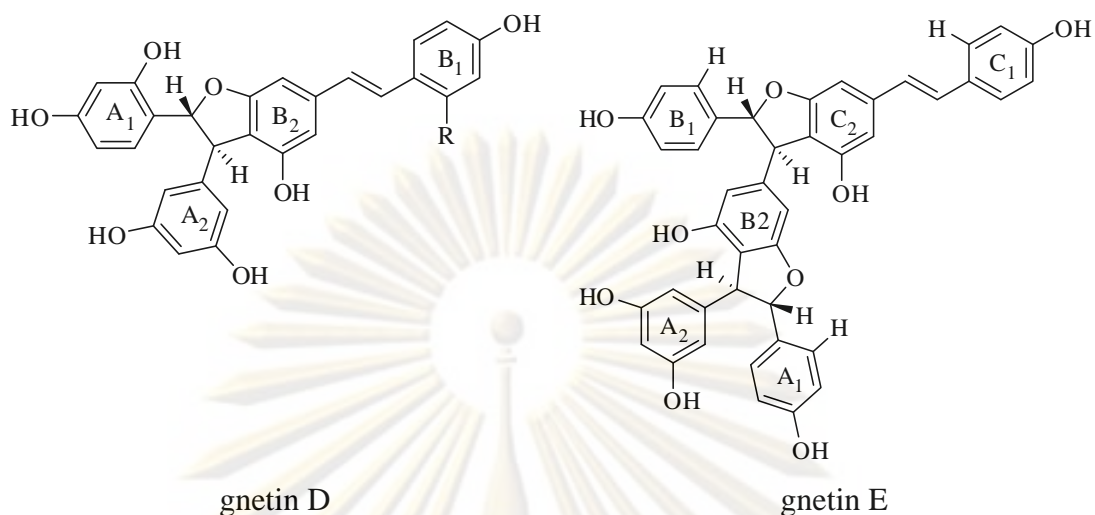


Figure 1.3 Stilbenoids from *G. ula*, *G. venosum*, *G. leyboldii* and *G. schwackeanum* (cont.)

Gnetofurans A-C and dihydropinosylvindiol were isolated from the methanol soluble extract of the stems of *G. klossii* together with gnetifolin F, gnetulin, latifolol, gnetol, (-)- ϵ -viniferin, gnetins E and C and resveratrol [31] (Fig 1.4).

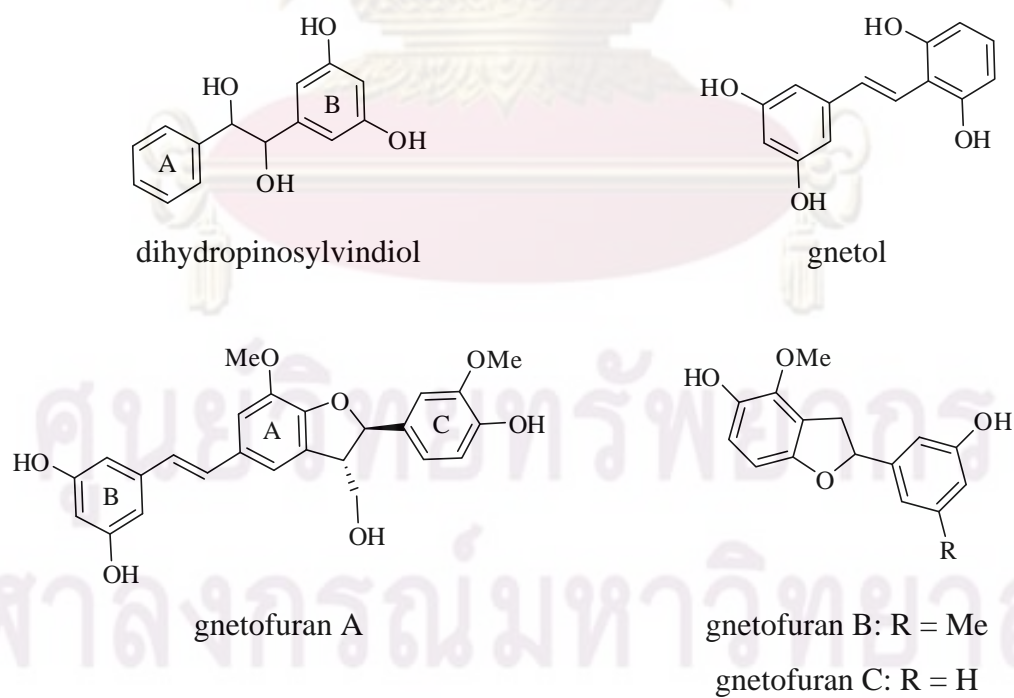


Figure 1.4 Stilbenoids from *G. klossii*

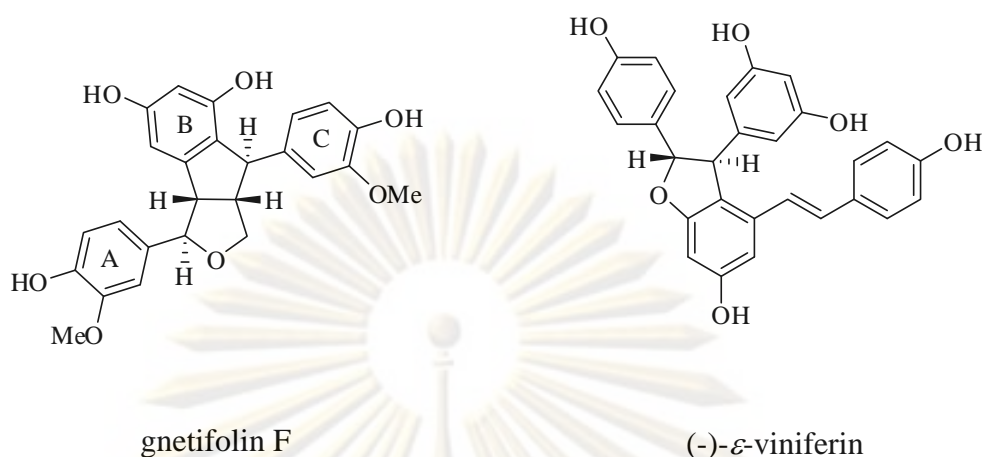


Figure 1.4 Stilbenoids from *G. klossii* (cont.)

Furthermore, resveratrol, gnetin C, (-)- ϵ -viniferin, gnetins E and D, latifolol and gnemons A, B, D, E, F, K, L, M, gnemonside K, gnetol, isorhapontigenin, gnetifolin E, isorhapontigenin-3-*O*-D-glucopyranoside were isolated from the acetone fraction of lianas of *G. latifolium* and the acetone, methanol, 70% methanol extracts of the roots of *G. gnemon* Linn [32-34] (Fig 1.5). Gnemons K-L, (-)- ϵ -viniferin, gnetol, resveratrol, isorhapontigenin and latifolol also showed antioxidant activities on lipid peroxidation and superoxide scavenging stronger than vitamin E.

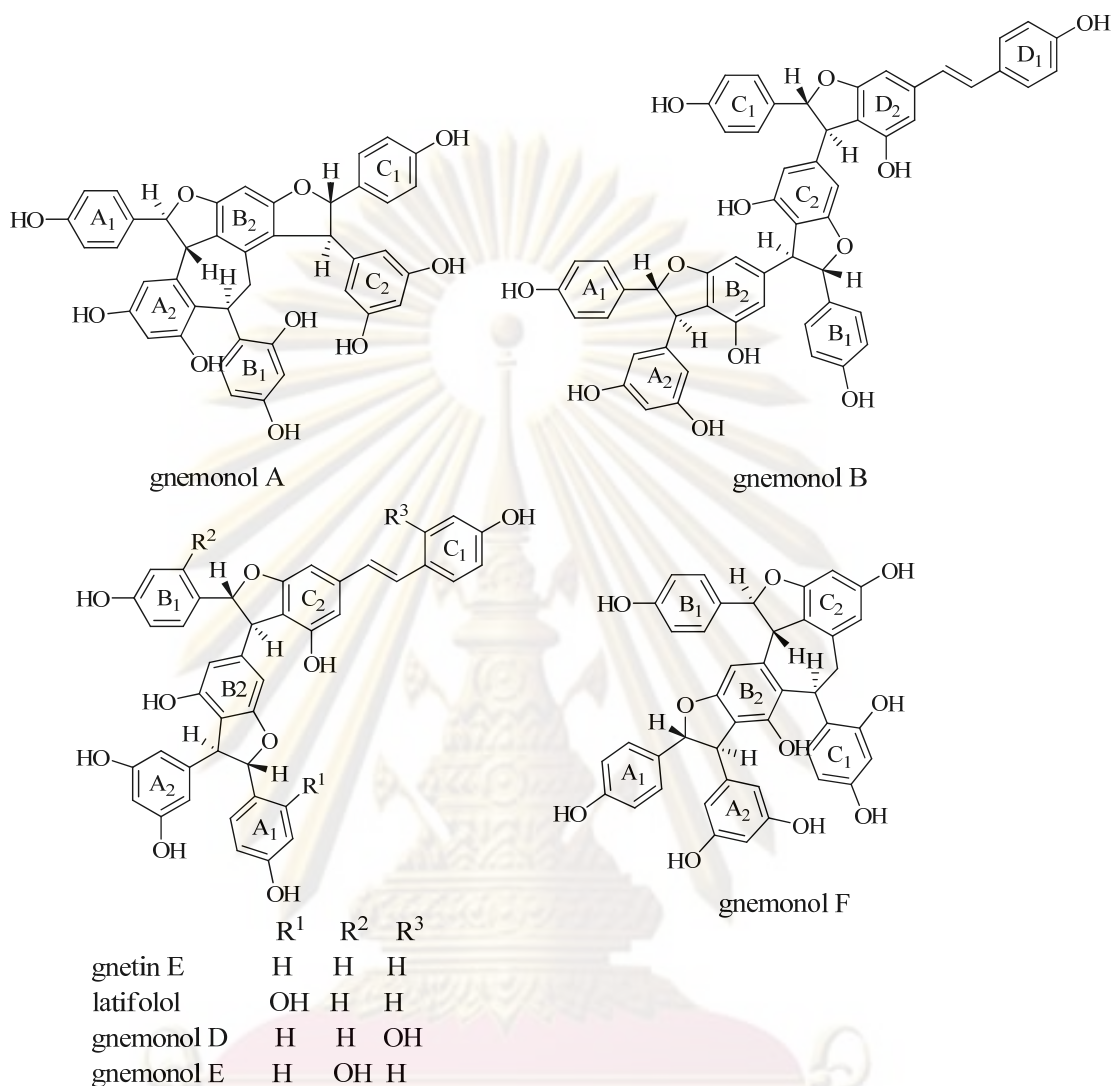


Figure 1.5 Stilbenoids from *G. latifolium* and *G. gnetum*.

Gnetum parvifolium grows in the southern part of China and has been used in the treatment of bronchitis and arthritis in folk medicine. Parvifolols A-D and 2b-hydroxyampelopsin F were isolated from the lianas of this plant (Fig 1.6). Among isolated compounds, 2b-hydroxyampelopsin F showed potent inhibitory activity ($IC_{50} = 10 \mu\text{g/mL}$) in the Maillard reaction which is one of the causes of diabetic complications and aging of the skin [7].

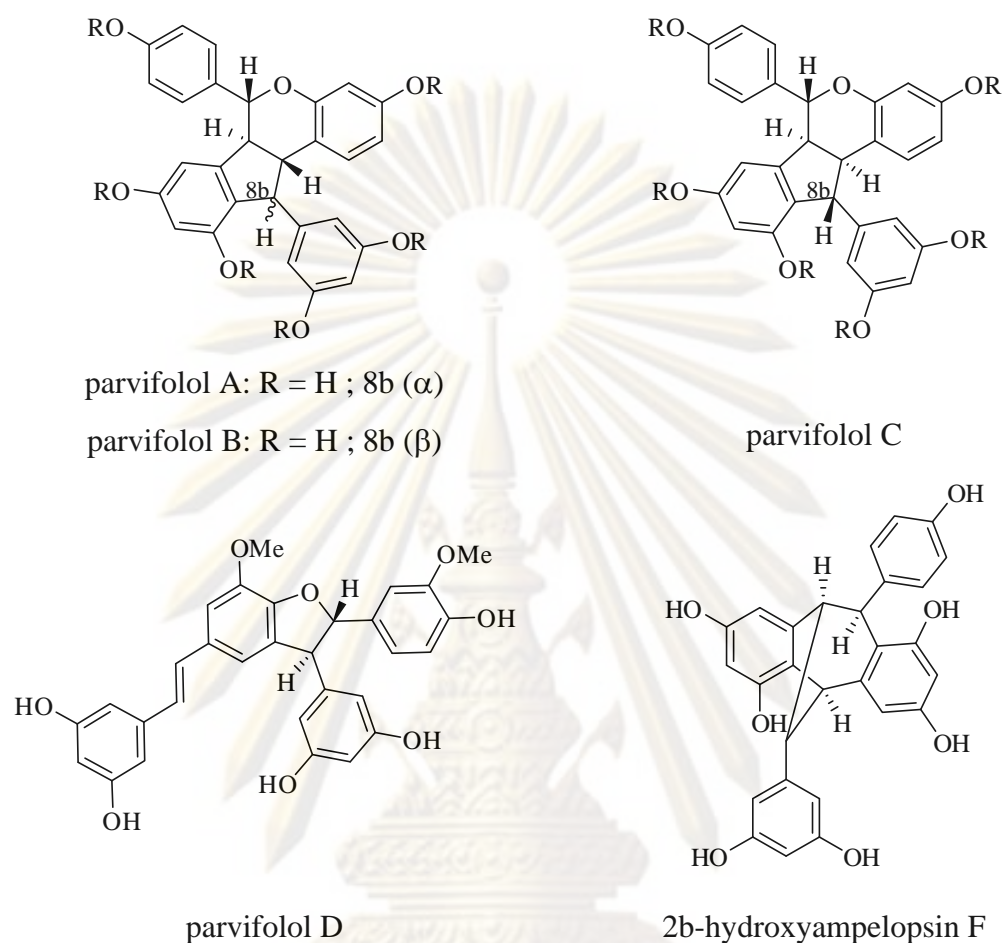


Figure 1.6 Stilbenoids from *G. parvifolium*

Furthermore, bisorrhapontigenin A, *cis*-shegansu B, gnetuhainin P and gnutulin were isolated from the lianas of *G. cleistostachyum* [35]. The pharmacological activities of these compounds have been tested for antiinflammatory activity and antioxidant activity. Bisorrhapontigenin A showed antiinflammatory activity, while gnetuhainin P revealed the antioxidant activity.

In addition, gnetuhainins A-J were obtained from the ethanolic extract of the lianas *G. hainanense* [8, 36] (Fig 1.7).

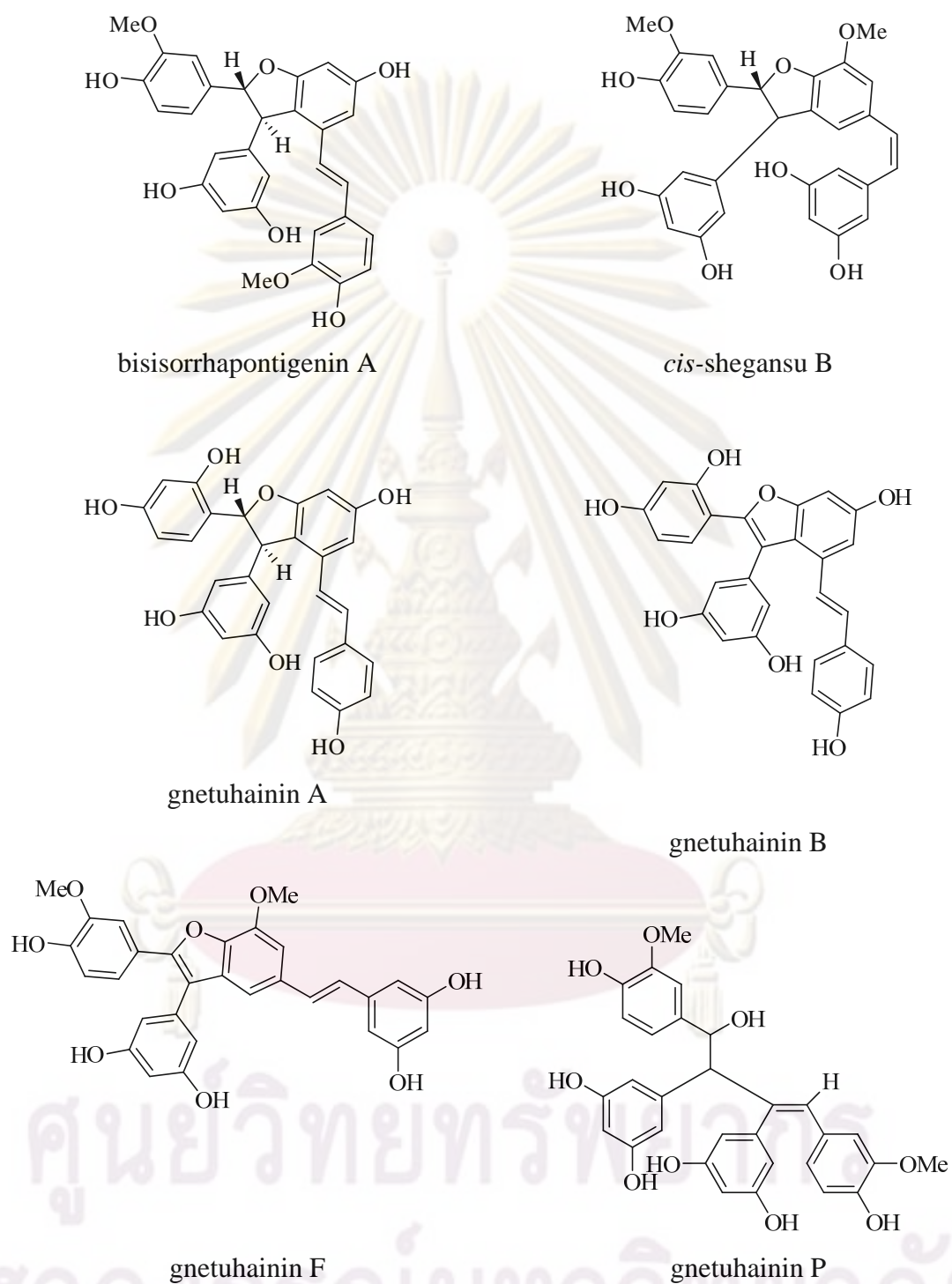


Figure 1.7 Stilbenoids from *G. cleistostachyum* and *G. hainanense*.

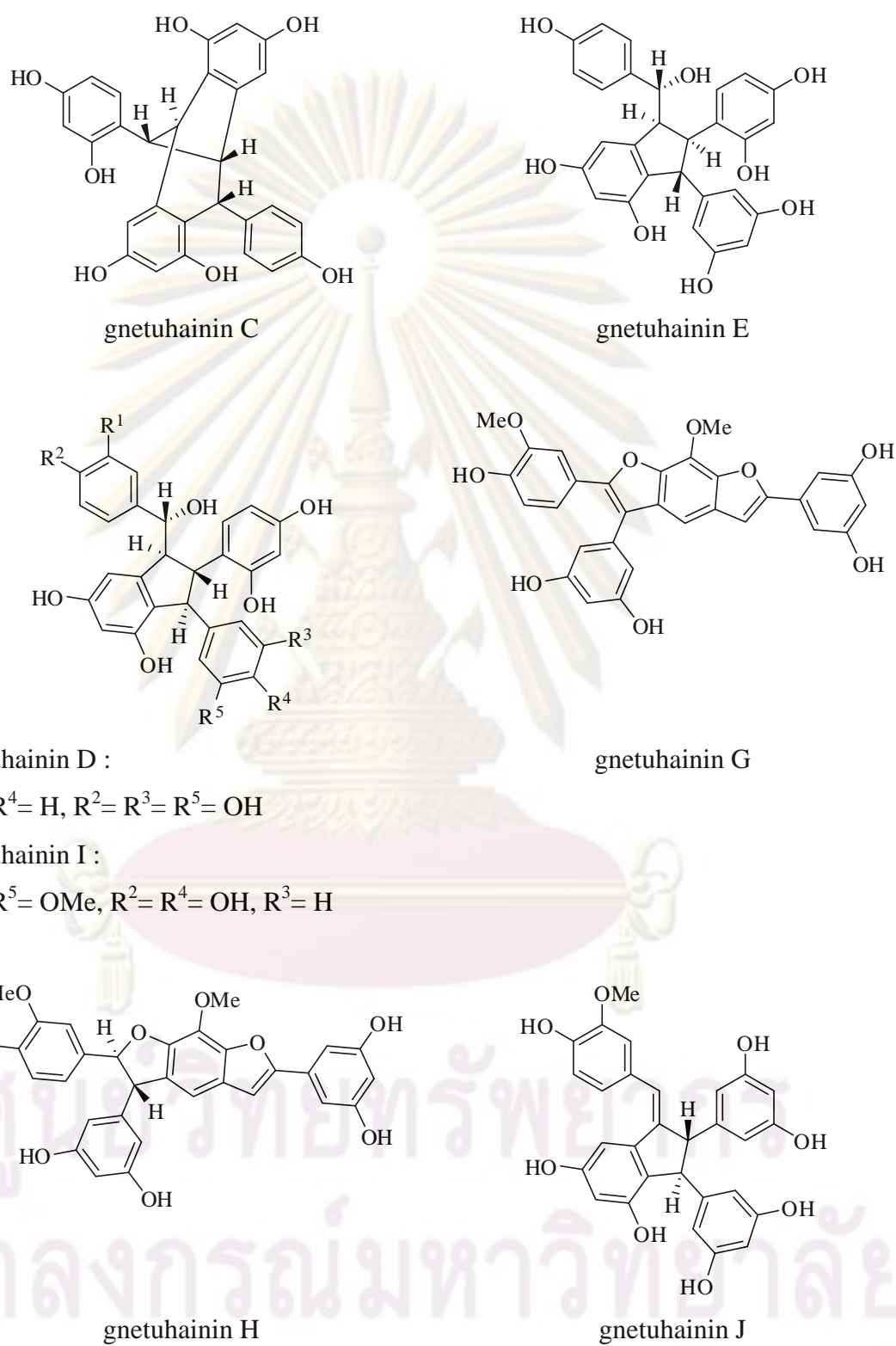


Figure 1.7 Stilbenoids from *G. cleistostachyum* and *G. hainanense* (cont.).

However, the isolation of the lianas of *G. africanum* gave gneaffricanins C-F along with gnetin F, gnetin D and gnetuhainin A (Fig 1.8). In addition, gneaffricanins C-E showed inhibition in lipid peroxide ($IC_{50} = 13, 50$ and $32 \mu M$) and scavenging activity of superoxide ($IC_{50} = 10, 34$ and $30 \mu M$) [10].

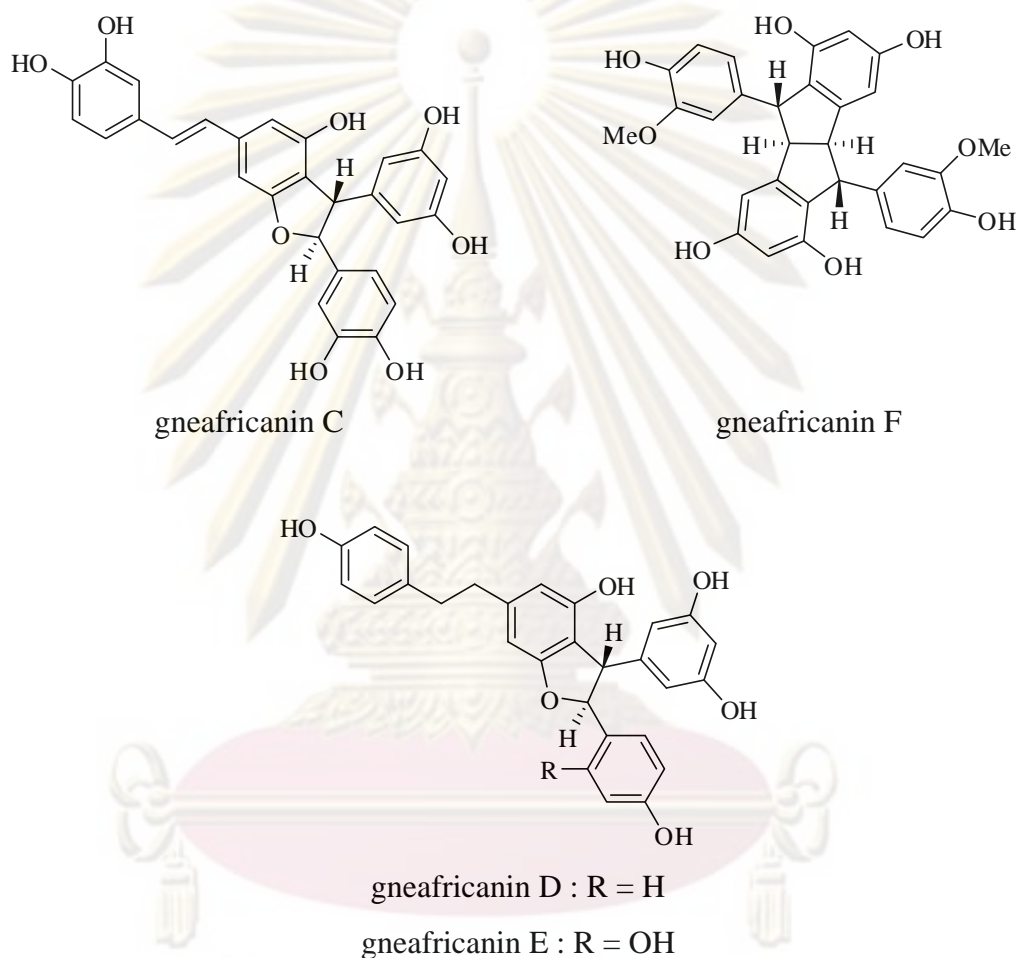


Figure 1.8 Stilbenoids from *G. africanum*.

Many stilbenoids were also isolated from the EtOAc soluble fraction of *G. montanum* [37] and *G. montanum* f. *megalocarpum* [38]. They were gnetifolin M, gnetumontanins A-D, gnetifolin, isorhapontigenin, resveratrol, gnetol, gnetupendin B, (-)- ϵ -viniferin, gnetulin, gnetin D, gnetuhainin M, isorhapontigenin 3-*O*- β -D-glucoside, and isorhapontigenin 12- β -D-glucoside (Fig 1.9).

Gnetumontanin A was the first stilbene dimer derived from two oxyresveratrol units while gnetumontanins C and D were novel skeleton having δ -lactone moieties. Gnetumontanin B showed tumor necrosis factor inhibitory activities (IC_{50} 1.49 μ M while dexamethasone was used as a positive control with an IC_{50} 1 μ M).

Gnetupendins A and B were obtained together with resveratrol and isorhapontigenin from *G. pendulum*. They contained new stilbenoid skeletons, in which C-2 of 3,5-dihydroxybenzene ring (B) of the isorhapontigenin unit was substituted by 4-hydroxybenzyl and 3,4-dihydroxybenzyl groups, respectively (Fig 1.9). Moreover, gnetupendin B showed cyclooxygenase-II inhibitory activity, which the inhibitory rate of it was 24.4% at the concentration of 10^{-7} mol/l, with meloxicam used as a positive control IC_{50} at 2.86×10^{-8} mol/l [39].

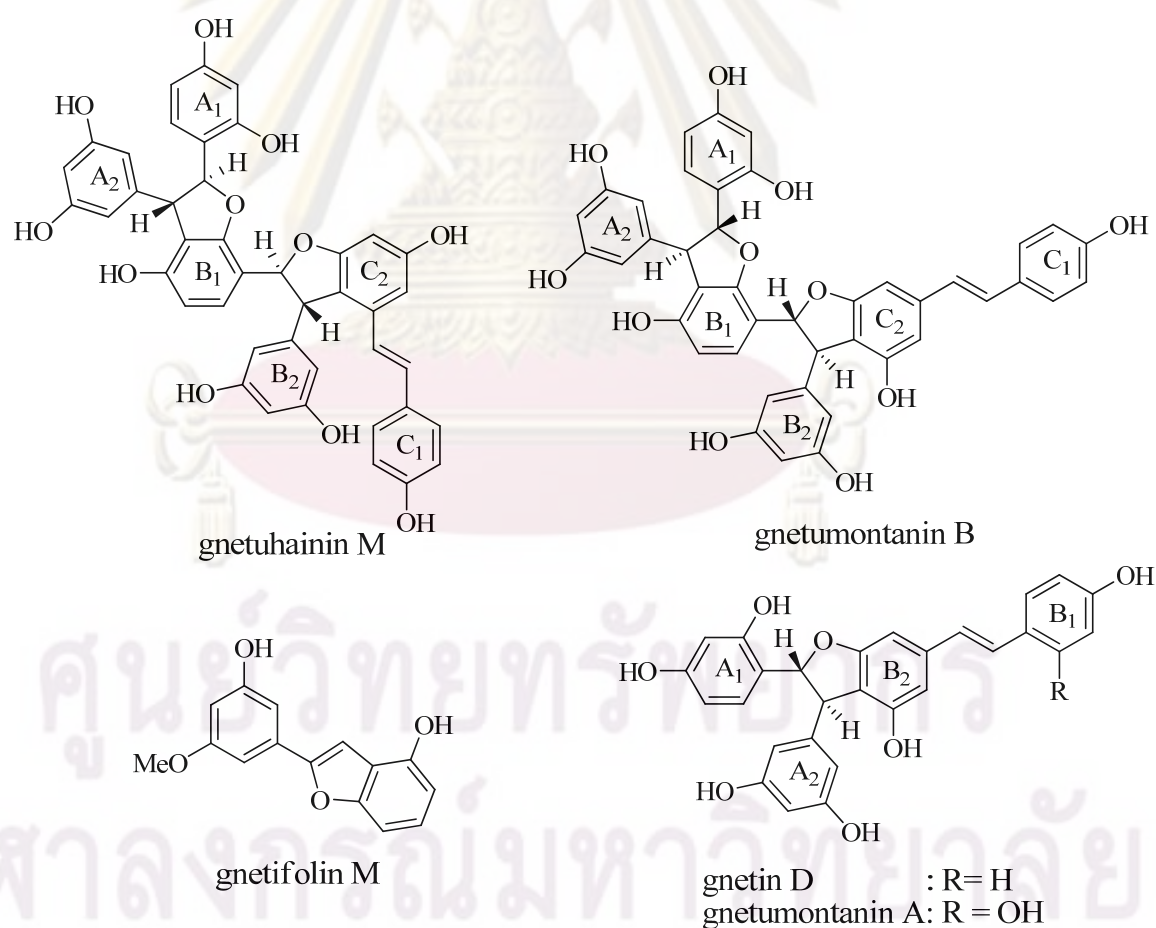


Figure 1.9 Stilbenoids from *G. montanum* and *G. montanum* f. *megalocarpum*.

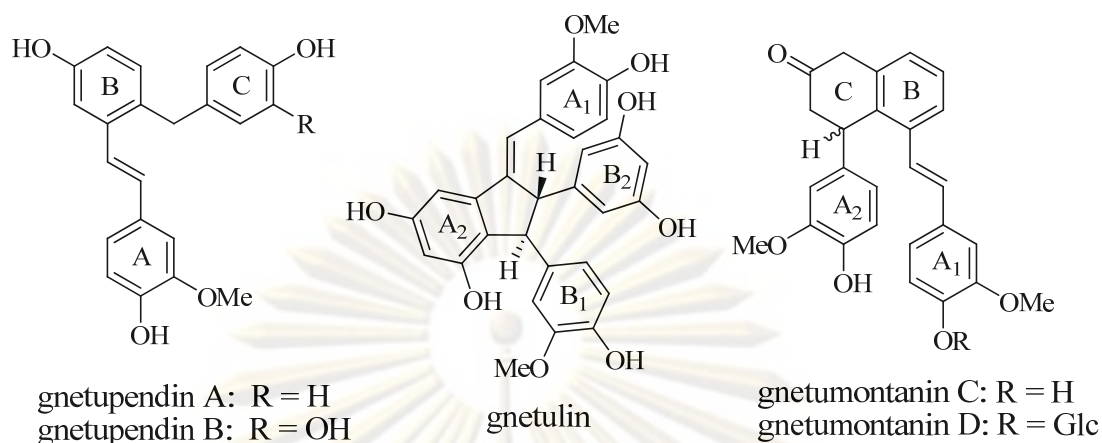


Figure 1.9 Stilbenoids from *G. montanum* and *G. montanum* f. *megalocarpum*. (cont.)

1.1.2 Botanical aspect and distribution

Gnetaceae is a monogeneric family, *Gnetum* being the only genus. *Gnetum* is evergreen dioecious (rarely monoecious) trees, shrubs, or woody climbers. There are about 30 species in the tropical lowlands of the world, from northeastern South America, tropical West Africa, south China to Southeast Asia. In Thailand, eight species are found in rainforests below 1800 metres [40-41], consist of

G. gnemon Linn. var. *gnemon* (Shrub tree) Pisae (ปีแซ)

G. gnemon Linn. var. *tenerum* Markgr. (Shrub) Phak miang (ผักเมียง)

G. tenuifolium Ridl. (Woody climber) Muai nok (เมื่อยนง)

G. macrostachyum Hook. f. (Woody climber) Muai duk (เมื่อยดุก)

G. microcarpum Bl. (Woody climber) Muai nok (เมื่อยนง)

G. cuspidatum Bl. (Woody climber) Muai dam (เมื่อยดำ)

G. leptostachyum Bl. (Woody climber)

G. montanum Markgr. (Woody climber) Muai (เมื่อย)

G. latifolium Bl. var. *funiculare* Markgraf. (Woody climber) Mamuai (มะม้วย)

Gnetum macrostachyum Hook. f. is the woody climber plant in genus of *Gnetum*, Gnetaceae family.

Leaves: oblong to lanceolate-oblong, coriaceous, brown when dry, 14-16 by 4-5 cm; apex cuspidate; base acute to rounded or sometimes suboblique; secondary nerves curved, distinctly anastomosing; petiole \pm 1 cm.

Male inflorescences: axillary, simple, \pm 5 by 0.7 cm, sporphylls very short, embedded in the villous indumentum; hair twice as long as the collar rudimentary ovaries obliquely ovoid, about 10 in each collar.

Female inflorescences: simple cauline, \pm 9 by 1 cm, flowers globose, 8-10 in each collar.

Fruits: sessile, ellipsoid, 2 by 1.2 cm, surrounded basally by very striking long brown hairs.

Thailand: North-Eastern: Nong Khai; Eastern: Nakhon Ratchasima, Surin; Central: Nakhon Nayok; South-Eastern: Trat, Chon Buri; Peninsular: Ranong, Surat Thani, Nakhon Si Thammarat.

Distribution: Tenasserim, Indochina, Malaysia (type, Malaya).

Ecology: Mostly by streams in evergreen forest, alt. 200-900 m.

Flowering: January-February; fruiting February-March.

Vernacular: Muai duk (เมื่อยดุก), Muai (เมื่อย), Muai (ม่วย), Muai luat (ม่วยเลือด).



ศูนย์วิทยทรัพยากร
จุฬาลงกรณ์มหาวิทยาลัย

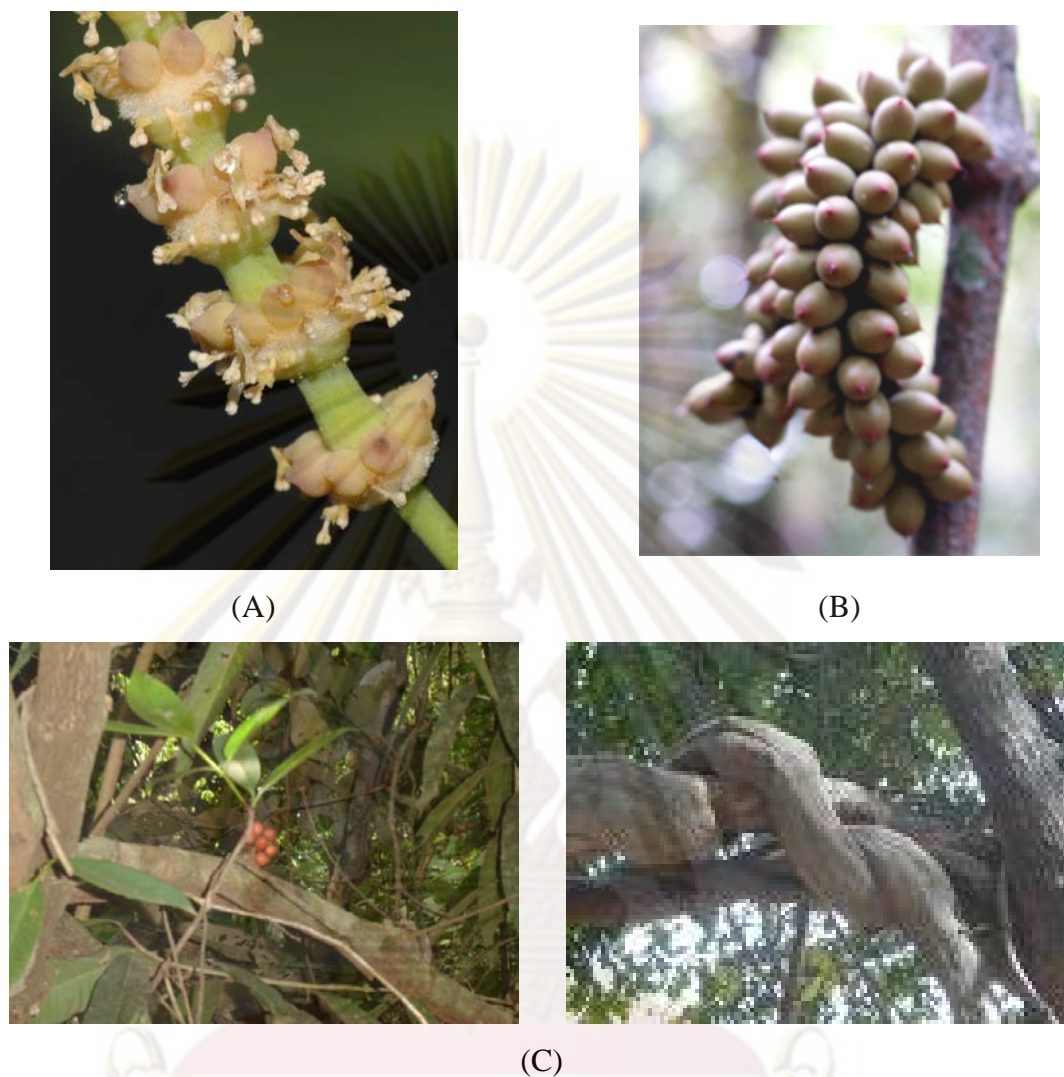


Figure 1.10 Flowers (A), seeds (B) and lianas (C) of *G. macrostachyum*

The objective of this research:

1. To extract and isolate compounds from the lianas of *G. macrostachyum*.
2. To elucidate the structures of all isolated compounds.
3. To determine the biological activities of the isolated compounds.

1.2 Results and Discussion

1.2.1 Extraction and isolation

The dried and powdered lianas of *G. macrostachyum* were extracted successively in a soxhlet extractor with CH₂Cl₂, acetone and MeOH, respectively. A part of acetone extract was stirred with acetone to yield acetone soluble and insoluble fractions. The acetone soluble fraction was fractionated by a combination of chromatographic procedures to afford two new compounds, 5,7,2'-trihydroxy-5'-methoxyflavone (**1.1**) and stilbenoid tetramer (**1.10**), together with eight known compounds (**1.2-1.9**), 5,7,4'-trihydroxy-3'-methoxyflavanone (**1.2**) [42], resveratrol (**1.3**) [30], 3-methoxyresveratrol (**1.4**) [30], shegansu B (**1.5**) [35], gnetulin (**1.6**) [29], gnetuhainin C (**1.7**) [8], parvifolol B (**1.8**) [7] and pallidol (**1.9**) [43]. The structures of isolated flavonoids and its derivatives and stilbenoids are summarized in Figure 1.11.

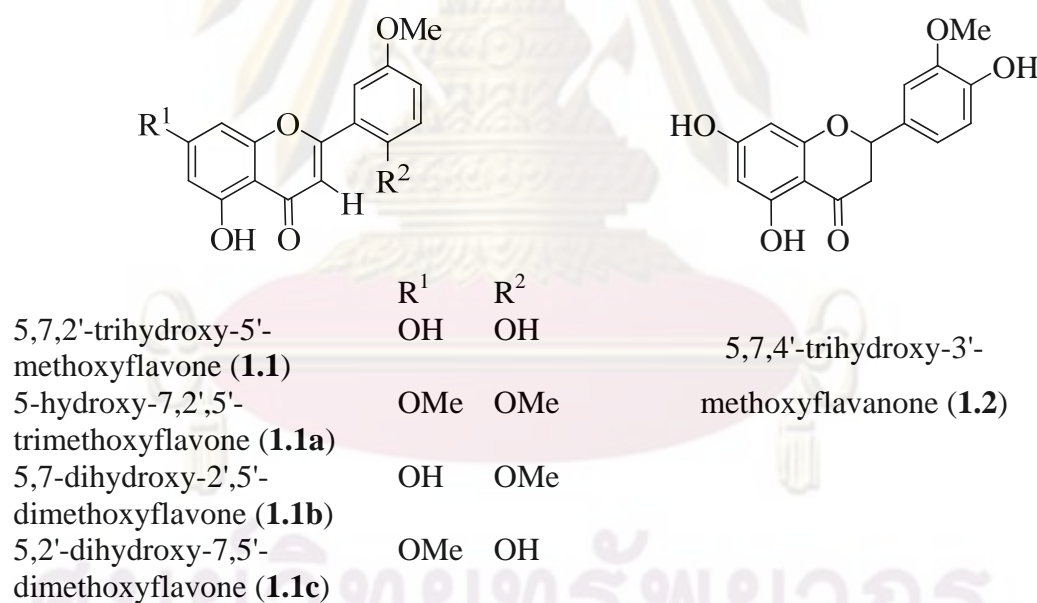
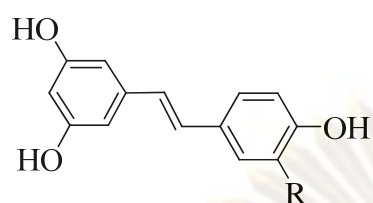


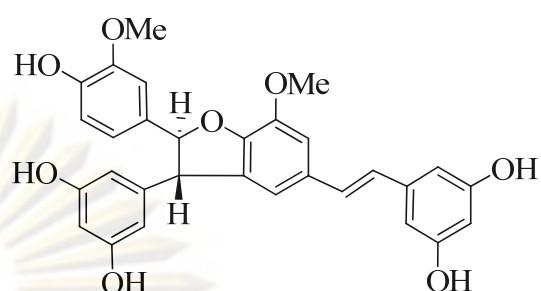
Figure 1.11 Flavonoids and its derivatives and stilbenoids isolated from *G.*

macrostachyum lianas.

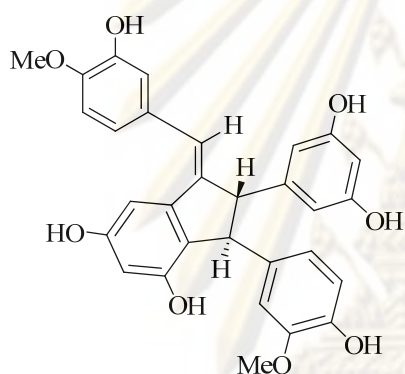


resveratrol (1.3): R = H

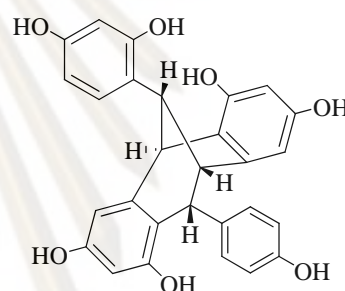
3-methoxyresveratrol (1.4): R = OMe



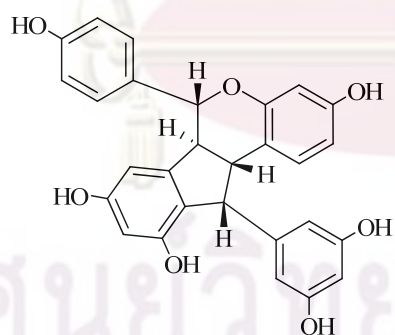
shegansu B (1.5)



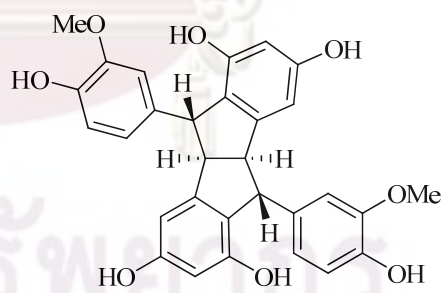
gnetullin (1.6)



gnetuhainin C (1.7)

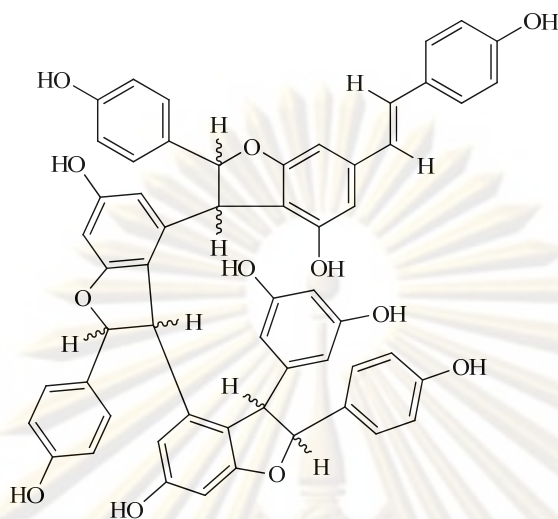


parvifolol B (1.8)



pallidol (1.9)

Figure 1.11 Flavonoids and its derivatives and stilbenoids isolated from *G. macrostachyum lianas* (continued).



stilbenoid tetramer **1.10**

Figure 1.11 Flavonoids and its derivatives and stilbenoids isolated from *G. macrostachyum* lianas (continued).

1.2.2 Properties and structural elucidation of isolated compounds

Structure elucidation of 5,7,2'-trihydroxy-5'-methoxyflavone (**1.1**)

5,7,2'-Trihydroxy-5'-methoxyflavone (**1.1**) was isolated as an amorphous yellow solid [mp 269°C (dec)]. The molecular formula was established to be $C_{16}H_{12}O_6$ based on the $[M+Na]^+$ ion peak at m/z 323.0517 (calcd for $C_{16}H_{12}O_6Na$, 323.0526) and ^{13}C NMR data. The UV spectrum of **1.1** exhibited maximal absorption bands at 270 and 345 nm, which were typical of a flavonoid moiety.

The IR spectrum showed absorptions of hydroxyl group (3347 cm^{-1}), carbonyl group (1647 cm^{-1}), carbon ether bond (1347 cm^{-1}), and aromatic moiety ($1600\text{-}1400\text{ cm}^{-1}$). The 1H NMR spectrum (Fig A-1.1) revealed the singlet resonance of a chelated hydroxyl proton at δ_H 12.90 (5-OH), in addition to a pair of exchangeable hydroxyl

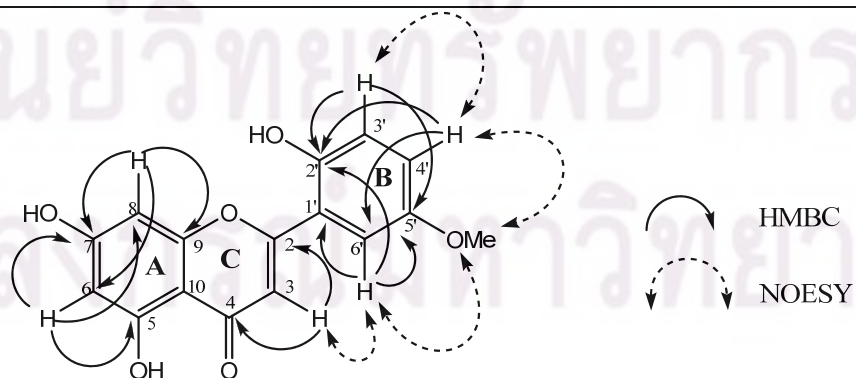
protons (δ_{H} 10.42 and 9.30). The signals in aromatic region (δ_{H} ca 6.0-7.8) was assigned as two isolated spin systems; 6.20 and 6.46 (each 1H, d, $J = 2.0$ Hz) for AB system as well as 6.95 (1H, d, $J = 8.4$ Hz), 7.51 (1H, d, $J = 8.4$ Hz), and 7.53 (1H, brs) for ABX system. The ^{13}C NMR spectrum (Fig A-1.2) showed 16 signals; three of which (δ_{C} 182.1, 164.0 and 103.3) were indicative of a flavone moiety.

The overall structure of **1.1** was deduced based mainly on HMBC data. In ring A, the correlations of 5-OH/C-5, C-6, and C-10 and 7-OH/C-6, C-7, and C-8 indicated that C-5 and C-7 were accommodated by two hydroxyl groups. The methoxy group (δ_{H} 3.95) was placed in ring B at C-5' (δ_{C} 149.3), which was in turn coupled to H-3' and H-6'. This assignment was further confirmed by NOESY cross peaks of 5'-OMe to H-4' and H-6', in addition to those of H-3'/H-4' and H-3/H-6'. The presence of hydroxyl groups was also supported by the formation of methyl ethers of **1.1**. Treatment of **1.1** with TMSCHN₂ yielded **1.1a** as the major product, together with two minor methyl ethers **1.1b** and **1.1c**. Two additional methoxy groups newly generated in **1.1a** indicated the presence of 7-OH and one hydroxyl group on ring B, in addition to the chelated 5-OH. Therefore, the structure of 5,7,2'-trihydroxy-5'-methoxyflavone was depicted for **1.1**.

5, 7, 2'-Trihydroxy-5'-methoxyflavone (1.1) : Amorphous yellow solid : ^1H NMR (acetone-*d*₆, 400 MHz) : δ 12.90 (1H, s, OH-5), 10.42 (1H, s, OH-7), 9.30 (1H, s, OH-2'), 7.53 (1H, brs, H-6'), 7.51 (1H, brd, $J = 8.4$ Hz, H-4'), 6.95 (1H, d, $J = 8.4$ Hz, H-3'), 6.65 (1H, s, H-3), 6.46 (1H, d, $J = 2.0$ Hz, H-8), 6.20 (1H, d, $J = 2.0$ Hz, H-6), 3.93 (3H, s, OMe-5'). ^{13}C NMR (acetone-*d*₆, 100 MHz): δ 182.1 (C-4), 164.2 (C-7), 164.0 (C-2), 162.0 (C-5), 157.8 (C-9), 150.9 (C-2'), 149.3 (C-5'), 122.4 (C-1'), 120.3 (C-4'), 115.7 (C-3'), 109.7 (C-6'), 104.0 (C-10), 103.3 (C-3), 99.0 (C-6), 93.9 (C-8), 55.7 (OMe-5').

Table 1.1 ^1H and ^{13}C NMR spectral data (acetone- d_6) of **1.1**.

Position	δ_{H} (mult, J in Hz)	δ_{C}	HMBC
1			
2		164.0	
3	6.65 (s)	103.3	C-2, 4, 10, 1'
4		182.1	
5		162.0	
6	6.20 (d, 2.0)	99.0	C-5, 7, 8, 10
7		164.2	
8	6.46 (d, 2.0)	93.9	C-6, 7, 9, 10
9		157.8	
10		104.0	
1'		122.4	
2'		150.9	
3'	6.95 (d, 8.4)	115.7	C-1', 2', 5'
4'	7.51 (brd, 8.4)	120.3	C-2', 6'
5'		149.3	
6'	7.53 (brs)	109.7	C-2, 1', 2', 4', 6'
5-OH	12.90 (s)		C-5, 6, 10
7-OH	10.42 (s)		C-6, 7, 8,
2'-OH	9.30 (brs)		
5'-OMe	3.93 (s)	55.7	C-5'

**Figure 1.12** Key HMBC and NOESY correlations of **1.1**

Structure elucidation of the stilbenoid tetramer (1.10)

Compound **1.10** was obtained as a brown amorphous powder. The negative ESIMS exhibited an $[M-H]^-$ ion peak at m/z 905.74 which established the tentative molecular formula as $C_{56}H_{42}O_{12}$, corresponding to a resveratrol tetramer.

The 1H NMR spectrum (Fig A-1.5) showed integrating signals for nine protons from δ 7.98 to 8.45, thus confirming the presence of nine phenolic hydroxyl groups. Furthermore, the 1H NMR spectrum showed eight sets of *ortho*-coupled aromatic protons in A_2B_2 system on the *para*-substituted phenyl moieties, assignable to four 4-hydroxyphenyl groups (rings A_1 , B_1 , C_1 and D_1) and signals from three sets of *meta*-coupled protons in the AB system on 1,3,4,5-tetrasubstituted benzene rings (rings B_2 , C_2 and D_2) and one set of protons in A_2X system on the 1,3,5-trisubstituted benzene ring (ring A_2).

In the HMBC spectral data of ring A, the H-7a (δ 5.34) and H-8a (δ 4.33) proton doublets, one of the three sets methine proton showed correlation with C-2a (6a) and C-10a (14a), respectively. This suggested that C-7a and C-8a were attached to 4-hydroxyphenyl group at C-1a and 3,5-dihydroxyphenyl group at C-9a, respectively. The chemical shifts of H-7a at δ 5.34 and its corresponding carbon at δ 92.8 suggesting that C-7a was attached to dihydrofuran oxygen. Additional HMBC correlations between H-7a and H-8a with the quaternary aromatic carbons C-11b at δ 162.0 and C-9b at δ 145.7 in ring B_2 further indicated that H-7a and H-8a were a part of a dihydrofuran entity. It was further determined that OH-11a (13a) at δ 7.98 shared indicative HMBC correlations with C-10a (14a) at δ 107.5 and OH-4a at δ 8.45 with C-3a (5a) suggested that three hydroxyl groups were attached at C-11a, C-13a and C-4a, respectively.

In the ring B, the H-7b (δ 5.31) and H-8b (δ 4.33) proton doublets showed HMBC correlations with C-2b (6b) and C-10b (14b), respectively. It indicated that C-7b and C-8b were attached to 4-hydroxyphenyl group at C-1b and 3,5-dihydroxyphenyl group at C-9b, respectively. Furthermore, the H-12b (δ 6.20) exhibited HMBC correlations with C-10b, C-11b and C-14b, while the H-14b (δ 6.11) shared HMBC correlations with C-10b and C-12b, thus confirming the attachment of ring B_2 with a dihydrofuran ring. It was further determined that HMBC correlations

between H-7b with C-11c and H-8b with C-9c, confirming the attachment of ring B and ring C with a dihydrofuran ring.

In the ring C, the H-7c (δ 5.21) and H-8c (δ 4.24) proton doublets showed also correlations with C-2c (6c) and C-10c (14c), respectively. It suggested that C-7c and C-8c were attached to 4-hydroxyphenyl group at C-1c and 3,5-dihydroxyphenyl group at C-9c, respectively. In addition, the HMBC correlations between H-8c with C-11d, C-12d and C-13d suggested that the dihydrofuran ring attached between C-11d and C-12d whereas OH-13d showed correlations with C-12d and C-14d, thus confirming the hydroxyl group at C-13d.

In the ring D, the ^1H NMR spectra also exhibited signals at δ 6.82 (d, $J = 16.6$ Hz, H-8d) and δ 6.96 (d, $J = 16.6$ Hz, H-7d) for a set of *trans*-couple olefinic protons in the resveratrol unit. The HMBC correlations between H-7d with C-2d (6d), C-9d and H-8d with C-1d, C-10d (14d) indicated that olefinic carbon attached at C-1d in ring D₁ and C-9d in ring D₂, respectively. Additional HMBC correlation of H-7c with C-11d, while H-8c shared HMBC correlations with C-11d and C-12d confirmed that ring D₂ attached with a dihydrofuran ring at C-11d and C-12d. Furthermore, the hydroxyl group at δ 8.39 (C-4d) showed correlation with C-3d (5d), thus confirming the presence of a hydroxyl group at C-4d. The Key HMBC correlations of **1.10** are shown in Figure 1.13.

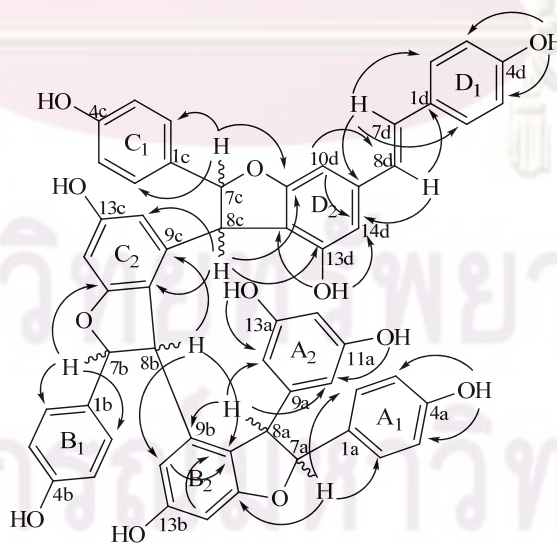


Figure 1.13 Selected HMBC correlations of **1.10**

In addition, the relative stereochemistry of **1.10** could not be assigned from the basis of the analysis of the NOESY NMR spectrum due to the decomposition of this compound. Therefore, the proposed structure of **1.10** is shown in Figure 1.14.

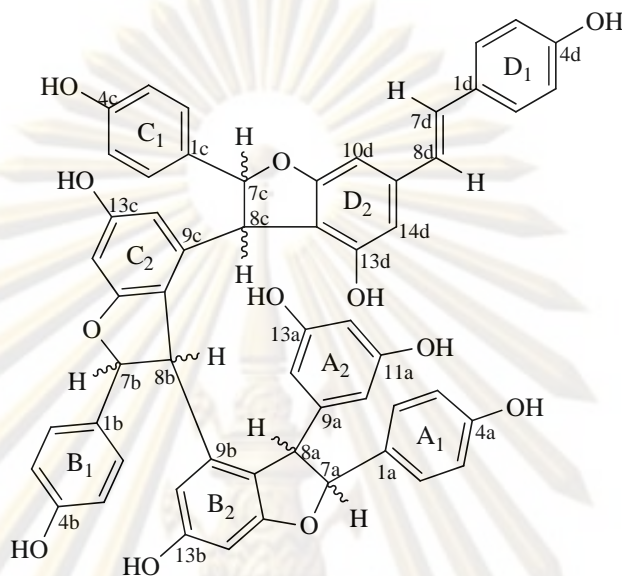


Figure 1.14 The proposed structure of **1.10**.

Table 1.2 ^1H , ^{13}C , HMBC and ^1H - ^1H COSY NMR data of tetramer **1.10** in acetone- d_6

Position	δ_{C}	δ_{H} (mult., J in Hz)	HMBC	COSY
1a	133.8	-	-	-
2a, 6a	126.9	7.10 (d, 8.0)	C-3a, C-4a, C-6a, C-7a	H-3a, H-5a
3a,5a	115.4	6.71 (d, 6.0)	C-1a, C-2a, C-4a	H-2a,6a
4a	157.4	-	-	-
7a	92.8	5.34 (d, 4.4)	C-1a, C-2a, C-6a, C-9a, C-10b, C-11b	H-8a
8a	55.0	4.33 (d, 4.0)	C-1a, C-9a, C-10a,14a, C-9b, C-10b, C-11b	H-7a
9a	145.7	-	-	-
10a, 14a	107.5	6.11 (brs)	C-8a, C-11a,13a, C-12a	H-12a
11a, 13a	154.6	-	-	-
12a	100.2	6.15 (brs)	C-10a,14a, C-11a,13a	H-10a,14a
1b	133.8	-	-	-
2b, 6b	127.1	7.08 (d, 8.4)	C-3b,5b, C-4b, C-7b	H-3b,5b
3b, 5b	115.4 ^a	6.71 ^f (d, 6.0)	C-1b, C-2b,6b, C-4b	H-2b,6b

Table 1.2 ^1H , ^{13}C , HMBC and ^1H - ^1H COSY NMR data of tetramer **1.10** in acetone- d_6 (continued)

Position	δ_{C}	δ_{H} (mult., J in Hz)	HMBC	COSY
4b	157.4 ^b	-	-	-
7b	92.8	5.31 (d, 4.8)	C-1b, C-2b,6b, C-8b, C-9b C-10c, C-11c	H-8b
8b	55.0 ^c	4.33 (d, 4.0)	C-1b, C-7b, C-9b, C- 10b, C-14b, C-10c, C-11c	H-7b
9b	145.7	-	-	-
10b	113.4 ^d	-	-	-
11b	162.0	-	-	-
12b	100.3	6.20 (brs)	C-10b, C-11b, C-14b	-
13b	154.6 ^e	-	-	-
14b	107.5 [*]	6.11 ^g (brs)	C-8b, C-10b, C-12b, C- 13b,	-
1c	132.9	-	-	-
2c, 6c	127.2	7.04 (d, 8.4)	C-7c, C-4c	H-3c,5c
3c, 5c	115.4 ^a	6.71 ^f (d, 6.0)	C-1c, C-2c,6c, C-4c	H-2c,6c
4c	157.4 ^b	-	-	-
7c	92.9	5.21 (d, 5.6)	C-2c,6c, C-8c, C-9c, C- 11d	H-8c
8c	55.1 ^c	4.24 (d, 5.6)	C-1c, C-7c, C-9c, C- 10c, C-14c, C-11d, C-12d, C-13d	H-7c
9c	145.2	-	-	-
10c	113.6 ^d	-	-	-
11c	162.0	-	-	-
12c	101.2	6.09 (brs)	C-10c, C-13c, C-14c	-
13c	158.6 ^e	-	-	-
14c	106.0	6.03 ^g (brs)	C-8c, C-10c, C-13c	-
1d	128.9	-	-	-
2d, 6d	127.9	7.30 (d, 8.4)	C-1d, C-2d,6d, C-4d	H-3d,5d
3d, 5d	115.4	6.71 ^f (d, 6.0)	C-1d, C-2d, C-4d	H-2d,6d
4d	157.4 ^b	-	-	-
7d	129.1	6.96 (d, 16.6)	C-2d,6d, C-8d, C-9d	H-8d
8d	125.9	6.82 (d, 16.6)	C-1d, C-7d, C-9d, C- 10d, C-14d	H-7d
9d	140.5	-	-	-
10d	98.3	6.58 (brs)	C-8d, C-11d, C-12d, C- 14d	H-14d
11d	162.3	-	-	-
12d	114.2	-	-	-
13d	154.5 ^e	-	-	-

Table 1.2 ^1H , ^{13}C , HMBC and ^1H - ^1H COSY NMR data of tetramer **1.10** in acetone- d_6 (continued)

Position	δ_{C}	δ_{H} (mult., J in Hz)	HMBC	COSY
14d	107.3*	6.48 (brs)	C-8d, C-10d, C-12d	H-10d
4a-OH		8.45 (brs)	C-3a,5a	
11a,				
13a-OH		7.98 (brs)	C-10a,14a	
4b-OH		8.39 ^h (brs)	C-3b,5b	
13b-OH		8.11 (brs)	C-12b, C-14b	
4c-OH		8.38 ^h (brs)	C-3c,5c	
13c-OH		8.07 (brs)	C-12c, C-14c	
4d-OH		8.39 (brs)	C-3d,5d	
13d-OH		8.22 (brs)	C-12d, C-14d	

^{a-h} Overlaped

* Data can be interchanged

1.2.3 Antioxidant activity of isolated compounds

Nine isolated compounds (**1.1-1.9**) were subjected to examine for their radical scavenging against DPPH (Table 1.3). Compound **1.1** showed slightly weak activity with IC_{50} value of 19.9 mM. Conversely resveratrol (**1.3**) and other stilbenoids (**1.4-1.9**) displayed stronger inhibition with IC_{50} values in range of 0.21-4.23 mM; of which, gnetulin (**1.6**) was the most active. Stilbenes have been recognized as potent oxygen radical scavengers possibly through oxidative coupling reaction, forming stable oligostilbenes. A recent investigation has shown that stilbenes undergo oxidation by nitrite ions (NO_2^-), a key mediator in the inflammatory response and carcinogenesis [44]. A comprehensive study on radical scavenging of stilbenes towards causative reactive species would provide an insight into prevention of pathological diseases.

Table 1.3. Antioxidant activity of nine isolated compounds (1.1-1.9)

Test compound	DPPH radical scavenging (IC ₅₀ , mM)
5,7,2'-trihydroxy-5'-methoxyflavone (1.1)	19.9
5,7,4'-trihydroxy-3'-methoxyflavanone (1.2)	1.48
resveratol (1.3)	0.40
3-methoxyresveratol (1.4)	0.30
shegansu B (1.5)	0.78
gnetulin (1.6)	0.21
gnetuhainin C (1.7)	2.90
parvifolol B (1.8)	4.23
pallidol (1.9)	0.53
ascorbic acid*	0.11

* Standard antioxidant

ศูนย์วิทยทรัพยากร
จุฬาลงกรณ์มหาวิทยาลัย

1.3 Experimental section

1.3.1 Plant material

The lianas of *G. macrostachyum* were collected in April 2006 from Nakornphanom. The plant material was identified by the Plants of Thailand Research Unit, Department of Botany, Faculty of Science, Chulalongkorn University, and the voucher specimen (BKF 108547) has been deposited in the herbarium of Royal Forest Department, Bangkok, Thailand.

1.3.2 General experimental procedures

NMR spectra were recorded with a Varian model Mercury⁺ 400 operated at 400 MHz for ¹H and 100 MHz for ¹³C nuclei. The chemical shift in δ (ppm) was assigned with reference to the signal from the residual protons in deuterated solvents and using TMS as an internal standard in some cases. Most solvents used in this research were commercial grade and were distilled prior to use. Adsorbents such as silica gel 60 Merck cat. No. 7731, 7734 and 7749 were used for quick column chromatography, open column chromatography and radial thin layer chromatography, respectively. Thin-layer chromatography (TLC) was performed on precoated Merck silica gel 60 F254 plates (0.25 mm thick layer). ESIMS data were obtained from a mass spectrometer model VG TRIO 2000. High resolution mass spectra were recorded by Micromass LCT and Bruker MICROTOF models. UV-visible absorption spectra were recorded on a UV-2552PC UV-Vis spectrometer, a UV-spectrometer, microtiter plate reader, model sunrise.

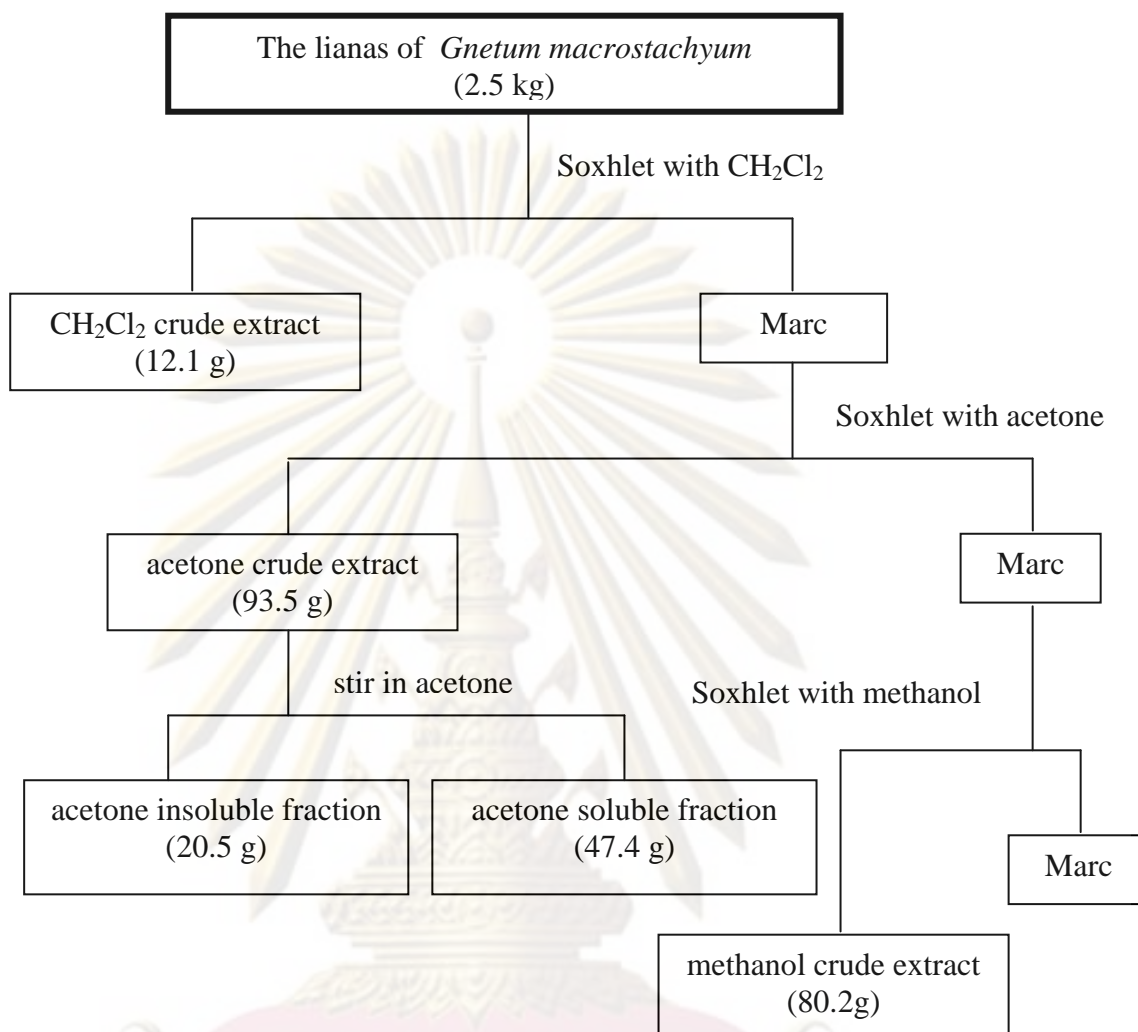
1.3.3 Extraction and purification

The dried and powdered lianas of *G. macrostachyum* (2.5 kg) were extracted successively in a Soxhlet extractor with CH₂Cl₂, acetone, and MeOH, respectively. A part of the acetone extract was stirred with acetone, yielding acetone soluble and insoluble fractions. The acetone soluble fraction (47.4 g) was fractionated on vacuum liquid chromatography (VLC) eluted with CH₂Cl₂, MeOH-CH₂Cl₂ (10:90 → 50:50),

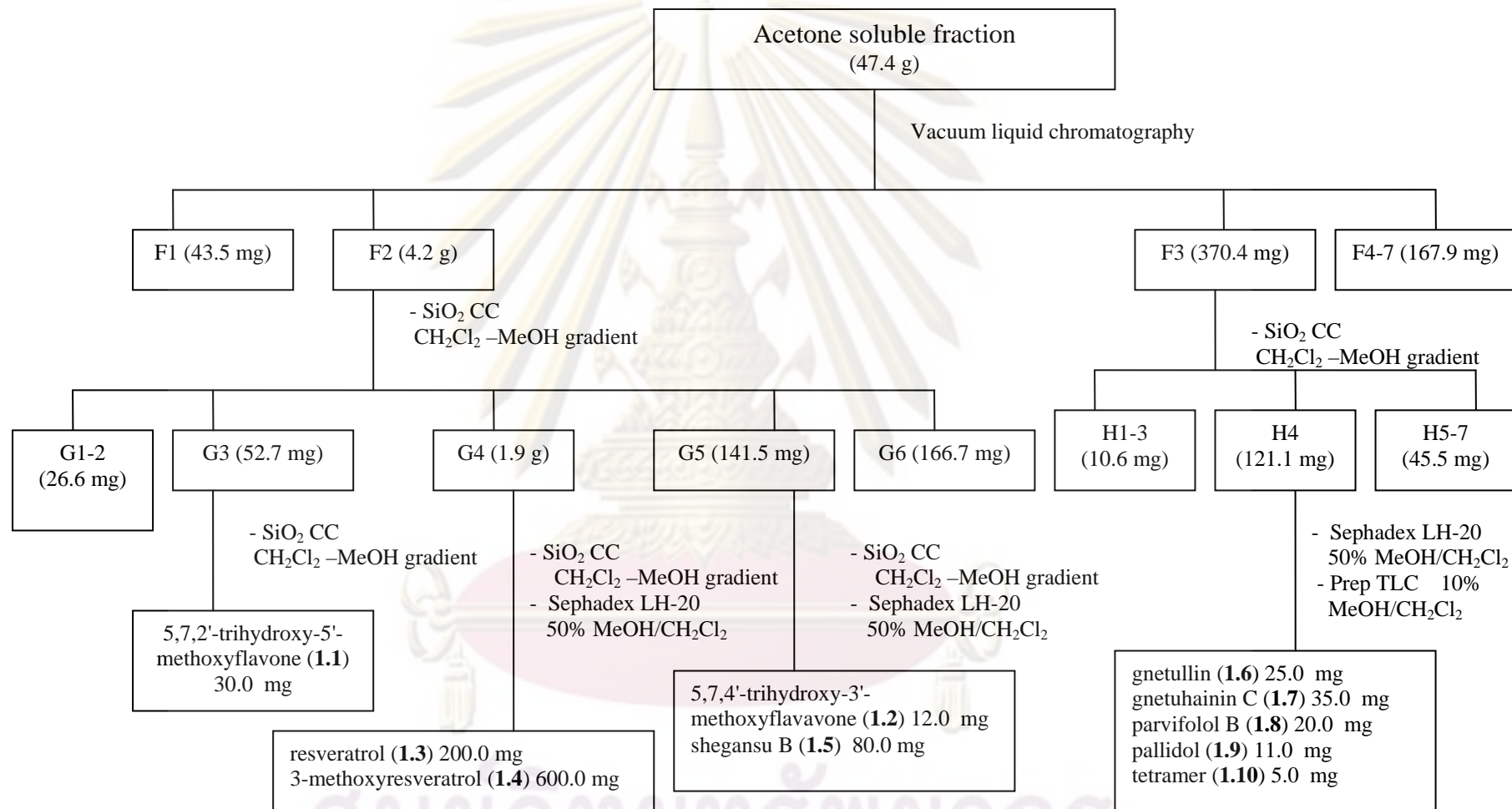
and MeOH, yielding seven fractions (F1-F7). Fraction F2 was purified on silica gel CC using CH_2Cl_2 , MeOH- CH_2Cl_2 (5:95 \rightarrow 50:50), and MeOH to afford six fractions (G1-G6). Fraction G3 was subsequently purified on silica gel CC using MeOH- CH_2Cl_2 (0:100 \rightarrow 100:0) to afford 5,7,2'-trihydroxy-5'-methoxyflavone (**1.1**, 30.0 mg). A portion of fraction G4 (21 g) was purified on silica gel CC using CH_2Cl_2 and MeOH- CH_2Cl_2 (0:100 \rightarrow 100:0) and further purified on a Sephadex LH 20 column using MeOH- CH_2Cl_2 (50:50) to give resveratrol (**1.3**, 200.0 mg) and 3-methoxyresveratrol (**1.4**, 600.0 mg). Fraction G5 was purified on silica gel CC using CH_2Cl_2 , MeOH- CH_2Cl_2 (0:100 \rightarrow 100:0), and further purified on a Sephadex LH 20 column using MeOH- CH_2Cl_2 (50:50) to yield 5,7,4'-trihydroxy-3'-methoxyflavanone (**1.2**, 12.0 mg) and shegansu B (**1.5**, 80.0 mg). Fraction F3 was purified on silica gel CC using CH_2Cl_2 , MeOH- CH_2Cl_2 (5:95 \rightarrow 50:50), and MeOH to afford seven fractions (H1-H7). Fraction H4 was purified on a Sephadex LH 20 column using MeOH- CH_2Cl_2 (50:50) and further purified by preparative TLC using 10% MeOH- CH_2Cl_2 to afford gnetulin (**1.6**, 25.0 mg), gnetuhainin C (**1.7**, 35.0 mg), parvifolol B (**1.8**, 20.0 mg), pallidol (**1.9**, 11.0 mg), and a stilbenoid tetramer (**1.10**, 5.0 mg). The extraction and isolation procedures of all isolated compounds were shown in Schemes 1.1 and 1.2.



ศูนย์วิจัยทรัพยากร
จุฬาลงกรณ์มหาวิทยาลัย



Scheme 1.1 The extraction procedure of *G. macrostachyum* lianas



Scheme 1.2 The isolation procedure of the acetone soluble fraction.

5,7,2'-Trihydroxy-5'-methoxyflavone (1.1) : Amorphous yellow solid; mp 269 °C (dec) ; UV (MeOH) λ_{\max} (log ϵ) 227 (3.09), 270 (2.93), 345 (3.06) ; IR (KBr) 3347, 3082, 1647, 1621, 1517, 1347, 1269, 1204, 1165, 826 cm^{-1} ; HRESIMS m/z $[\text{M}+\text{Na}]^+$ 323.0517 (calcd for $\text{C}_{16}\text{H}_{12}\text{O}_6\text{Na}$, 323.0526) ^1H NMR ($\text{DMSO-}d_6$, 400 MHz) and ^{13}C NMR ($\text{DMSO-}d_6$, 100 MHz) see Table 1.1.

Preparation of methyl ethers of 5,7,2'-trihydroxy-5'-methoxyflavone (1.1)

5,7,2'-Trihydroxy-5'-methoxyflavone **1.1** (10.0 mg) dissolved in MeOH (2 mL) was added dropwise 2.0 M trimethylsilyldiazomethane (TMSCHN_2) in hexane until yellow solution persisted. The mixture was stirred at room temperature for 1 h. After the reaction mixture was evaporated to dryness, the residue was purified on preparative TLC developed with MeOH- CH_2Cl_2 (5:95) to afford 5-hydroxy-7,2',5'-trimethoxyflavone **1.1a** (7.0 mg), 5,7-dihydroxy-2',5'-dimethoxyflavone **1.1b** (2.0 mg) and 5,2'-dihydroxy-7,5'-dimethoxyflavone **1.1c** (2.0 mg).

5-hydroxy-7,2',5'-trimethoxyflavone **1.1a**: yellow powder; ^1H NMR (CDCl_3) δ 12.90 (1H, OH-5), 7.55 (1H, d, $J = 8.4$ Hz, H-4'), 7.50 (1H, s, H-6'), 7.03 (1H, d, $J = 8.4$ Hz, H-3'), 6.60 (1H, s, H-3), 6.43 (1H, d, $J = 2.0$ Hz, H-8), 6.13 (1H, d, $J = 2.0$ Hz, H-6), 3.86 (3H, s, OMe-5'), 3.84 (3H, s, OMe-2'), 3.79 (3H, s, OMe-7).

5,7-dihydroxy-2',5'-dimethoxyflavone **1.1b**: yellow powder; ^1H NMR (CDCl_3) δ 12.90 (1H, OH-5), 7.60 (1H, d, $J = 8.4$ Hz, H-4'), 7.50 (1H, s, H-6'), 7.05 (1H, d, $J = 8.4$ Hz, H-3'), 6.65 (1H, s, H-3), 6.60 (1H, d, $J = 2.0$ Hz, H-8), 6.20 (1H, d, $J = 2.0$ Hz, H-6), 3.82 (3H, s, OMe-5'), 3.80 (3H, s, OMe-2').

5,2'-dihydroxy-7,5'-dimethoxyflavone **1.1c**: yellow powder; ^1H NMR (CDCl_3) δ 12.90 (1H, OH-5), 7.55 (1H, s, H-6'), 7.50 (1H, d, $J = 8.4$ Hz, H-4'), 6.90 (1H, d, $J = 8.4$ Hz, H-3'), 6.65 (1H, s, H-3), 6.59 (1H, d, $J = 2.0$ Hz, H-8), 6.20 (1H, d, $J = 2.0$ Hz, H-6), 3.85 (3H, s, OMe-5'), 3.80 (3H, s, OMe-7).

5,7,4'-Trihydroxy-3'-methoxyflavanone (1.2) : Amorphous yellow solid; ^1H NMR (CD_3COCD_3 , 400 MHz): δ 12.06 (1H, s, OH-5), 9.53 (1H, s, OH-7), 7.68 (1H, s, OH-4'), 7.06 (1H, s, H-2'), 6.86 (1H, s, H-6'), 6.73 (1H, s, H-5'), 5.84 (1H, d, $J = 4.8$ Hz,

H-8), 5.82 (1H, d, $J = 4.8$ Hz, H-7), 5.30 (1H, dd, $J = 13.2, 2.4$ Hz, H-2), 3.75 (3H, s, OMe-3'), 3.10 (1H, brs, H- α), 2.58 (1H, d, $J = 17.2, 2.4$ Hz, H- β). ^{13}C NMR (CD_3COCD_3 , 100 MHz): δ 198.0 (C-4), 165.0 (C-5), 163.0 (C-9), 147.0 (C-3'), 146.0 (C-4'), 130.0 (C-1'), 119.0 (C-8'), 114.5 (C-5'), 110.5 (C-2'), 102.0 (C-10), 96.0 (C-6), 95.0 (C-8), 79.5 (C-2), 55.3 (OMe-3'), 42.8 (C-3).

Resveratrol (1.3): white crystals; ^1H NMR (CD_3COCD_3 , 400 MHz): δ 7.41 (2H, d, $J = 8.0$ Hz, H-2', 6'), 7.01 (1H, d, $J = 16.4$ Hz, H- β), 6.88 (1H, d, $J = 16.4$ Hz, H- α), 6.83 (2H, d, $J = 8.4$ Hz, H-3', 5'), 6.53 (2H, d, $J = 2.0$ Hz, H-2, 6), 6.26 (1H, d, $J = 2.0$ Hz, H-4). ^{13}C NMR (CD_3COCD_3 , 100 MHz): δ 159.4 (C-3, 5), 158.5 (C-4'), 140.9 (C-1), 130.5 (C-1'), 129.3 (C- β), 128.9 (C-2', 6'), 127.8 (C- α), 116.5 (C-3', 5'), 105.7 (C-2, 6), 103.1 (C-4).

3-Methoxyresveratrol (1.4): Brown oil; ^1H NMR (CD_3COCD_3 , 400 MHz): δ 8.35 (2H, brs, OH-3', 5'), 7.80 (1H, brs, OH-4), 7.20 (1H, brs, H-2), 7.02 (1H, d, $J = 16.4$ Hz, H- α), 7.01 (1H, brd, $J = 6.4$ Hz, H-6), 6.91 (1H, d, $J = 16.4$ Hz, H- β), 6.83 (1H, d, $J = 8.0$ Hz, H-5), 6.51 (2H, brd, $J = 1.8$ Hz, H-2', 6'), 6.30 (1H, brt, $J = 1.6$ Hz, H-4'), 3.88 (3H, s, OMe-3). ^{13}C NMR (CD_3COCD_3 , 100 MHz): δ 158.7 (C-3', 5'), 147.7 (C-3), 146.7 (C-4), 140.0 (C-1'), 129.6 (C-1), 128.6 (C- α), 126.2 (C- β), 120.3 (C-6), 114.1 (C-5), 109.3 (C-2), 104.8 (C-2', 6'), 101.8 (C-4'), 55.4 (OMe-3).

Shigansu B (1.5): brown amorphous powder; ^1H NMR (CD_3COCD_3 , 400 MHz): δ 8.36 (2H, s, OH-11a, 13a), 8.35 (2H, s, OH-11b, 13b), 7.80 (1H, s, OH-4a), 7.18 (1H, s, H-2b), 7.05 (1H, s, H-6a), 7.04 (1H, d, $J = 16.4$ Hz, H-7b), 6.94 (1H, d, $J = 16.4$ Hz, H-8b), 6.85 (1H, brs, H-2a), 6.84 (1H, brs, H-6b), 6.83 (1H, brs, H-5a), 6.54 (2H, d, $J = 2.2$ Hz, H-10b, 14b), 6.28 (1H, t, $J = 2.2$ Hz, H-12a), 6.26 (1H, t, $J = 2.2$ Hz, H-7a), 6.21 (2H, d, $J = 2.2$ Hz, H-10a, 14a), 5.45 (1H, d, $J = 8.8$ Hz, H-7a), 4.53 (1H, d, $J = 8.8$ Hz, H-8a), 3.90 (3H, s, OMe-3b), 3.80 (3H, s, OMe-3a). ^{13}C NMR (CD_3COCD_3 , 100 MHz): δ 158.8 (C-11a, C-13a), 158.6 (C-11b, C-13b), 148.2 (C-4b), 147.5 (C-3a), 146.6 (C-4a), 144.5 (C-3b), 144.0 (C-5b), 139.8 (C-9a, 9b), 131.7 (C-1b), 131.6 (C-1a), 128.4 (C-7b), 126.5 (C-8b), 119.3 (C-2a), 115.7 (C-6b), 114.8 (C-5a), 110.5

(C-2b), 109.8 (C-6a), 106.6 (C-10a, 14a), 104.8 (C-10b, 14b), 101.8 (C-12b), 101.5 (C-12a), 93.6 (C-7a), 57.1 (C-8a), 55.4 (OMe-3b), 55.3 (OMe-3a).

Gnetulin (1.6): brown amorphous powder; ^1H NMR (CD_3COCD_3 , 400 MHz): δ 8.16 (1H, s, OH-13a), 8.08 (2H, s, OH-11b, 13b), 7.79 (1H, s, OH-11a), 7.46 (1H, s, OH-4a), 7.17 (1H, s, OH-4b), 6.92 (1H, s, OH-7a), 6.76 (1H, d, $J = 1.6$ Hz, H-2a), 6.72 (1H, dd, $J = 8.0, 1.6$ Hz, H-6a), 6.66 (1H, d, $J = 1.6$ Hz, H-14a), 6.61 (1H, d, $J = 1.6$ Hz, H-2b), 6.56 (1H, d, $J = 8.1$ Hz, H-5a), 6.51 (1H, d, $J = 8.0$ Hz, H-5b), 6.36 (1H, dd, $J = 8.0, 1.6$ Hz, H-6b), 6.21 (2H, d, $J = 1.6$ Hz, H-10b, 14b), 6.17 (1H, d, $J = 2.0$ Hz, H-12a), 6.07 (1H, brs, H-12b), 4.14 (1H, brs, H-7b), 4.06 (1H, brs, H-8b), 3.59 (3H, s, OMe-3a), 3.44 (3H, s, OMe-3a). ^{13}C NMR (CD_3COCD_3 , 100 MHz): δ 158.9 (C-11b, C-13b), 158.8 (C-13a), 155.0 (C-11a), 148.2 (C-9b), 147.16 (C-3b), 147.11 (C-3a), 146.4 (C-9a), 145.7 (C-4a), 144.8 (C-4b), 141.8 (C-8a), 137.5 (C-1b), 129.2 (C-1a), 123.5 (C-10a), 122.9 (C-6a), 122.3 (C-7a), 119.0 (C-6b), 114.6 (C-5a, 5b), 111.1 (C-2a), 110.7 (C-2b), 105.3 (C-10b, 14b), 102.8 (C-12a), 100.6 (C-12b), 97.4 (C-14a), 59.7 (C-8b), 57.0 (C-7b), 55.2 (OMe-3a), 55.3 (OMe-3b).

Gnetuhainin C (1.7): brown amorphous powder; ^1H NMR (CD_3COCD_3 , 400 MHz): δ 8.13 (1H, s, OH-4a), 8.02 (1H, brs, OH-13a), 8.00 (2H, s, OH-2b, 13b), 7.95 (1H, s, OH-4b), 7.80 (1H, s, OH-11a), 7.37 (1H, s, OH-11b), 6.95 (2H, d, $J = 8.4$ Hz, H-2a, 6a), 6.57 (2H, d, $J = 8.4$ Hz, H-3a, 5a), 6.46 (1H, d, $J = 1.6$ Hz, H-14a), 6.42 (1H, d, $J = 2.4$ Hz, H-6b), 6.30 (1H, d, $J = 2.0$ Hz, H-14b), 6.14 (1H, d, $J = 2.4$ Hz, H-3b), 6.00 (1H, d, $J = 8.4$ Hz, H-12b), 5.90 (1H, d, $J = 2.0$ Hz, H-12a), 5.88 (1H, dd, $J = 8.4, 2.4$ Hz, H-5b), 4.04 (1H, brs, H-7a), 3.99 (3H, s, OMe-8b), 3.77 (3H, s, OMe-7b), 3.25 (1H, brs, H-2a). ^{13}C NMR (CD_3COCD_3 , 100 MHz): δ 157.3 (C-13a), 156.9 (C-11b), 156.3 (C-2b, 13b), 156.1 (C-4b), 155.1 (C-4a), 152.4 (C-11a), 147.7 (C-9a), 147.3 (C-9b), 137.5 (C-1a), 129.1 (C-2a), 128.1 (C-6b), 127.0 (C-10a), 120.7 (C-1b), 114.5 (C-3a, 5a), 112.5 (C-10b), 105.5 (C-5b), 104.8 (C-14b), 102.7 (C-14a), 102.0 (C-3b), 100.8 (C-12a), 100.7 (C-12b), 54.7 (C-8a), 48.5 (C-8b), 46.3 (C-7a), 44.3 (C-7b).

Parvifolol B (1.8): brown amorphous powder; ^1H NMR (CD_3COCD_3 , 400 MHz): δ 8.46 (1H, s, OH-4a), 8.24 (1H, s, OH-4b), 8.17 (2H, s, OH-11b, 13b), 7.99 (1H, s, OH-13a), 7.18 (2H, d, $J = 8.4$ Hz, H-2a, 6a), 6.84 (2H, d, $J = 8.4$ Hz, H-3a, 5a), 6.76 (1H, s, OH-11a), 6.64 (1H, d, $J = 8.4$ Hz, H-6b), 6.32 (1H, m, H-3b), 6.32 (1H, m, H-5b), 6.29 (2H, brs, H-10b, 14b), 6.29 (1H, brs, H-12b), 6.12 (1H, d, $J = 2.0$ Hz, H-12a), 5.58 (1H, d, $J = 1.2$ Hz, H-14a), 4.66 (1H, d, $J = 8.8$ Hz, H-7a), 4.14 (1H, d, $J = 8.0$ Hz, H-8b), 3.54 (1H, m, H-8a), 3.52 (1H, m, H-7b). ^{13}C NMR (CD_3COCD_3 , 100 MHz): δ 158.4 (C-11b), 157.5 (C-11a), 157.1 (C-4a), 156.6 (C-13b), 156.4 (C-4b), 155.4 (C-2b), 154.0 (C-13a), 146.4 (C-9b), 130.9 (C-1a), 130.0 (C-6b), 129.2 (C-2^a, 6a), 121.7 (C-10a), 115.7 (C-1b), 114.7 (C-3a, 5a), 108.2 (C-3b, 12b), 104.5 (C-14a), 104.7 (C-14a), 102.8 (C-5b, 14b), 101.9 (C-12a), 100.8 (C-10b), 78.2 (C-7a), 56.3 (C-8b), 49.5 (C-7b), 48.3 (C-8a).

Pallidol (1.9): brown amorphous powder; ^1H NMR (CD_3COCD_3 , 400 MHz): δ 8.09 (2H, s, OH-2, 8), 7.82 (2H, s, OH-4, 10), 7.28 (2H, s, OH-4', 4''), 6.80 (2H, s, OH-6', 6''), 6.64 (2H, d, $J = 8.0$ Hz, H-3', 3''), 6.61 (2H, brs, H-1, 7), 6.51 (2H, d, $J = 8.0$ Hz, H-2', 2''), 6.17 (2H, d, $J = 1.6$ Hz, H-3, 9), 4.54 (2H, brs, H-5, 11), 3.83 (2H, brs, H-6, 12), 3.75 (6H, s, OMe-5', 5''). ^{13}C NMR (CD_3COCD_3 , 100 MHz): δ 158.4 (C-2, 8), 154.2 (C-4, 10), 149.5 (C-6a, 12a), 147.0 (C-5', 5''), 144.6 (C-4', 4''), 137.4 (C-1', 1''), 122.0 (C-4a, 10a), 119.4 (C-2', 2''), 114.4 (C-3', 3''), 111.2 (C-6', 6''), 102.5 (C-1, 7), 101.6 (C-3, 9), 59.6 (C-6, 12), 55.3 (OMe-5', 5''), 53.6 (C-5, 11).

Stilbenoid tetramer 1.10: brown amorphous powder; negative ion ESIMS m/z : 905.74 $[\text{M}-\text{H}]^-$; ^1H NMR (CD_3COCD_3 , 400 MHz) and ^{13}C NMR (CD_3COCD_3 , 100 MHz) see Table 1.2.

1.3.4 DPPH Radical scavenging activity

There are several methods or models to determine the antioxidative properties of the compounds. DPPH was selected in activity directed fractionation of free radical scavenging activity because it is rapid, convenient, reliable, inexpensive, sensitive,

and require little material. DPPH is classified as nitrogen centered radical and stable at room temperature because it has virtual of the delocalization of the spare electron over the molecule. The radical scavenging of plant extracts against stable DPPH was determined spectrophotometrically. DPPH radical reacts with antioxidant compound which can donate hydrogen. Antioxidants scavenging DPPH radical by converting DPPH to DPPHn (2,2-diphenyl-1-picrylhydrazine). The changing of color (from deep violet to light yellow) was measured at 517 nm on a visible light spectrophotometer. Radical scavenging activity is reported in term of IC₅₀ (inhibition concentration at 50 %) (Figure 1.15) [45].

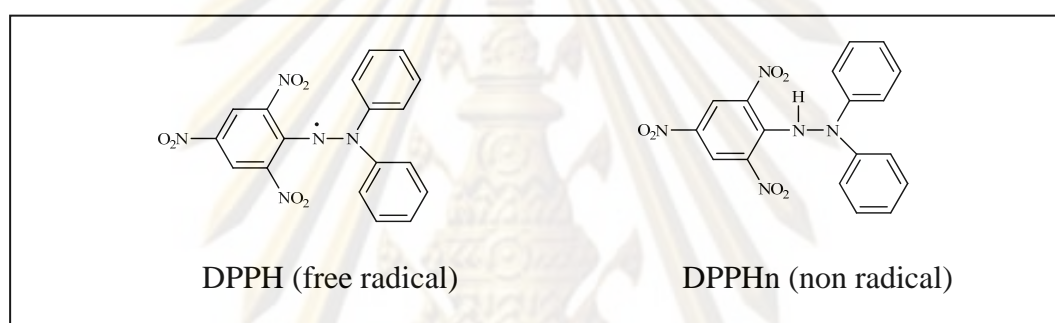


Figure 1.15 Structures of DPPH and DPPHn

After isolation and purification, activities of pure compounds were quantified in this assay. Various concentrations of sample dissolved in methanolic solution (50 μ L) were added to DPPH radical methanolic solution (0.3 mM, 200 μ L). After 30 minutes incubation at room temperature in the dark, the absorbance was measured at 517 nm with a UV-Vis spectrophotometer. All tests were run in triplicate and the data were averaged. The scavenging activity was evaluated from the decreased value of 517 nm absorption, which was calculated by the following equation.

$$\% \text{ Radical scavenging} = [1 - (A_{\text{sample}}/A_{\text{blank}})] \times 100$$

The activities was shown as IC₅₀ values that the concentration of sample required scavenging 50% DPPH free radicals.

CHAPTER II

BIOACTIVE COMPOUNDS FROM THE ROOTS OF *Alangium salviifolium*

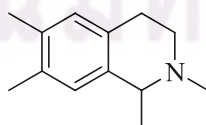
2.1 Introduction

The genus *Alangium* consists of trees and shrubs which are found in the old world tropics throughout India and Southeast Asia. The genus *Alangium* has been recognized as a rich source of various metabolites including alkaloids, iridoids, flavonoids and terpenoids. The major phytochemical constituents of this genus was alkaloids which were also found in the other plants of Rubiaceae family. The alkaloids have been tested for various pharmacological activity such as antimicrobial activity, anticancer agent [46], cytotoxicity activity [47], antifertility activity [48] and antibacterial activity [49]. Moreover, the alkaloids can also serve as agents capable of mediating DNA cleavage and useful for clinical antitumor drugs.

2.1.1 Chemical constituents from *Alangium* species and their biological activities.

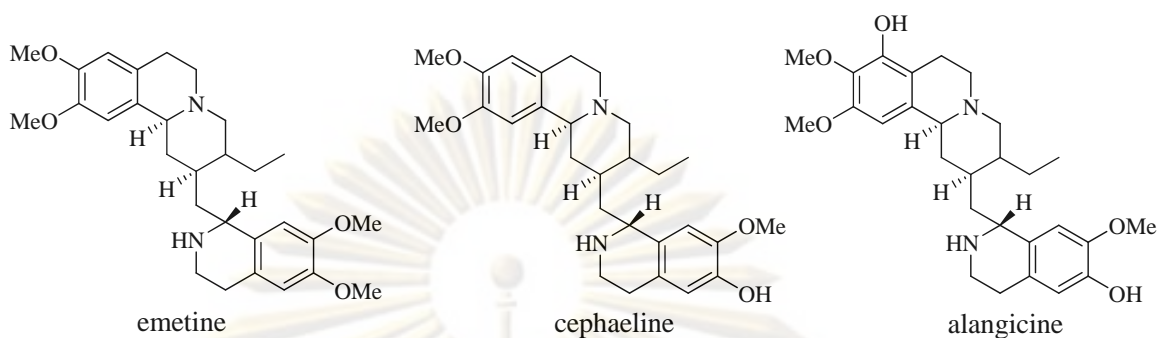
Phytochemical studies on the genus *Alangium* resulted in the isolation of several alkaloids, flavonoid glycosides, phenolic compounds, megastigmane glycoside, iridoid glucoside and xyloglucosides of some alcohols. This genus is also known to be rich in alkaloids. Alkaloids have a complex structures and limited distribution in the plant kingdom. Among the large number of alkaloids containing an isoquinoline nucleus, there are a small group of alkaloids characterized by an isoquinoline portion and a portion of monoterpene origin. The most previous known alkaloids in this genus belong to four types as followed.

1. Benzoquinolizidine is a typical skeleton of tetrahydroisoquinoline.

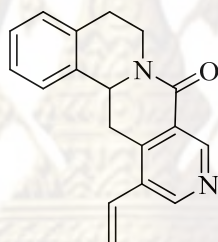


tetrahydroisoquinoline skeleton

The alkaloids bearing this skeleton are emetine, cephaeline and alangiside.

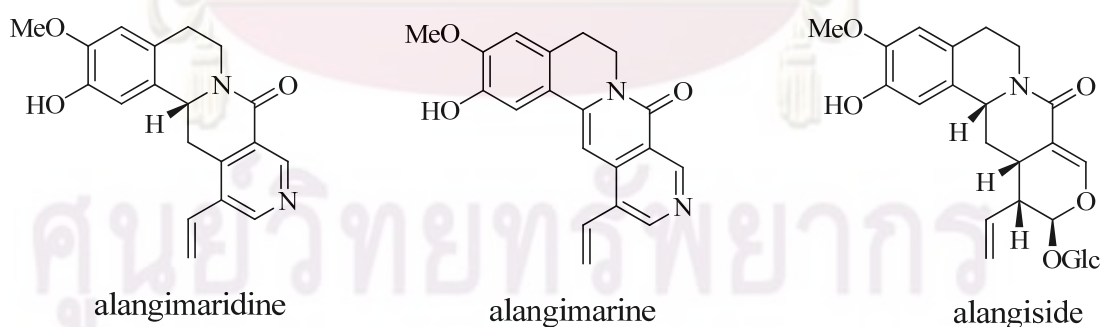


2. Benzopyridoquinolizine is a typical skeleton of tetrahydroisoquinoline connecting with a pyridine ring.

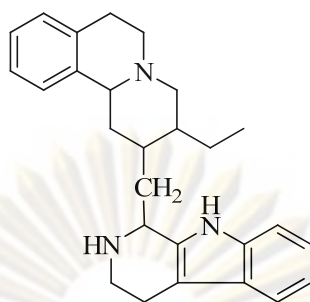


benzopyridoquinolizine skeleton

The alkaloids in this type are alangimaridine, alangimarine and alangiside.

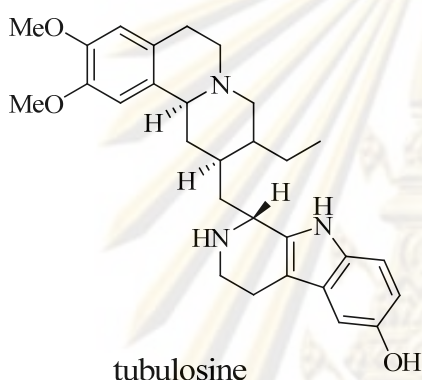


3. Indolobenzoquinolizidine is a hybrid structure of an isoquinoline and a β -carboline moiety.

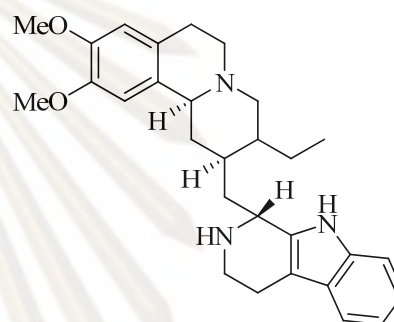


indolobenzoquinolizidine

The alkaloids in this type are tubulosine and deoxytubulosine.

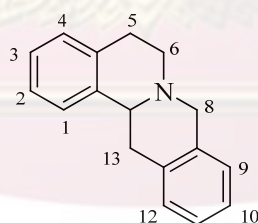


tubulosine



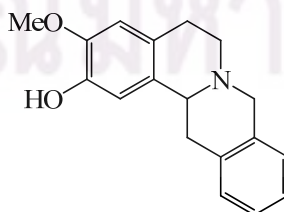
deoxytubulosine

4. Tetrahydroprotoberberine is the tetracyclic structure such as a unique tetrahydroisoquinoline monoterpene alkaloid.



tetrahydroprotoberberine skeleton

The alkaloids in this type almostly are substituted at C-2 and C-3 such as bharatamine.



bharatamine

Emetine is a typical member of the alkaloid which is considered to be derived biosynthetically from two molecules of dopamine and the monoterpene glycoside secologanin. In plants, emetine occurs together with a number of structurally related alkaloids such as cephaeline, alangiside and tubulosine. The proposed biosynthetic pathway of them is shown in Figure 2.1 [50].

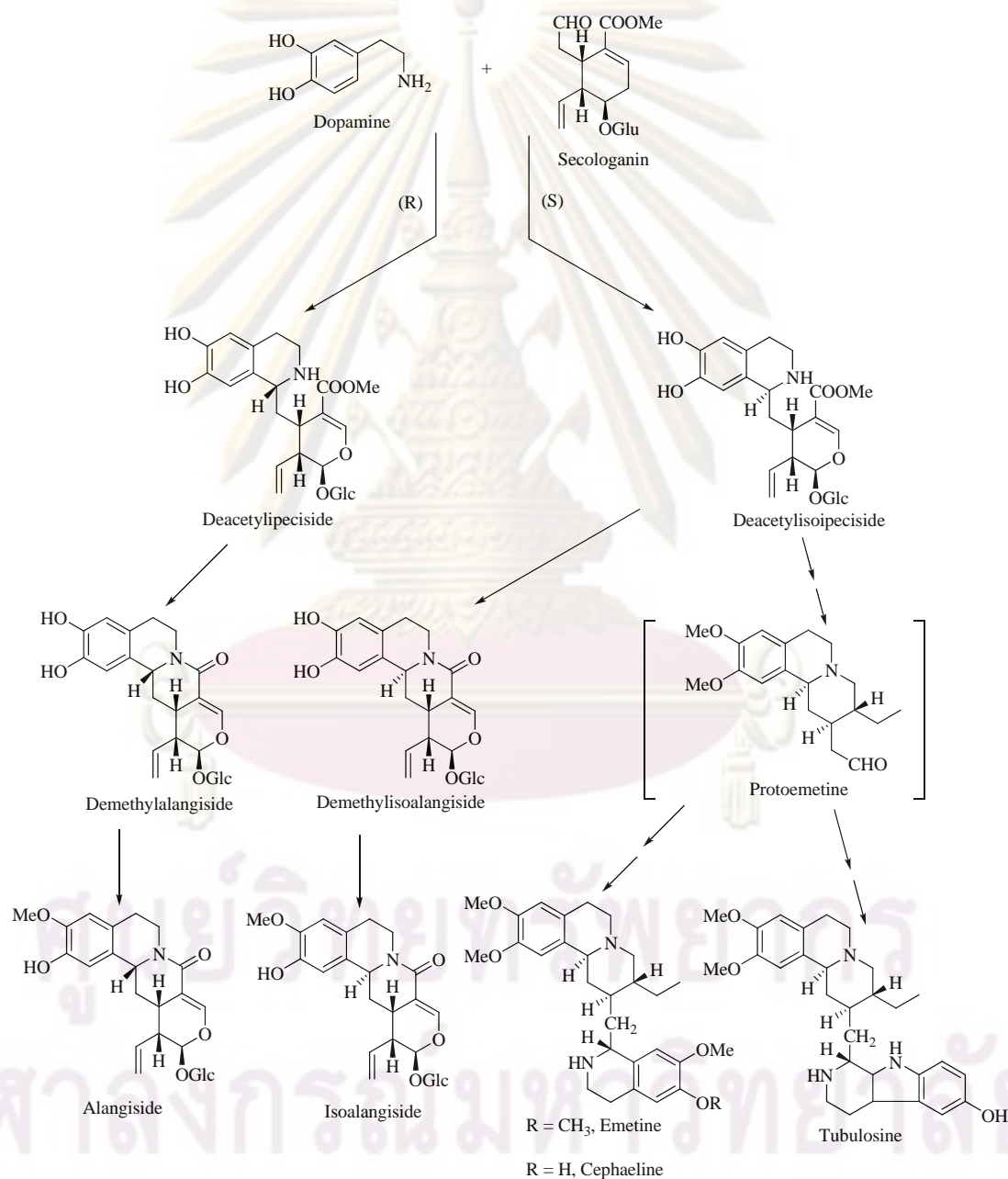
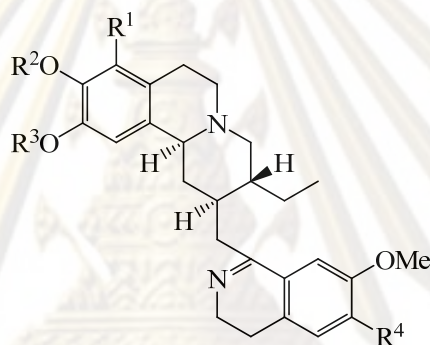


Figure 2.1 Proposed biosynthesis sequence of the alkaloids and nitrogenous glucosides in *Alangium lamarckii*.

The alangium alkaloids were isolated from various parts of *Alangium lamarckii* because this plant is a traditional plant in India. It used as anthelmintic, purgative, emetic and febrifuge and for the treatment of leprosy and other skin disease. Recently, the leaves extract of *A. lamarckii* has shown mild adrenolytic, antispasmodic, hypotensive and anticholinesterase activity [51]. In addition, it has also shown biphasic action on blood pressure of intact cats.

The root bark of *A. lamarckii* was isolated to give cephaeline, emetine, psychotrine, tubulosine, demethyltubulosine, isotubulosine, demethylpsychotrine and alangicine [52]. All of these structures are summarized in Figure 2.2.



psychotrine ; $R^1 = H, R^2 = R^3 = R^4 = OMe$

demethylpsychotrine ; $R^1 = H, R^2 = OH, R^3 = R^4 = OMe$

alangicine ; $R^1 = OH, R^2 = R^3 = R^4 = OMe$

emetine ; $R^1 = H, R^2 = R^3 = R^4 = OMe$

cephaeline ; $R^1 = R^4 = H, R^2 = R^3 = OMe$

Figure 2.2 Benzoquinolizidine and indolobenzoquinolizidine alkaloids from the root bark of *A. lamarckii*.

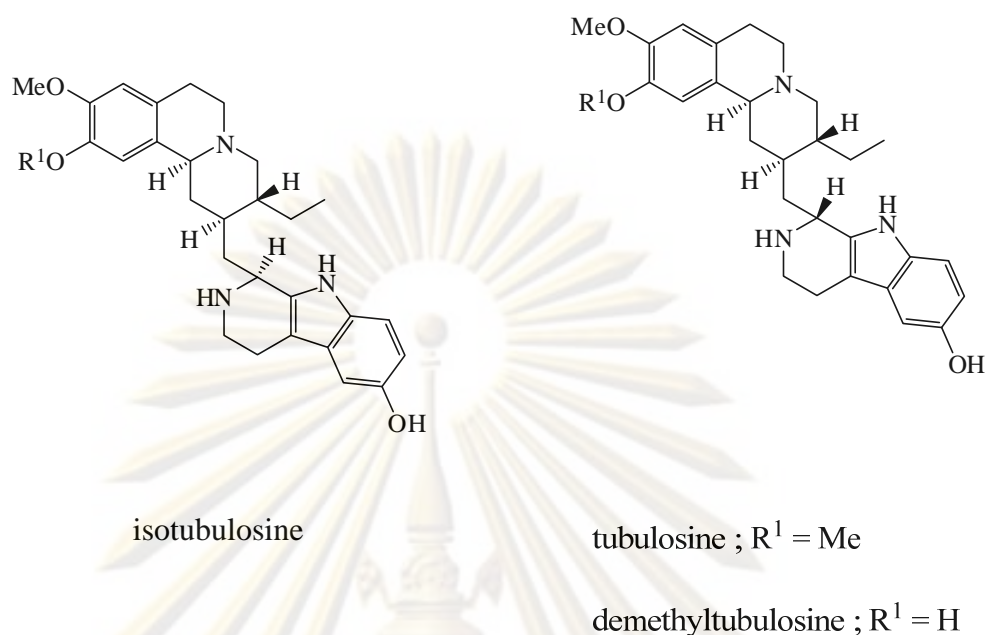
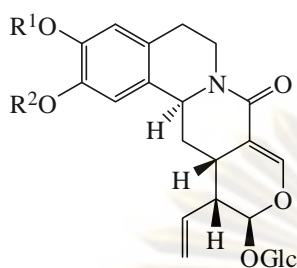


Figure 2.2 Benzoquinolizidine and indolobenzoquinolizidine alkaloids from the root bark of *A. lamarckii*. (cont.)

The hot methanolic fraction of *A. lamarckii* fruits was isolated to give alangiside, alangimarine, methylisolangiside, isolangiside, demethylneolangiside, neolangiside, 3-*O*-demethyl-2-*O*-methylisolangiside, 10-hydroxyvincoside lactam, 3-*O*-demethyl-2-*O*-methylalangiside, 7-*O*-methylpecoside, 6-*O*-methylpecoside, 1', 2'-dehydrotubulosine, alangine, tubulosine, isotubulosine, 6'-*O*- β -D-glucopyranosyl alangiside, 3'-*O*- β -D-glucopyranosylalangiside, 6'-*O*- α -D-glucopyranosylalangiside, 6'-*O*- α -D-glucopyranosyl-3-*O*-demethyl-2-*O*-methylalangiside, 6'-*O*- α -D-xylopyranosylalangiside, 2'-*O*-*trans*-feruloyldemethylalangiside, 2'-*O*-*trans*-feruloylalangiside, 2'-*O*-*trans*-feruloyl-3-*O*-demethyl-2-*O*-methylalangiside, 2'-*O*-*trans*-sinapoyldemethylalangiside, 2'-*O*-*trans*-sinapoylalangiside, 2'-*O*-*trans*-sinapoyl-3-*O*-demethyl-2-*O*-methylalangiside, 2'-*O*-*trans*-[4-(1,3-dihydroxypropoxy)-3-methoxycinnamoyl] alangiside [53]. These structures are summarized in Figure 2.3.

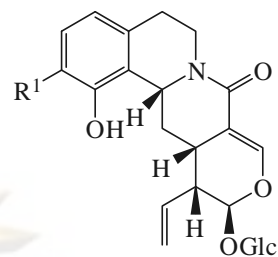


methylisolangiside ; $R^1 = R^2 = \text{Me}$

isolangiside ; $R^1 = \text{Me}, R^2 = \text{H}$

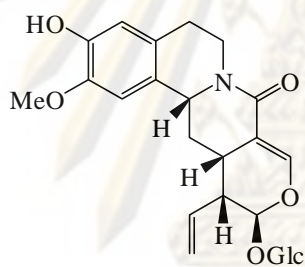
3-*O*-demethyl-2-*O*-methylisoalangiside ;

$R^1 = \text{H}, R^2 = \text{Me}$



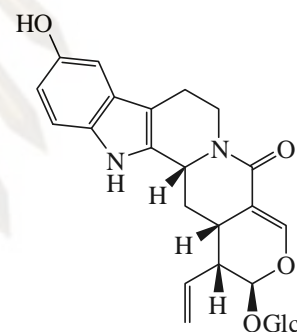
demethylneoalangiside ; $R^1 = \text{OH}$

neoalangiside ; $R^1 = \text{OMe}$

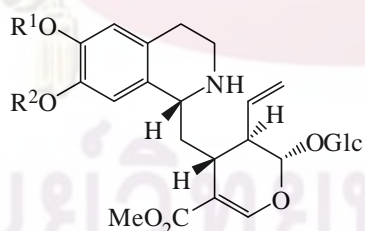


3-*O*-demethyl-2-*O*-methylalangiside ;

$R^1 = \text{H}, R^2 = \text{Me}$

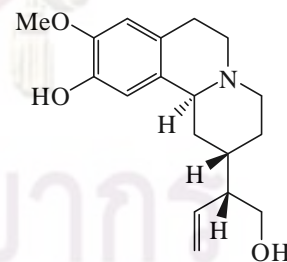


10-hydroxyvincoside lactam



7-*O*-methylpecoside ; $R^1 = \text{H}, R^2 = \text{Me}$

6-*O*-methylpecoside ; $R^1 = \text{Me}, R^2 = \text{H}$



alangine

Figure 2.3 Tetrahydroisoquinoline monoterpene glucosides from the hot methanolic fraction of *A. lamarckii* fruits.

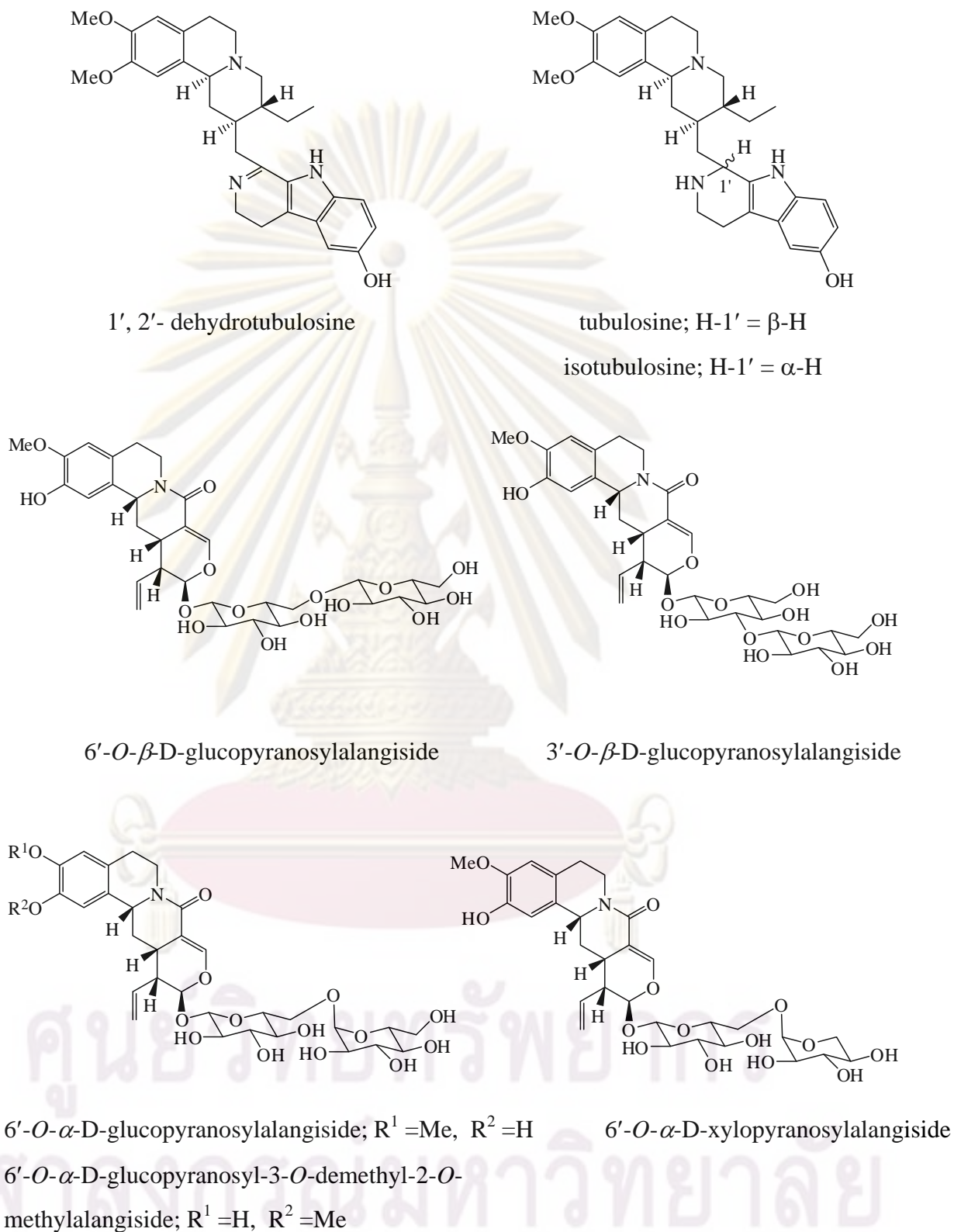
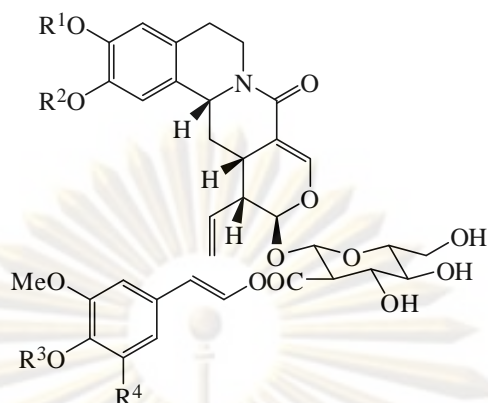


Figure 2.3 Tetrahydroisoquinoline monoterpene glucosides and indolobenzoquinolizidine from the hot methanolic fraction of *A. lamarckii* fruits (cont.).

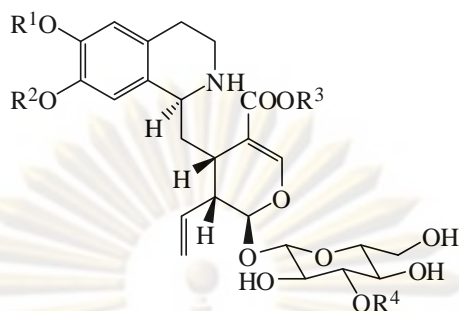


- 2'-*O*-*trans*-feruloyldemethylalangiside ; $R^1 = R^2 = R^3 = R^4 = H$
 2'-*O*-*trans*-feruloylalangiside ; $R^1 = Me, R^2 = R^3 = R^4 = H$
 2'-*O*-*trans*-feruloyl-3-*O*-demethyl-2-*O*-methylalangiside ; $R^1 = R^3 = R^4 = H, R^2 = Me$
 2'-*O*-*trans*-sinapoyldemethylalangiside ; $R^1 = R^2 = R^3 = H, R^4 = OMe$
 2'-*O*-*trans*-sinapoylalangiside ; $R^1 = Me, R^2 = R^3 = H, R^4 = OMe$
 2'-*O*-*trans*-sinapoyl-3-*O*-demethyl-2-*O*-methylalangiside ;
 $R^1 = R^3 = H, R^2 = Me, R^4 = OMe$
 2'-*O*-*trans*-[4-(1,3-dihydroxypropoxy)-3-methoxycinnamoyl] alangiside ;
 $R^1 = Me, R^2 = R^4 = H, R^4 = CH(CH_2OH)_2$

Figure 2.3 Tetrahydroisoquinoline monoterpene glucosides from the hot methanolic fraction of *A. lamarckii* fruits (cont.).

On the other hand, the water soluble fraction of *A. lamarckii* fruits was separated to afford 6-*O*-methyl-*N*-deacetylisoipecosidic acid, 7-*O*-methyl-*N*-deacetylisoipecosidic acid, 6,7-di-*O*-methyl-*N*-deacetylisoipecosidic acid, 6''-*O*- α -D-glucopyranosyl-6-*O*-methyl-*N*-deacetylisoipecosidic acid, 6'-*O*- α -D-glucopyranosylloganic acid, 6-*O*-methyl-*N*-deacetylisoipecosidic acid and loganic acid [54-55].

These structures are summarized in Figure 2.4.



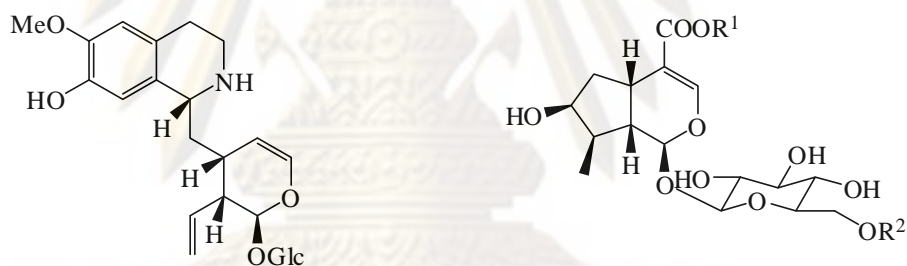
6-*O*-methyl-*N*-deacetylisoipecosidic acid ; $R^1 = \text{Me}, R^2 = R^3 = R^4 = \text{H}$

7-*O*-methyl-*N*-deacetylisoipecosidic acid ; $R^1 = R^3 = R^4 = \text{H}, R^2 = \text{Me}$

6,7-di-*O*-methyl-*N*-deacetylisoipecosidic acid ; $R^1 = R^2 = \text{Me}, R^3 = R^4 = \text{H}$

6'-*O*- α -D-glucopyranosyl-6-*O*-methyl-*N*-deacetylisoipecosidic acid ;

$R^1 = \text{Me}, R^2 = R^3 = \text{H}, R^4 = \alpha\text{-Glc}$



6-*O*-methyl-*N*-deacetylisoipecosidic acid

6'-*O*- α -D-glucopyranosylloganin

; $R^1 = \text{H}, R^2 = \alpha\text{-Glc}$

loganin ; $R^1 = R^2 = \text{H}$

Figure 2.4 Iridoid glucoside from the water soluble fraction of *A. lamarckii* fruits.

However, the chemical studies on the other plants of the family Alangiaceae led to the isolation of various compounds such as iridoid glucoside, flavonoid glucoside, phenolic glycoside and megastigmane glycoside were isolated. Iridoid glucoside, 10-*O*-benzoyladoxosidic was isolated along with alangiside,

demethylalangiside and four flavonoid glycosides from the leaves of *A. kurzii* [56]. All of these structures are summarized in Figure 2.5.

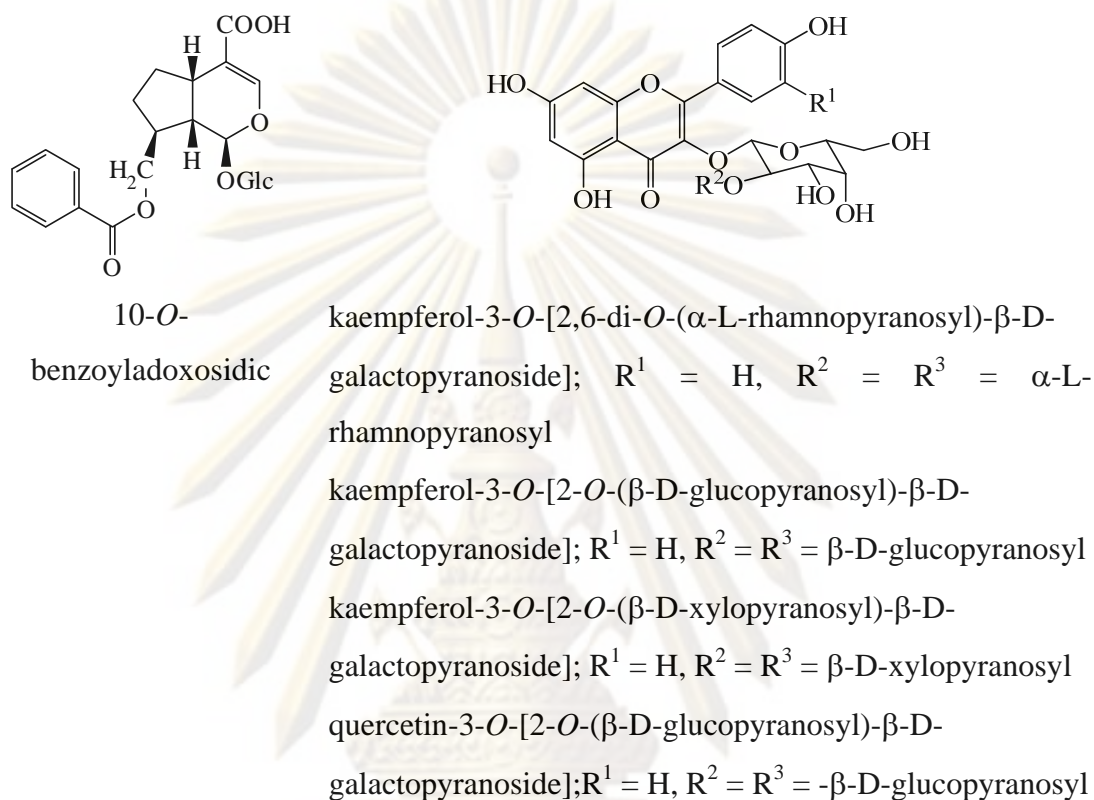
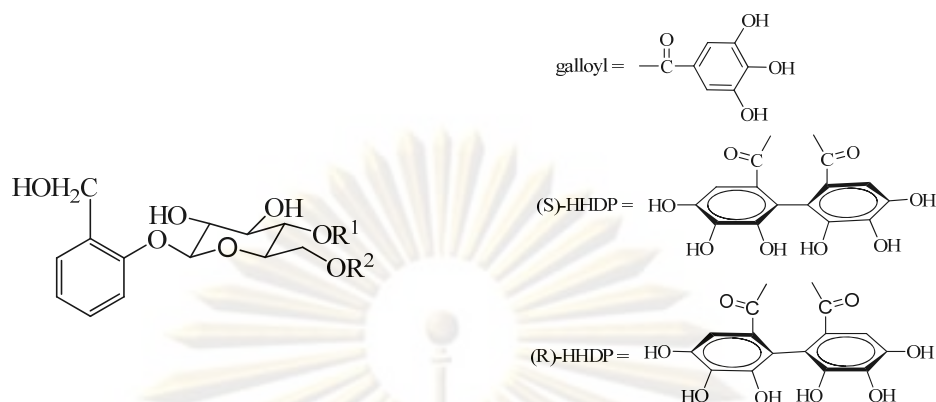


Figure 2.5 Iridoid glucoside and flavonoids glucoside from *A. kurzii* leaves.

The roots, flowers and leaves of *A. chinense* have been documented for used as a muscle relaxant and analgesic agent [57]. A phytochemical studied on this plant revealed the isolation of phenolic glucosides and demethylalangiside. These structures are summarized in Figure 2.6.



6'-*O*-galloylsalicin ; $R^1 = H$, $R^2 = \text{galloyl}$

4', 6'-di-*O*-galloylsalicin ; $R^1 = R^2 = \text{galloyl}$

4', 6'-di-*O*-(*S*)-hexahydroxydiphenoylsalicin ; $R^1 = R^2 = (\text{S})$ -
hexahydroxydiphenoyl (HHDP)

4', 6'-di-*O*-(*R*)-hexahydroxydiphenoylsalicin ; $R^1 = R^2 = (\text{R})$ -
hexahydroxydiphenoyl (HHDP)

Figure 2.6 Phenolic glucoside from *A. chinense*.

Furthermore, the stem bark extract of *A. longiflorum* was isolated to give alangium alkaloids. Among them, 10-*O*-demethylisocephaline was isolated for the first time as a naturally occurring product from a plant source and it exhibited potent cytotoxic activity against human lung carcinoma (A549) and breast adenocarcinoma (MCF-7) with ED_{50} values of 0.013 and 0.062 μM , respectively. The opposite stereochemistry at C-1' of 10-*O*-demethylisocephaline had 10-fold less active than 10-*O*-demethylisocephaline (ED_{50} values of 0.15 and 0.55 μM against A549 and MCF-7, respectively) [58] and their structures are summarized in Figure 2.7.

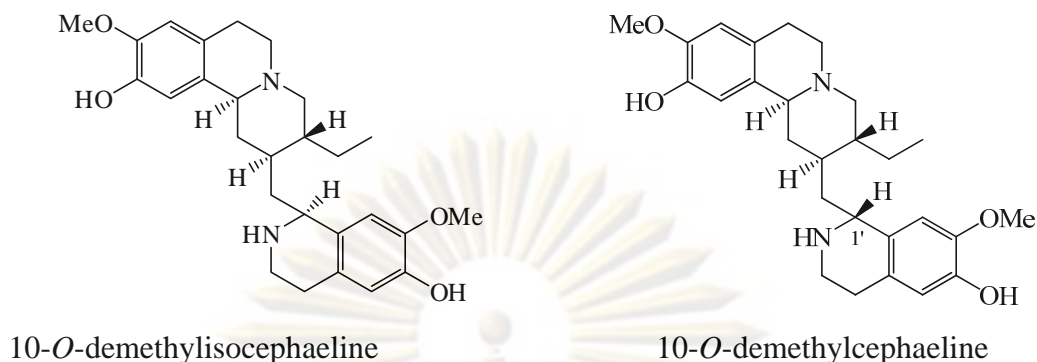


Figure 2.7 Benzoquinolizidine from *A. longiflorum*.

A. salviifolium is mainly used as a folk medicine in India, China and Phillipines. The different parts of this plant are reported to possess acrid, astringent, emollient, anthelmintic, diuretic and purgative properties [48]. These results indicated that this plant produced mainly abortifacient activity and less antiimplantation activity. In addition, the methanolic extract of *A. salviifolium* flowers showed a wide spectrum of antibacterial activity against both gram-positive and gram-negative bacteria [49,59].

In the previous phytochemical studies on roots and leaves of this plant have been found the psychotrine, demethylpsychotrine, emetine, tubulosine and mixture of alangimarckine and dehydroalangimarckine [60]. These structures are summarized in Figure 2.8.

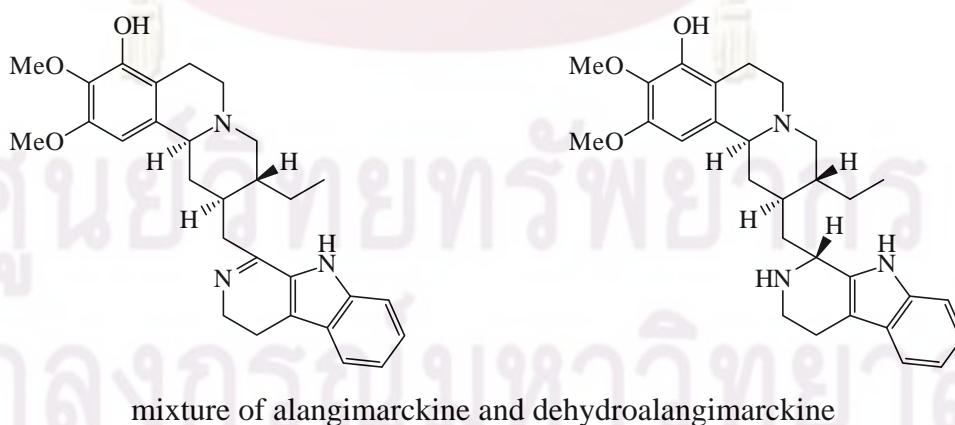


Figure 2.8 Indolobenzoquinolizidine from *A. salviifolium*.

2.1.2 Botanical aspect and distribution

The family Alangiaceae is a small family with only one genus (*Alangium*) and consist of 17 species which occurs in tropical and subtropical Africa and Asia. In Thailand, there were three species of the genus *Alangium* ; as follows:

A. Chinense: Khaao yen (ข้าวเย็น)

A. Kurzii : Champaathong (จำปาทอง)

A. salviifolium: Pruu (ปู้)

Alangium salviifolium belongs to the family Alangiaceae. It is distributed in the Central, Eastern, North-Eastern and Northern of Thailand, which is known in Thai as Pruu (ปู้), Phluu (พลู, Central), Pruu (ปู้, North-Eastern and Northern), Ma Kluea Kaa (มะเกลือกา, Prachin Buri) and Ma taa puu (มะต่าปู้, Chiang Mai). It is a small deciduous tree, shrub and lianas with rough light brown bark.

Leaves : cuneate or rounded at the base, rounded or acute at the apex, at first pubescent later glabrous, 3-23 cm. long and 1.4-9 cm. wide, petiole up to 1.5 cm. long ; lateral nerves 3-9, venation openly reticulate, prominent below.

Flowers : 1.2-3.3 cm., cream or pale yellow, bisexual, in shortly branched clusters (cymes) of 3-17 flowers at leaf axils or behind leaves, 1.4-2.3 cm. individual stalks 0.2-0.8 cm., shortly and densely hairy, main stalks very short, 0.2-0.4 cm.

Fruit : 0.9-1.8 cm., red turning jet black, spherical or oval with persistent calyx at top, smooth or sparsely hairy, sometimes very slightly 12 ribbed, stone with 1 seed.

ศูนย์วิทยทรัพยากร

จุฬาลงกรณ์มหาวิทยาลัย

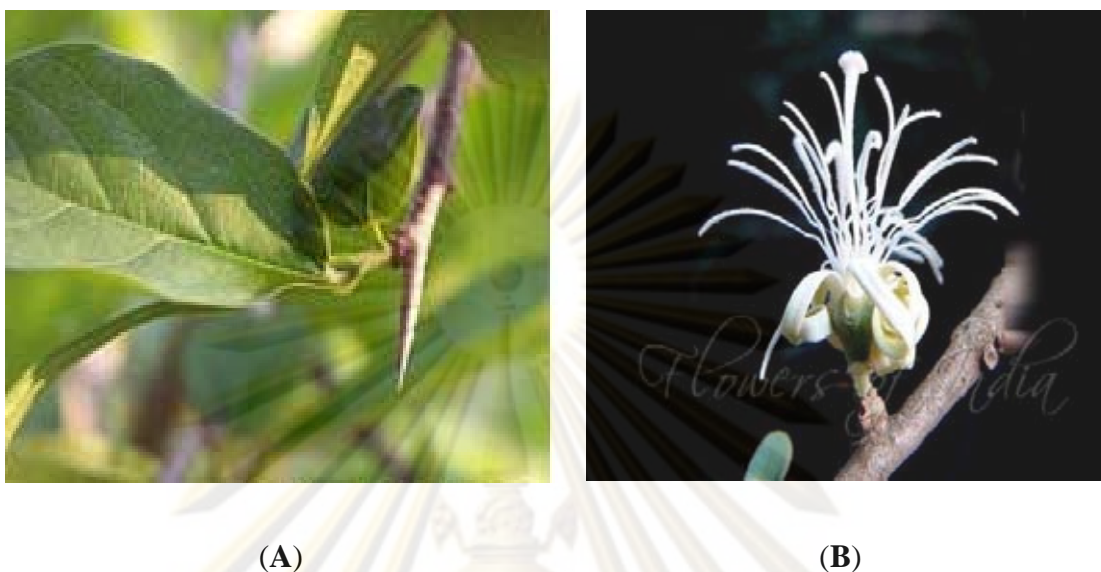


Figure 2.9 Leaves (A) and flowers (B) *Alangium salviifolium* (www.toptropicals.com/pics/garden).

The objective of this research:

The main objectives in this investigation are as follows:

1. To carry out a comprehensive chemical separation and structure determination of constituents from the roots of *A. salviifolium* by chromatographic and spectroscopic techniques, respectively.
2. To investigate the cytotoxic activity against KB and HeLa cells of all isolated compounds.

ศูนย์วิจัยทรัพยากร
จุฬาลงกรณ์มหาวิทยาลัย

2.2 Results and Discussion

2.2.1 Structural elucidation of alangium alkaloids

The roots of *A. salviifolium* were extracted with MeOH in a soxhlet extractor and the MeOH extract was successively partitioned between H₂O/CH₂Cl₂ and H₂O/*n*-BuOH. The *n*-BuOH crude extract were separated by a combination of chromatographic procedures to afford five known alkaloids (**2.1-2.5**) [61-67], which were identified as psychotrine (**2.1**), alangiside (**2.2**), 3-*O*-demethyl-2-*O*-methylalangiside (**2.3**), alangicine (**2.4**) and demethylalangiside (**2.5**). The water crude extract was also separated by a combination of chromatographic procedures to obtain two known alkaloids (**2.6-2.7**) [52,74], which were identified as 1', 2'-dehydrotubulosine (**2.6**) and demethylpsychotrine (**2.7**).

All of isolated alkaloids were divided into three groups. The first group was benzoquinolizidine: psychotrine (**2.1**), alangicine (**2.4**) and demethylpsychotrine (**2.7**). The second group was indolobenzoquinolizidine: 1', 2'-dehydrotubulosine (**2.6**) and the last group was benzopyridoquinolizidine: alangiside (**2.2**), 3-*O*-demethyl-2-*O*-methylalangiside (**2.3**) and demethylalangiside (**2.5**). All of these alkaloids are summarized in Figure 2.10.

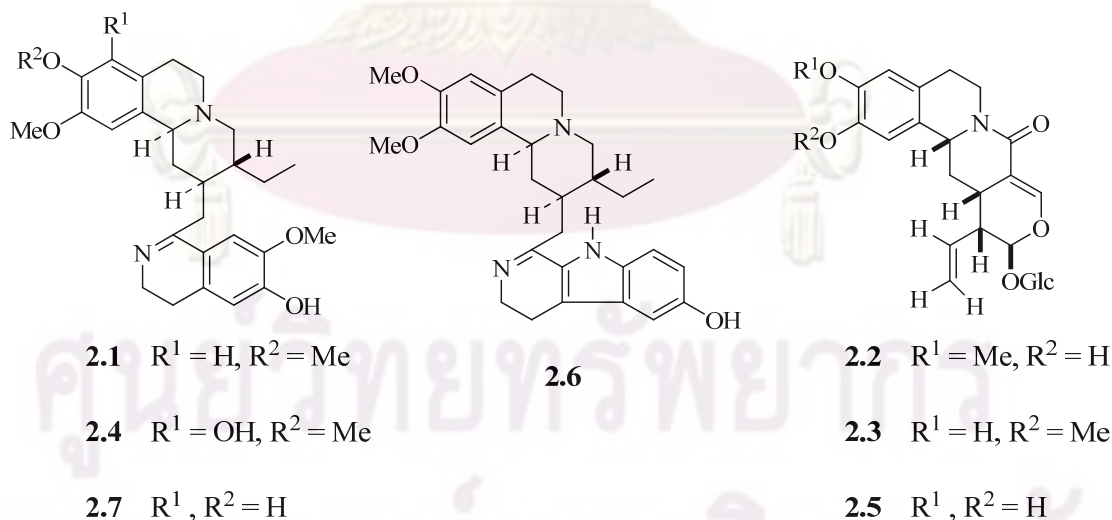


Figure 2.10 Structure of alkaloids **2.1-2.7** from the butanolic and water extracts of *A. salviifolium* roots

Psychotrine (**2.1**) was obtained as amorphous powder. Its ESIMS indicated a pseudomolecular ion $[M+H]^+$ at m/z 465.11, compatible with molecular formula of $C_{28}H_{36}N_2O_4$. The 1H NMR spectra exhibited four singlets of aromatic protons at δ 6.49, 6.51, 6.66 and 7.09, three singlets of methoxyl groups at δ 3.68, 3.77 and 3.81 and signals for an ethyl group at δ 0.95, 1.29-1.33 and 1.93. In HMBC spectra showed correlation cross peaks from H-11 (δ 6.51) to C-11b (δ 61.8) and C-9 (δ 147.0) and from H-8 (δ 6.66) to C-7 (δ 27.7) and C-10 (δ 150.0). This data indicated that H-8 and H-11 were 1,4-disubstituted protons attached at C-8 and C-11 on the upper aromatic ring of 9, 10-dimethoxybenzo[a]quinolizidine moiety, respectively. On the other hand, the signal of H-8' (δ 7.09) showed the correlation to C-1' (δ 171.0), C-4'a (δ 136.0) and C-6' (δ 167.0) and the signal of H-5' (δ 6.49) also showed the correlation to C-4' (δ 26.2) and C-7' (δ 147.0). This data suggested that H-8' and H-5' were 1,4-disubstituted protons attached at C-8' and C-5' on the lower aromatic ring of 3,4-dihydroisoquinoline moiety, respectively. In addition, the signals H-8' (δ 7.09) and H-3' (δ 3.64) exhibited the correlation with a quaternary carbon at C-1' (δ 171.0), suggesting that this compound contained endocyclic double bond at C-1'.

Thus, this compound was determined to be psychotrine by comparison of its 1H , ^{13}C and 2D NMR spectral data with those in literature [61-62]. The key HMBC correlation of **2.1** is shown in Figure 2.11. Therefore, the structure of **2.1** was characterized as psychotrine.

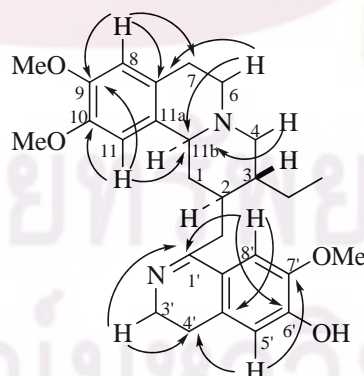


Figure 2.11 The key HMBC correlations of **2.1**

Alangiside (**2.2**) was obtained as amorphous powder. The 1H NMR spectral data showed a terminal vinyl protons at δ 5.30 (1H, dd, $J = 17.0, 1.4$ Hz) and 5.50

(1H, dd, $J = 17.0, 1.4$ Hz), two aromatic protons at δ 6.69 and 6.80, a doublet for an olefinic proton at δ 7.41 (1H, d, $J = 2.3$ Hz), a doublet for an acetal proton at δ 5.50 (1H, d, $J = 1.8$ Hz), a doublet for an anomeric proton at δ 4.70 (1H, d, $J = 8.0$ Hz) and a singlet for a methoxyl group at δ 3.83. All of the above data suggested the possibility of a tetrahydroisoquinoline monoterpene glucoside skeleton. In the HMBC spectral data showed correlation cross peak between H-6, H-9 and H-13a with carbonyl carbon at C-8 position. In addition, it showed correlation between anomeric proton at δ 4.70 and terminal vinyl proton at δ 5.54 (H-14) with C-11, indicated that the location of vinyl group and glucose unit were attached at C-12 and C-11, respectively. The HMBC correlation was shown in Figure 2.12. Finally, the spectral data of **2.2** was confirmed by comparison with the spectroscopic data in the literature [63-64]. Therefore, alkaloid **2.2** was assigned to be alangiside.

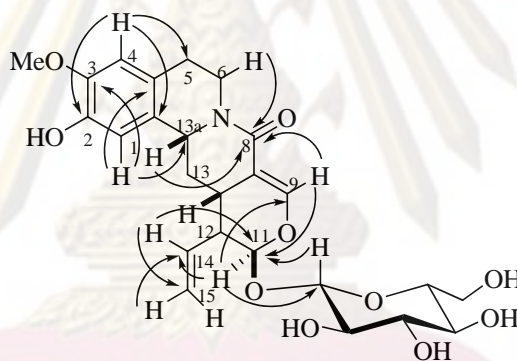


Figure 2.12 The key HMBC correlations of **2.2**

3-*O*-Demethyl-2-*O*-methylalangiside (**2.3**) was also obtained as amorphous powder. The ^1H and ^{13}C NMR spectral data of **2.3** was structurally similar to **2.2**, although there are significant differences between the chemical shifts of the aromatic protons. In the ^1H NMR spectral data of **2.3** showed two singlets aromatic protons at δ 6.57 (H-4) and 6.78 (H-1), instead of two singlets aromatic protons at δ 6.68 (H-4) and 6.70 (H-1) as in **2.2**. The ^{13}C NMR spectra of **2.3** was also superimposable on those of **2.2**, except for the signals arising from its aromatic moiety. In the HMBC spectrum of **2.3** showed correlation peak similar to those of **2.2**, indicating the location of vinyl group and glucose unit were attached at C-12 and C-11, respectively. The key HMBC correlation was shown in Figure 2.13. All these results demonstrated that **2.3** was an isomer of alangiside (**2.2**) with the position of phenolic hydroxyl and

methoxyl groups interchanged as well as comparison its spectral data with the reports in the literature [65]. Therefore, alkaloid **2.3** was assigned to be 3-*O*-demethyl-2-*O*-methylalangsine.

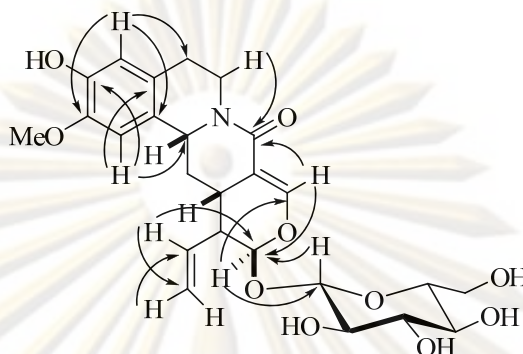


Figure 2.13 The key HMBC correlations of **2.3**

Alangicine (**2.4**) was obtained as amorphous powder. The positive ESIMS showed a pseudomolecular ion peak at m/z 481.11 $[M+H]^+$, indicating an elemental molecular formula at $C_{28}H_{36}N_2O_5$. The 1H NMR spectral features of **2.4** was closely similar to that of **2.1**, except for the absence of a singlet aromatic proton, which appeared at δ 6.66 (H-8) in **2.1**. In the HMBC spectrum still showed correlation peak between H-8', H-3' and C-1'; H-3', H-5' and C-4', indicating presence of two aromatic protons at δ 7.08 and δ 6.48 in the lower aromatic ring. For the upper aromatic ring found that the only signal at δ 6.07 had correlated with C-11b in the HMBC spectrum. In addition, on the basis of mass spectral data suggested that the structure of **2.4** had a hydroxyl group attached at C-8. The spectral features of **2.4** were analogous to those of **2.1**, except for the absence of aromatic proton at C-8. Finally, this assumption was supported by a comparison with the spectral data in the literature [66]. The key HMBC correlation of **2.4** are shown in Figure 2.14. Thus, the structure of **2.4** was determined to be alangicine.

จุฬาลงกรณ์มหาวิทยาลัย

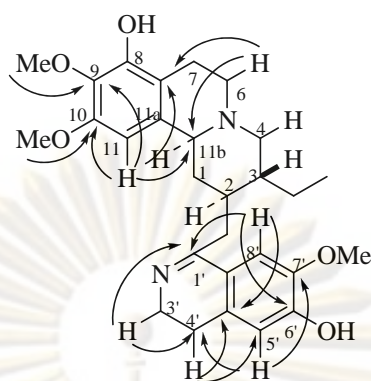


Figure 2.14 The key HMBC correlations of **2.4**

Demethylalangiside (**2.5**) was isolated as amorphous powder. Its ^1H and ^{13}C NMR spectral features were closely similar to those of **2.2**, except for the absence of a singlet methoxy proton at δ 3.83 in **2.2**. Furthermore, two singlets aromatic protons of **2.5** at δ 6.54 (H-4) and 6.64 (H-1) were deshielded to low field by compared with two singlets aromatic protons of **2.2**, indicated that they attached closely to hydroxyl groups. From these evidences, one hydroxyl group at C-3 of **2.5** was observed, instead of methoxyl group as **2.2**. In the HMBC spectrum of **2.5** showed correlation peak similar to those of **2.2** and **2.3**, indicating the location of vinyl group and glucose unit were attached at C-12 and C-11, respectively. The key HMBC correlation are shown in Figure 2.15. Finally, the spectral data of **2.5** was confirmed by comparison with the spectroscopic data in the literature [67]. Thus, compound **2.5** was assigned to be demethylalangiside.

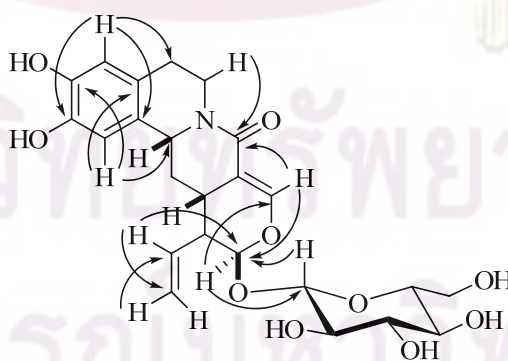


Figure 2.15 The key HMBC correlations of **2.5**

1',2'-Dehydrotubulosine (**2.6**) was obtained as amorphous powder. The ESIMS revealed a pseudomolecular ion peak $[\text{M}+\text{H}]^+$ at m/z 474.29, compatible with

molecular formula of $C_{29}H_{35}N_3O_3$. The 1H NMR spectral data exhibited signals for an ethyl group at δ 1.0, 1.2 and 1.85, singlets for two aromatic protons at δ 6.12 and 6.85, an AMX system for three aromatic protons at δ 6.54, 6.90 and 7.24, and singlets for two methoxy protons at δ 3.20 and 3.64. These spectral features were similar to those of tubulosine, except for the absence of the H-1' signal, which appeared at δ 4.11 in tubulosine [42]. In addition, the HMBC spectrum showed correlation of H-3' (δ 3.89) to C-1' (δ 166.5) and C-4'a (δ 120.5), suggested that **2.6** was the 1',2'-dehydrogenated analogue of tubulosine. The proposed structure of **2.6** was consistent with its HMBC spectrum, where C-1' (quaternary carbon) was observed at δ 166.5 instead of at δ 48.5 in tubulosine as well as comparison the chemical shifts with the reports in the literature [68]. The key HMBC correlations are shown in Figure 2.16. Therefore, alkaloid **2.6** was determined to be 1', 2'-dehydrotubulosine.

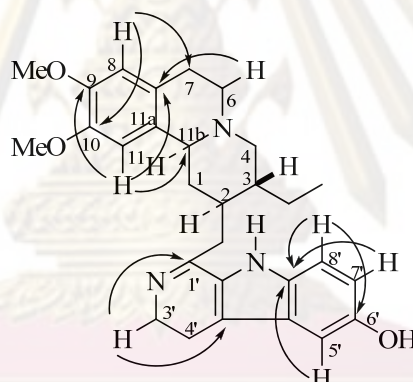


Figure 2.16 The key HMBC correlations of **2.6**

Demethylpsychotrine (**2.7**) was isolated as amorphous powder. The positive ESIMS showed a pseudomolecular ion peak at m/z 451.34 $[M+H]^+$, indicating an elemental molecular formula at $C_{27}H_{34}N_2O_4$. The 1H NMR spectra of **2.7** showed only two methoxy signals at δ 3.59 and δ 3.73, four singlets of aromatic protons at δ 6.35, 6.40, 6.42 and 7.02. These spectral features were similar to those of psychotrine (**2.1**), except that its 1H NMR spectra showed only two methoxy signals. In the HMBC spectrum showed correlation cross peak similar to those of **2.1**, indicating the presence of four aromatic protons in the molecule. The hydroxyl group at C-9 of **2.7** was observed, instead of methoxyl group of **2.1**. This evidence was confirmed through the mass spectrum and HMBC experiment. The key HMBC correlation was

shown in Figure 2.17. The spectral data of **2.7** was determined by comparison with the chemical shifts in the literature [52]. Therefore, compound **2.7** was assigned to be demethylpsychotrine.

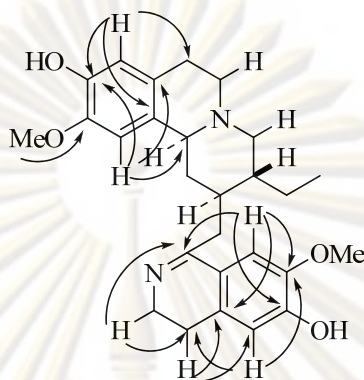


Figure 2.17 The key HMBC correlations of **2.7**

In conclusion, the chromatographic separation of the butanolic crude extracts led to the isolation of five known alkaloids (**2.1-2.5**), psychotrine (**2.1**), alangiside (**2.2**), 3-*O*-demethyl-2-*O*-methylalangiside (**2.3**), alangicine (**2.4**) and demethylalangiside (**2.5**). In addition, 1',2'-dehydrotubulosine (**2.6**) and demethylpsychotrine (**2.7**) were isolated from the water crude extracts. The structures of all isolated compounds were characterized by spectroscopic method as well as comparison with the previous literature data.

2.2.2 Cytotoxic activity against KB and HeLa cell lines of alangium alkaloids

The cytotoxic activity against HeLa and KB cell lines of all isolated compounds were determined using MTT assay and the result is shown in Table 2.1.

The evaluation for cytotoxicity against KB and HeLa cell lines showed that compound **2.1** has highest cytotoxicity against both KB cell and HeLa cell with IC_{50} value 1.00 and 0.70 $\mu\text{g/ml}$, respectively. The cytotoxicity results of **2.1** was in good agreement with earlier values reported in the literature [47, 69]. In addition, tetrahydroisoquinoline monoterpene glycoside (**2.2**, **2.3** and **2.5**) were inactive towards both KB and HeLa cell lines. However, previous bioactivities investigations demonstrated that compound **2.3** and **2.5** were inactive toward antitumor activity.

Accordingly, the presences of glycoside unit on the C-11 reduced cytotoxicity of **2.3** and **2.5** [70].

The future work may involve the synthesis of isolated compounds for increasing quantity and biological activity that could be developed into new drugs. Novel active compounds will afford the target for future synthesis and structure activity relationship studies as well. This will lead to the better understanding on the interaction between active compounds and diseases.

Table 2.1 Cytotoxic activity against HeLa and KB Cell lines of isolated compounds.

Isolated compounds	IC ₅₀ (µg/mL)	
	KB cell line	HeLa cell line
Psychotrine (2.1)	1.00	0.70
Alangiside (2.2)	99.00	99.00
3- <i>O</i> -Demethyl-2- <i>O</i> -methylalangiside (2.3)	>100.00	>100.00
Alangicine (2.4)	9.00	6.00
Demethylalangiside (2.5)	>100.00	20.50
1', 2'-Dehydrotubulosine (2.6)	40.00	10.00
Demethylpsychotrine (2.7)	18.00	4.00
Adriamycin*	0.018	0.018

KB cell line: Human epidermoid carcinoma

HeLa cell line: Human cervical carcinoma

Standard agent*

ศูนย์วิทยทรัพยากร
จุฬาลงกรณ์มหาวิทยาลัย

2.3 Experimental

2.3.1 Plant material

The roots of *Alangium salviifolium* were collected from Mahasarakham Province of Thailand in May, 2007 and identified by Ms. Suttira Khumkratok, a botanist at the Walai Rukhavej Botanical Research Institute, Mahasarakham University, where a voucher specimen (Khumkratok no. 70-07) is deposited.

2.3.2 General experimental procedures

NMR spectra were recorded with a Varian Mercury⁺ 400 NMR spectrometer operated at 400 MHz for ¹H and 100 MHz for ¹³C nuclei. The chemical shift in δ (ppm) was assigned with reference to the signal from the residual protons in deuterated solvents and using TMS as an internal standard in some cases. Most solvents used in this research were commercial grade and were distilled prior to use. Adsorbents such as silica gel 60 Merck cat. No. 7729, 7731, and 7734 were used for quick column chromatography, open column chromatography and radial chromatography, respectively. Thin-layer chromatography (TLC) was performed on precoated Merck silica gel 60 F254 plates (0.25 mm thick layer). ESIMS data were obtained from a VG TRIO 2000 mass spectrometer. High resolution mass spectra were recorded by Micromass LCT and Bruker MICROTOF models. UV-visible absorption spectra were recorded on UV-2552PC UV-Vis spectrometer (Shimadzu, Kyoto, Japan). Melting points were determined with Fisher-Johns Melting Point Apparatus. IR data was obtained from a Nicolet 6700 FT-IR spectrometer (Thermo Electron Corporation, Madison, WI, USA) equipped with a mercury-cadmium-telluride (MCT) detector.

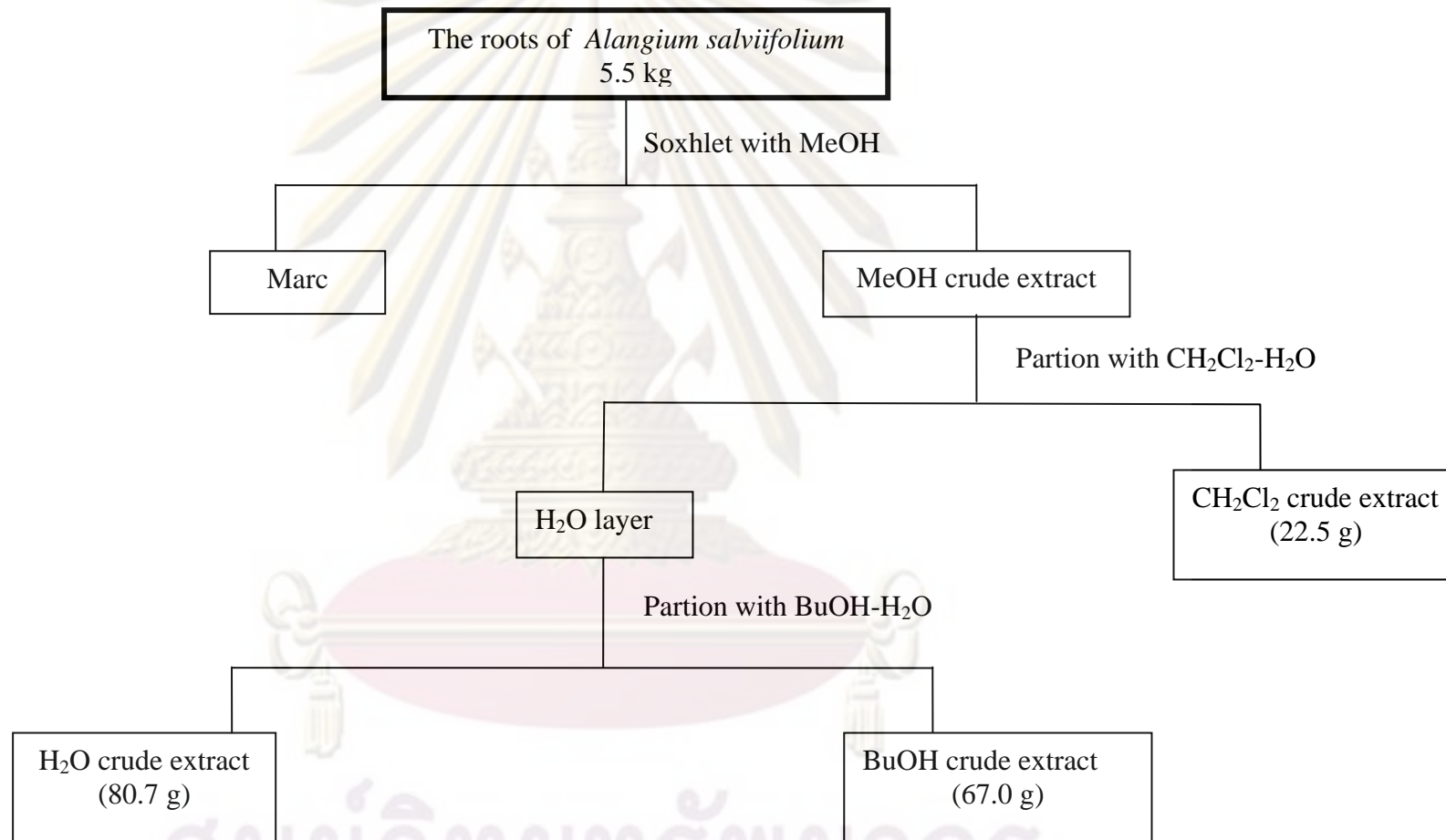
2.3.3 Extraction and purification

Air-dried and powdered roots of *A. salviifolium* (5.5 kg) were extracted with MeOH in a Soxhlet extractor. The MeOH crude extract was concentrated and

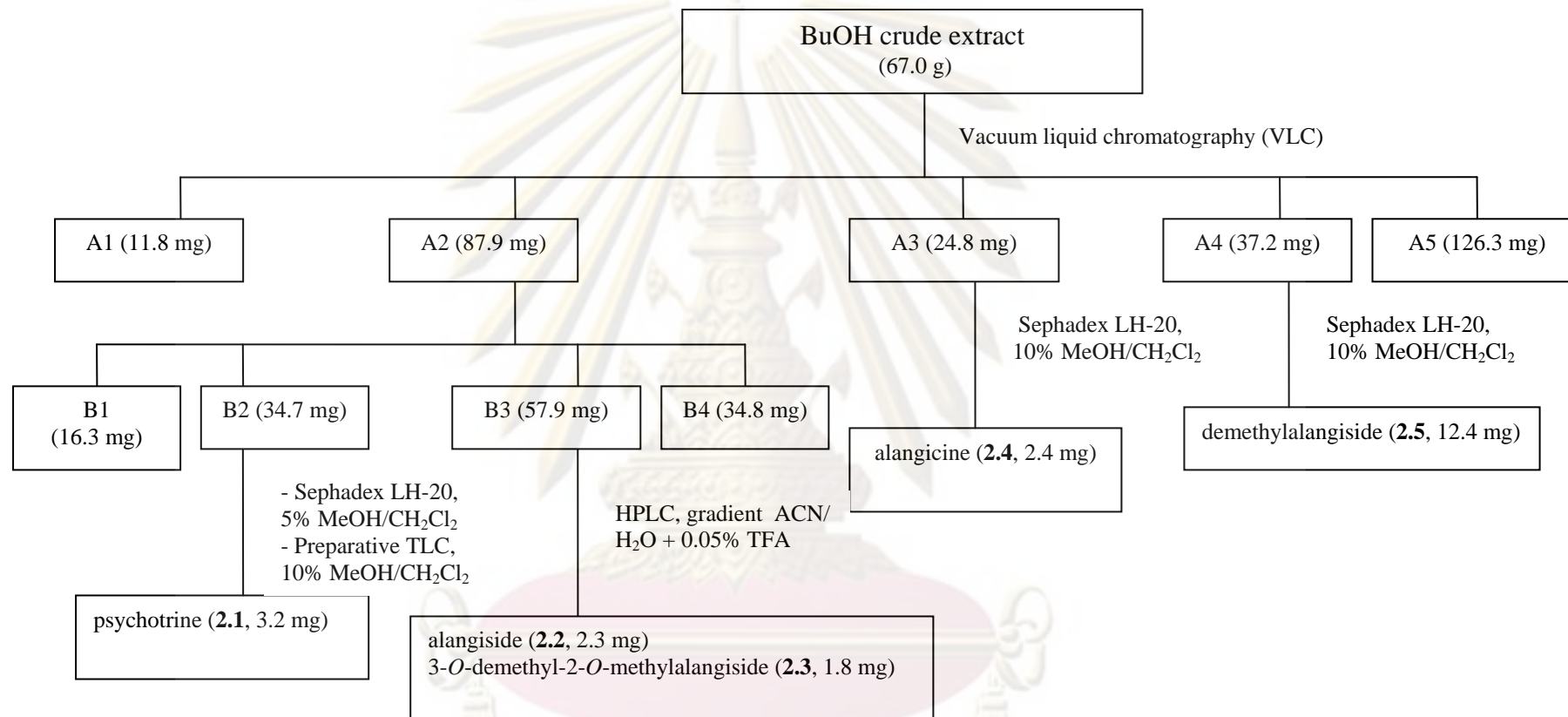
successively partitioned between H₂O/CH₂Cl₂ and between H₂O/*n*-BuOH to give CH₂Cl₂, *n*-BuOH and H₂O crude extracts, respectively. The *n*-BuOH crude extract was concentrated under vacuum to yield brown amorphous (67.0 g). This extract was fractionated by vacuum liquid chromatography (VLC) over silica gel (Merck Art. 7730), using CH₂Cl₂ and MeOH with increasing polarity to give five fractions (A1-A5). Fraction A-2 (2.0 g) was further purified by a Sephadex LH-20 column eluted with 5% MeOH-CH₂Cl₂ to yield four fractions (B1-B4). Fraction B-2 was purified by a Sephadex LH-20 column eluted with 5% MeOH-CH₂Cl₂, followed by preparative TLC (silica gel, 10% MeOH-CH₂Cl₂) to obtain psychotrine (**2.1**, 3.2 mg). Fraction B-3 was purified by HPLC with gradient elution [solvent (A) H₂O + 0.05% TFA, solvent (B) ACN] using the following standard gradient solvent system: 2 minutes of 5% ACN / H₂O; a linear gradient to 50% ACN / H₂O for 30 minutes; isocratic at 50% ACN / H₂O for another 4 minutes; then returned to 5% ACN / H₂O over 1 minutes and reequilibrated for 3 minutes to obtain alangiside (**2.2**, 2.3 mg) and 3-*O*-demethyl-2-*O*-methylalangiside (**2.3**, 1.8 mg). Fraction A-3 (2.5 g) was further purified by Sephadex LH-20 column eluted with 10% MeOH-CH₂Cl₂ to afford **2.1**, **2.2**, **2.3**, and alangicine (**2.4**, 2.4 mg). Fraction A-4 (4.0 g) was purified by Sephadex LH-20 column using 10% MeOH-CH₂Cl₂ as the eluent, yielding **2.1** and demethylalangiside (**2.5**, 12.4 mg).

The H₂O crude extract was concentrated under vacuum to yield 80.7 g. This extract was fractionated by vacuum liquid chromatography over silica gel (Merck Art. 7730), using CH₂Cl₂ and MeOH with increasing polarity to give four fractions (C1-C4). Fraction C-2 was further purified by preparative TLC (silica gel, 7% MeOH / CH₂Cl₂) to obtain **2.1** and 1', 2'-dehydrotubulosine (**2.6**, 1.8 mg). Fraction C-3 was purified by preparative TLC, using 10% MeOH-CH₂Cl₂ to give demethylpsychotrine (**2.7**, 2.2 mg).

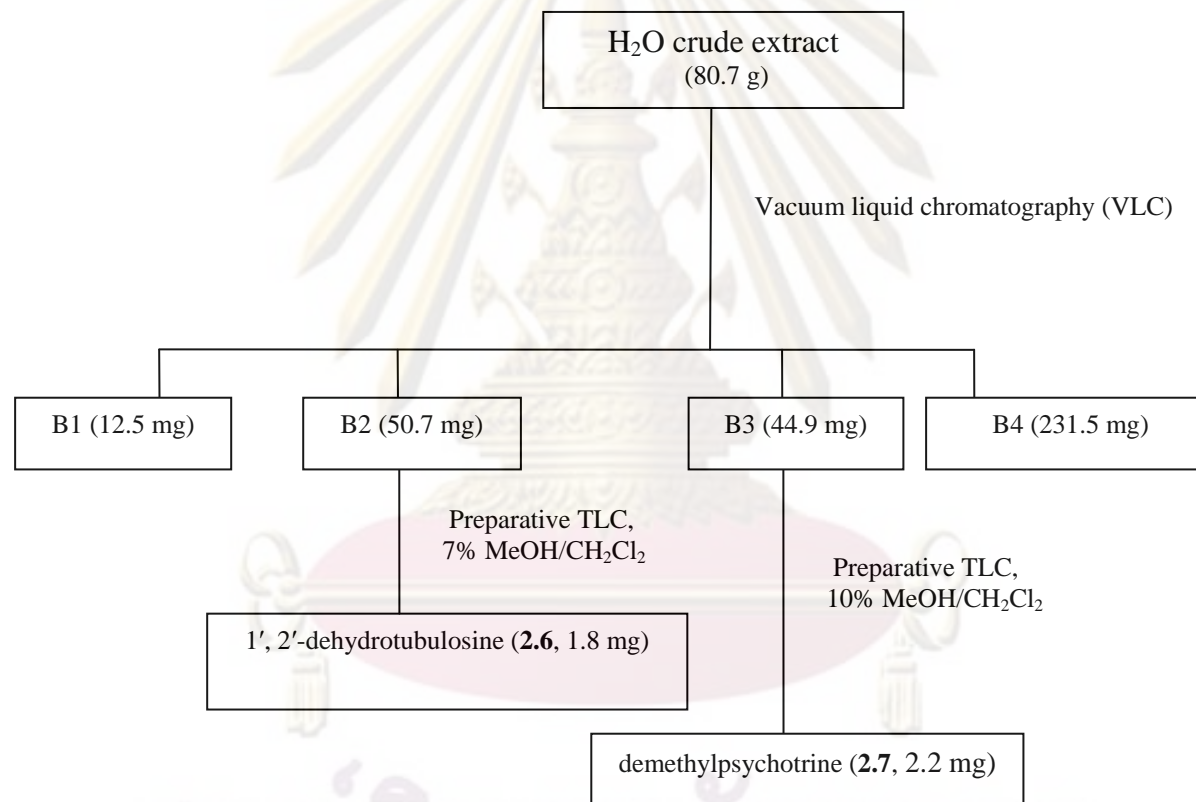
The extraction and purification of all isolated compounds from the roots of *A. salviifolium* were briefly summarized in Schemes 2.1, 2.2 and 2.3.



Scheme 2.1 Extraction procedure of *A. salviifolium* roots.



Scheme 2.2 Isolation procedure of the butanolic crude extract.



Scheme 2.3 Isolation procedure of the water crude extract

Psychotrine (2.1): amorphous powder; m.p. 117-120 °C; ^1H NMR (CD_3OD , 400 MHz): δ 7.09 (1H, s, H-8'), 6.66 (1H, s, H-8), 6.51 (1H, s, H-11), 6.49 (1H, s, H-5'), 3.81 (3H, s, OMe-10), 3.77 (3H, s, OMe-7'), 3.68 (3H, s, OMe-9), 3.64 (1H, m, H-3'), 3.13 (1H, dd, $J = 3.8, 11.0$ Hz, H-11b), 2.68-2.71 (1H, m, H-7), 2.53-3.07 (1H, m, H-6), 2.20-3.17 (1H, m, H-4), 1.80 (1H, m, H-2), 1.58 (1H, m, H-3), 1.52-1.93 (2H, m, H-12), 1.29-1.33 (2H, m, H-13), 1.23, 2.16 (2H, brt, $J = 12.0$ Hz, H-1), 0.95 (1H, t, $J = 8.5$, Hz, H-14). ^{13}C NMR (CD_3OD , 100 MHz): δ 171.0 (C-1'), 167.0 (C-6'), 150.0 (C-10), 147.0 (C-9, 7'), 136.0 (C-4'a), 128.0 (C-11a), 125.0 (C-7a), 116.9 (C-5', 8'a), 111.5 (C-8), 110.5 (C-8'), 108.0 (C-11), 61.8 (C-11b), 59.8 (C-4), 55.0 (OMe-9), 54.9 (OMe-7'), 54.7 (OMe-10'), 51.6 (C-6), 41.4 (C-3, 3'), 40.5 (C-2, 12), 36.0 (C-1), 27.7 (C-7), 26.2 (C-4'), 23.0 (C-13).

Alangiside (2.2): amorphous powder; m.p. 164-167 °C; ^1H NMR (CDCl_3 , 400 MHz): ^1H NMR (CD_3OD , 400 MHz): δ 7.41 (1H, d, $J = 2.3$ Hz, H-9), 6.70 (1H, s, H-1), 6.69 (1H, s, H-4), 5.50 (1H, d, $J = 1.8$ Hz, H-14), 5.30 (1H, dd, $J = 17.0, 1.4$ Hz, H-15a), 5.50 (1H, dd, $J = 17.0, 1.4$ Hz, H-15b), 4.72 (1H, m, H-13a), 4.71 (2H, m, H-6), 4.70 (1H, d, $J = 8.0$ Hz, H-1'), 3.83 (3H, s, OMe-3), 3.21 (1H, t, $J = 8.0$ Hz, H-12a), 2.89 (1H, m, H-6a), 2.66-2.79 (2H, m, H-5), 2.31 (1H, dt, $J = 12.0, 4.5$ Hz, H-12a). ^{13}C NMR (CD_3OD , 100 MHz): δ 164.5 (C-8), 147.4 (C-9), 146.6 (C-3), 144.9 (C-2), 132.5 (C-14), 128.0 (C-13b), 127.5 (C-4a), 114.7 (C-1), 111.9 (C-4), 98.2 (C-1'), 96.1 (C-11), 55.8 (OMe-3), 39.4 (C-6), 28.0 (C-5), 26.3 (C-12a).

3-*o*-demethyl-2-*o*-methylalangiside (2.3): amorphous powder; m.p. 275-277 °C; ^1H NMR (CD_3OD , 400 MHz): δ 7.41 (1H, d, $J = 2.5$ Hz, H-9), 6.78 (1H, s, H-1), 6.57 (1H, s, H-4), 5.53 (1H, dt, $J = 17.0, 10.0$ Hz, H-14), 5.49 (1H, d, $J = 1.5$ Hz, H-11), 5.28 (1H, dd, $J = 17.0, 2.0$ Hz, H-15b), 5.19 (1H, dd, $J = 10.0, 2.0$ Hz, H-15a), 4.76 (1H, dd, $J = 11.5, 3.5$ Hz, H-13a), 4.73 (1H, ddd, $J = 12.5, 4.5, 3.0$ Hz, H-6b), 4.69 (1H, d, $J = 8.0$ Hz, H-1'), 3.89 (1H, dd, $J = 12.0, 2.0$ Hz, H-6'b), 3.82 (3H, s, OMe-2), 3.67 (1H, dd, $J = 12.0, 5.5$ Hz, H-6'a), 3.38 (1H, t, $J = 9.0$ Hz, H-3'), 3.33 (1H, ddd, $J = 9.5, 5.5, 2.0$ Hz, H-5'), 3.28 (1H, dd, $J = 9.5, 9.0$ Hz, H-4'), 3.21 (1H, dddd, $J = 13.0, 5.5, 3.5, 2.5$ Hz, H-12a), 3.19 (1H, dd, $J = 9.0, 8.0$ Hz, H-2'), 2.84 (1H, td, $J =$

12.5, 3.0 Hz, H-6a), 2.71 (2H, ddd, $J = 15.5, 5.5, 1.5$ Hz, H-5b, 12), 2.60 (1H, dt, $J = 15.5, 3.0$ Hz, H-5a), 2.37 (1H, dt, $J = 13.0, 3.5$ Hz, H-13b), 1.36 (1H, td, $J = 13.0, 11.5$ Hz, H-13a). ^{13}C NMR (CD₃OD, 100 MHz): δ 166.0 (C-8), 148.8 (C-9), 148.2 (C-2), 146.5 (C-3), 134.0 (C-14), 128.9 (C-4a), 128.8 (C-13b), 120.4 (C-15), 116.1 (C-4), 110.3 (C-1), 109.3 (C-8a), 99.7 (C-1'), 97.6 (C-11), 78.4 (C-5'), 78.1 (C-3'), 74.9 (C-2'), 71.6 (C-4'), 62.7 (C-6'), 57.3 (C-13a), 56.7 (OMe-2), 44.5 (C-12), 40.8 (C-6), 35.5 (C-13), 29.4 (C-5), 27.9 (C-12a).

Alangicine (2.4): amorphous powder; m.p. 145-147 °C; ^1H NMR (CD₃OD, 400 MHz): δ 7.09 (1H, s, H-8'), 6.48 (1H, s, H-5'), 6.08 (1H, s, H-11), 3.80 (3H, s, OMe-7'), 3.72 (3H, s, OMe-9), 3.68 (3H, s, OMe-10), 3.64 (1H, m, H-3'), 3.41 (1H, m, H-12), 3.08 (1H, m, H-11b), 2.87 (1H, t, $J = 8$ Hz, H-4'), 2.72, 2.69 (2H, m, H-7), 2.48, 3.07 (2H, dt, $J = 11.5, 4.6$ Hz, H-6), 2.15, 3.14 (2H, m, H-4), 1.32, 1.92 (2H, m, H-13), 1.57 (1H, m, H-3), 1.79 (1H, m, H-2), 1.22, 2.11 (2H, m, H-1), 1.04 (1H, t, $J = 8.0$ Hz, H-14). ^{13}C NMR (CD₃OD, 100 MHz): δ 170.7 (C-1'), 150.3 (C-6'), 150.2 (C-7'), 147.5 (C-8), 134.7 (C-9), 132.0 (C-11a), 117.3 (C-5'), 116.0 (C-8'a), 114.7 (C-7a), 110.7 (C-8'), 99.1 (C-11), 62.3 (C-11b), 60.3 (C-4), 59.9 (OMe-10), 59.8 (OMe-9), 55.0 (OMe-7'), 51.7 (C-6), 41.6 (C-3',C-3), 40.9 (C-2), 36.3 (C-12), 36.1 (C-1), 26.4 (C-4'), 23.4 (C-13), 22.8 (C-7).

Demethylalangiside (2.5): amorphous powder; m.p. 180-182 °C; ^1H NMR (CD₃OD, 400 MHz): δ 7.40 (1H, d, $J = 2.0$ Hz, H-9), 6.64 (1H, s, H-1), 6.54 (1H, s, H-4), 5.53 (1H, dt, $J = 11.2, 17.0$ Hz, H-14), 5.48 (1H, d, $J = 12.0$ Hz, H-11), 5.25 (1H, brd, $J = 16.8$ Hz, H-5a), 5.16 (1H, dd, $J = 10.4, 1.2$ Hz, H-5b), 4.68 (1H, d, $J = 8.0$ Hz, H-1'), 4.64 (1H, brt, $J = 3.6$ Hz, H-13a), 4.63 (1H, dt, $J = 12.8, 3.6$ Hz, H-6a), 3.91 (1H, brd, $J = 12.0$ Hz, H-6'a), 3.68 (1H, dd, $J = 12.0, 5.2$ Hz, H-6'b), 3.37 (1H, t, $J = 8.8$ Hz, H-3'), 3.22 (1H, brt, $J = 8.1$ Hz, H-2'), 3.20 (1H, m, H-12a), 2.86 (1H, dt, $J = 12.8, 2.8$ Hz, H-6b), 2.57, 2.70 (2H, m, H-5), 2.66 (1H, m, H-12), 2.26 (1H, dt, $J = 12.8, 4.8$ Hz, H-13b), 1.34 (1H, td, $J = 12.8, 2.8$ Hz, H-13a). ^{13}C NMR (CD₃OD, 100 MHz): δ 164.5 (C-8), 147.3 (C-9), 143.8 (C-3), 143.8 (C-2), 132.6 (C-14), 127.6 (C-13b),

125.9 (C-4a), 111.9 (C-1), 114.6 (C-4), 98.1 (C-1'), 96.0 (C-11), 55.5 (13a), 39.7 (C-6), 27.9 (C-5), 26.2 (C-12a).

1', 2'-dehydrotubulosine (2.6): amorphous powder; m.p. 167-170°C (dec.); ¹H NMR (CD₃OD, 400 MHz): δ 7.24 (1H, d, *J* = 8.8 Hz, H-8'), 6.85 (1H, d, *J* = 8.8 Hz, H-7'), 6.83 (1H, s, H-5'), 6.54 (1H, s, H-8), 6.12 (1H, s, H-11), 3.84 (2H, m, H-3'), 3.64 (3H, s, OMe-9), 3.20 (3H, s, OMe-10), 3.04 (1H, m, H-11b). ¹³C NMR (CD₃OD, 100 MHz): δ 166.5 (C-1'), 152.0 (C-6'), 113.4 (C-8'), 111.4 (C-5'), 107.5 (C-11), 103.3 (C-7'), 102.6 (C-8), 62.0 (C-11b), 147.5 (C-9), 146.7 (C-10), 44.2 (C-3'), 51.5 (C-6), 27.9 (C-7).

Demethylpsychotrine (2.7): amorphous powder; m.p. 166-168 °C; ¹H NMR (CD₃OD, 400 MHz): δ 7.02 (1H, s, H-8'), 6.42 (1H, s, H-8), 6.40 (1H, s, H-5'), 6.35 (1H, s, H-11), 3.73 (3H, s, OMe-7'), 3.59 (3H, s, OMe-10), 2.70 (2H, m, H-7). ¹³C NMR (CD₃OD, 100 MHz): δ 171.0 (C-1'), 168.0 (C-7'), 150.0 (C-6'), 146.0 (C-9), 145.0 (C-10), 136.6 (C-4'a), 117.0 (C-5'), 114.7 (C-8), 110.5 (C-8'), 107.5 (C-11), 62.3 (C-11b), 59.5 (C-4), 51.5 (C-6), 27.9 (C-7).

2.3.4 The cytotoxic activity against HeLa and KB cell lines by MTT assay

All tested compounds (1 mg each) were tested for cytotoxic activity against HeLa and KB cell lines by MTT assay. This assay was kindly performed by Natural Products Research Section, Research Division, National Cancer Institute, Thailand.

CHAPTER III

BIOACTIVE COMPOUNDS FROM THE RHIZOMES OF *Curcuma longa*

3.1 Introduction

Curcuma longa or turmeric (Zingiberaceae) is a medicinal plant widely cultivated in tropical regions of Asia. It has been widely used as a yellow colorant and spice in many foods. The turmeric extract from the rhizomes, commonly called curcuminoids, mainly composes of curcumin (75-95%) together with a small amount of demethoxycurcumin and bisdemethoxycurcumin as shown in Figure 3.1.

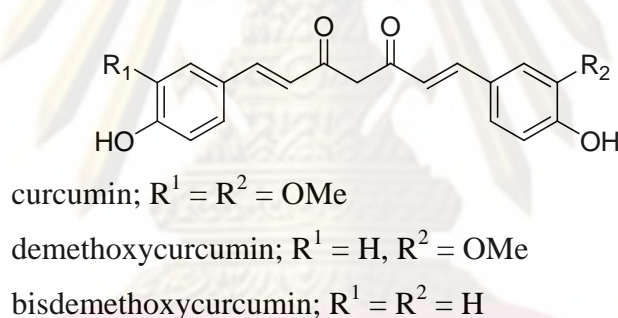


Figure 3.1 The structures of curcuminoids

Curcuminoids have been reported to possess a variety of biological and pharmacological activities, including antioxidant [71-72], antiinflammatory [73-74], antitumor [75-76], antiHIV protease [77-78] and antiangiogenic activity [79]. Recent experiments have shown that turmeric extract could reduce blood sugar, which may be used as a remedy to treat diabetes mellitus [80-81]. Du and coworkers synthesized curcuminoids and analogues by modifying β -diketo moiety and examined their inhibitory effect against α -glucosidase [82]. However, the inhibition of synthesized analogues was vary, indicating that β -diketo moiety is not crucial in blocking enzyme function. The results indicated that natural curcuminoids and their analogues could inhibit the activity of α -glucosidase. The interesting discovery of the α -glucosidase

inhibitory activity of phenolic compounds like curcuminoids prompted us to study a series of curcumin analogues.

In the present study, the natural curcuminoids and the synthetic curcumin analogues are synthesized and evaluated *in vitro* for the α -glucosidase inhibitory activity. The structure activity relationship is also discussed.

3.1.1 α -Glucosidase inhibitors

α -Glucosidase enzyme (α -D-glucoside glucohydrolase; EC. 3.2.1.20) is a group of membrane-bound enzymes that locates at the epithelium of the small intestine and is the key enzyme involved in breaking down carbohydrates. It specifically hydrolyses 1,4-glycosidic linkages, thereby releasing an α -D-glucose from starch as shown in Figure 3.2.

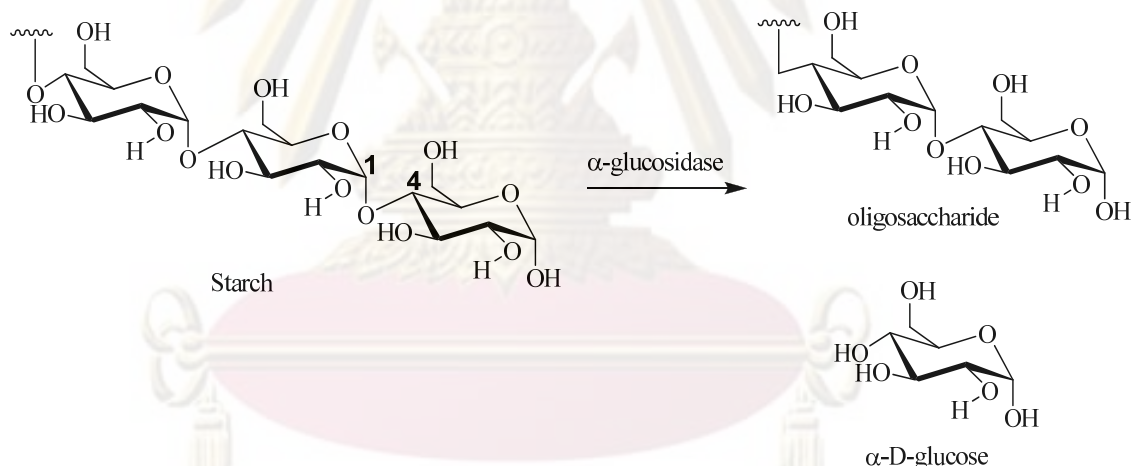


Figure 3.2 Hydrolysis of 1,4-glycosidic linkages

In digestive tract, starch is broken down by amylase enzyme to oligosaccharides such as maltose, which are further hydrolysed by membrane-bound intestinal α -glucosidase (sucrase, maltase and isomaltase) to monosaccharide such as glucose (Figure 3.3)[83].

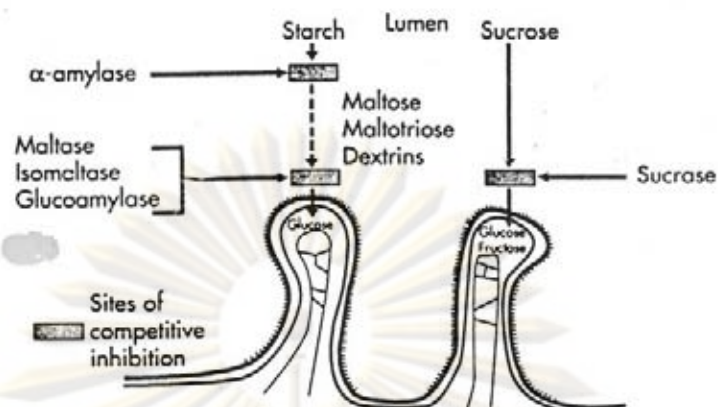


Figure 3.3 Digestion of starch in the small intestine by α -glucosidase enzyme

Most α -glucosidase inhibitors are saccharide-like compounds that display their inhibition by mimicking their structures as oligosaccharide substrate. They act as competitive inhibitors of α -glucosidase enzymes, which prevent the binding and enzymatic hydrolysis of the oligosaccharides substrate in the small intestine. Therefore, the inhibition activity of α -glucosidase results in lowering the high blood sugar in diabetic patients. The structures of particular α -glucosidase inhibitors are summarized in Figure 3.4

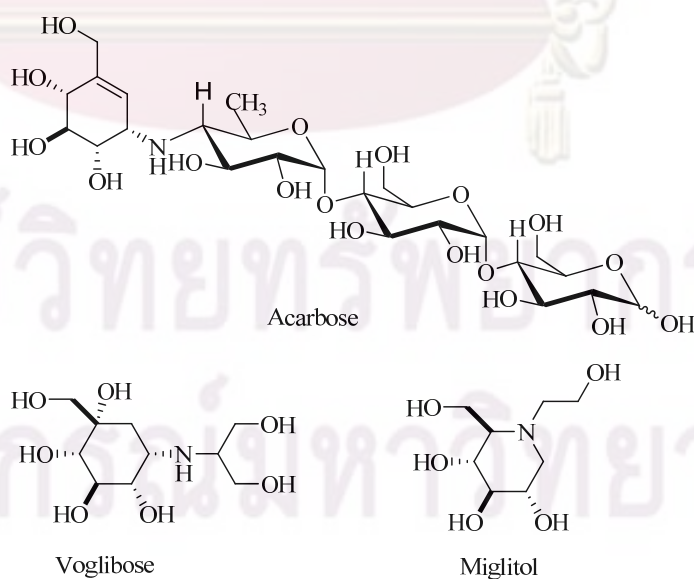


Figure 3.4 Structures of α -glucosidase inhibitors

3.2 Results and discussion

3.2.1 Isolation of curcuminoids

The air-dried rhizomes of *C. longa* were refluxed with 80% MeOH-H₂O to give the 80% MeOH-H₂O extract. The extract were partitioned with hexane. The hexane layer was evaporated under reduced pressure to yield yellow oil. The aqueous layer was adjusted to 50% MeOH-H₂O and partitioned with CH₂Cl₂ to give the CH₂Cl₂ extract. The CH₂Cl₂ extract was purified on silica gel CC using 1% MeOH-CH₂Cl₂ to afford three curcuminoids as shown in Scheme 3.1. The three isolated curcuminoids showed three single spots on TLC. They were identified as curcumin (**3.1**), demethoxycurcumin (**3.2**) and bisdemethoxycurcumin (**3.3**) by comparison on silica gel TLC with authentic samples (Figure 3.5).

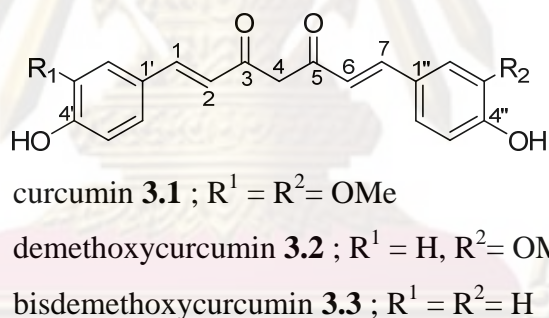
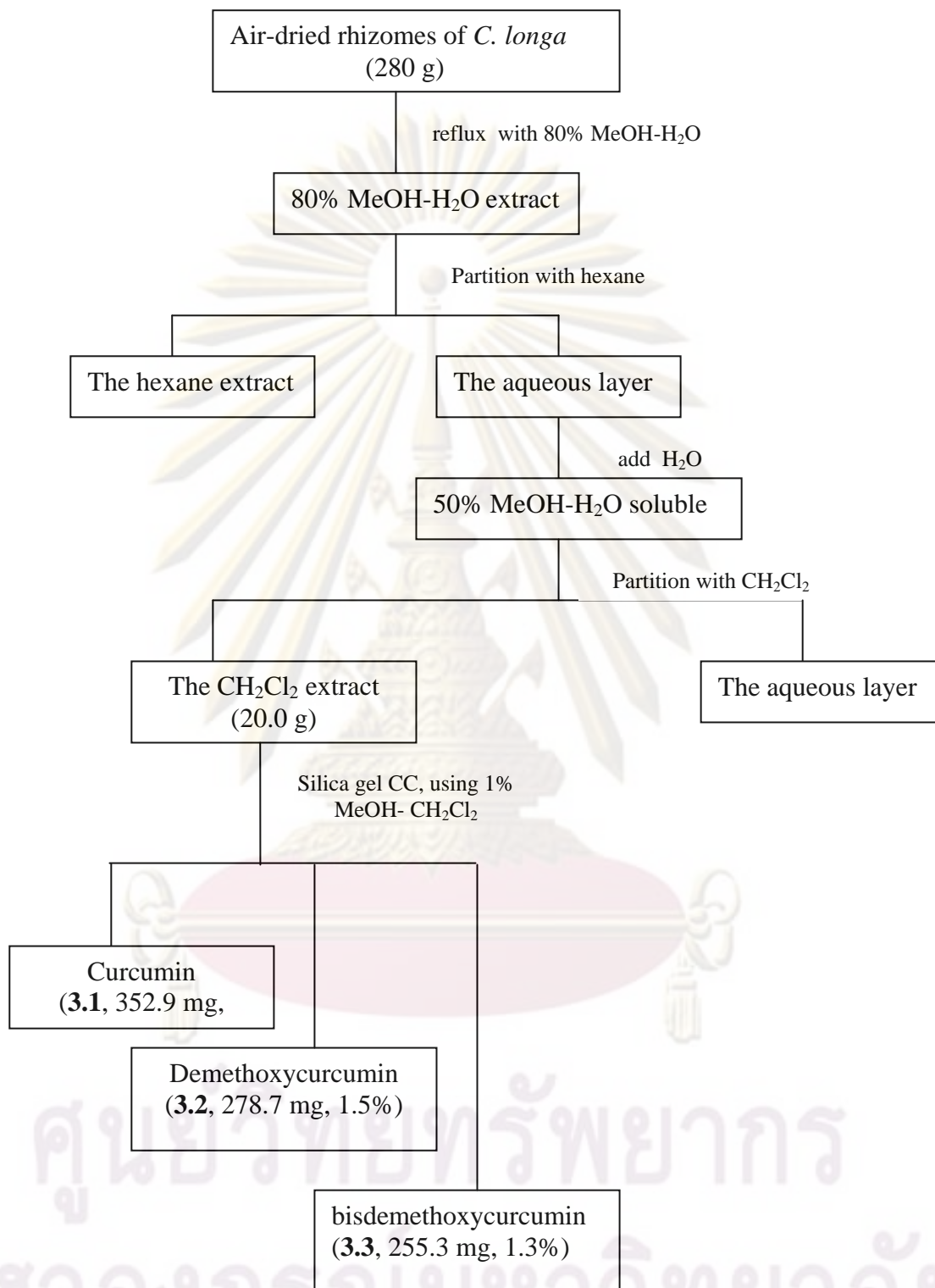


Figure 3.5 Curcuminoids from the *Curcuma longa* rhizomes

ศูนย์วิทยทรัพยากร
 จุฬาลงกรณ์มหาวิทยาลัย



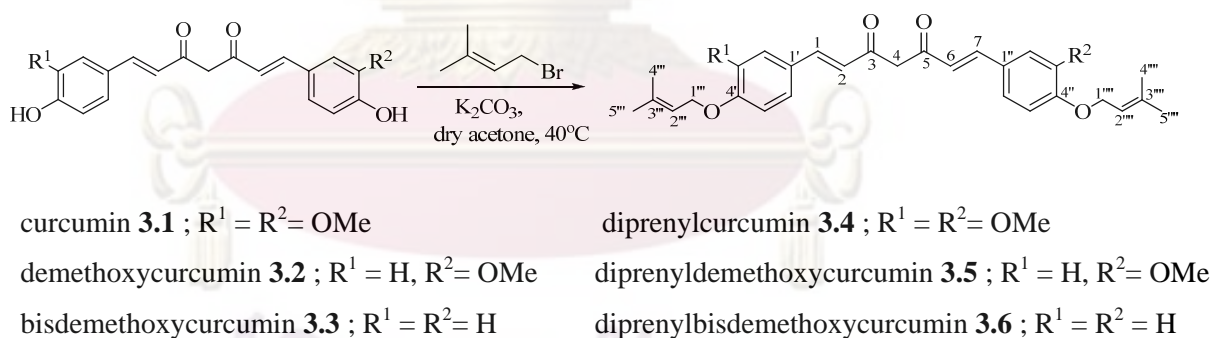
Scheme 3.1 The isolation procedure of curcuminoids from *Curcuma longa* rhizomes

3.2.2 Synthesis of curcumin analogues (3.3-3.14)

Curcuminoids (**3.1-3.3**) were modified by alkylation reactions : prenylation, acetylation and methylation. Of 11 synthesized curcuminoids analogues, four new (**3.4-3.6** and **3.9**) and seven known (**3.7, 3.8, 3.10, 3.11-3.14**) derivatives were obtained.

3.2.2.1 Prenylation of curcuminoids (3.1-3.3)

The prenylation of curcumin (**3.1**) was performed by adding 3-methylallyl bromide / acetone in the presence of K_2CO_3 . The reaction mixture was refluxed at $40^\circ C$ for 2 h. After typical work up, the crude product was purified on preparative TLC developed with 1% MeOH- CH_2Cl_2 to give diprenylcurcumin **3.4**. Similarly, demethoxycurcumin **3.2** and bisdemethoxycurcumin **3** were treated with the same protocol for the synthesis of **3.4** to give diprenyldemethoxycurcumin **3.5** and diprenylbisdemethoxycurcumin **3.6**, respectively (Scheme 3.2).



Scheme 3.2 Prenylation of curcuminoids (**3.1-3.3**)

Structural elucidation of diprenylcurcuminoids (3.4-3.6)

Diprenylcurcumin **3.4** was obtained as yellow solid. Its molecular formula of $C_{31}H_{36}O_6$ was established by LC-APCIMS (m/z 505.2537 $[M+H]^+$). In the 1H NMR spectrum of **4**, half of signals for the molecular formula were observed, indicating that **4** had a symmetrical structure. In the 1H NMR spectrum, signals

assignable to two sets of trisubstituted benzene at δ 7.04 (2H, d, J = 8.0 Hz, H-6' and H-6''), 7.00 (2H, s, H-2' and H-2''), 6.80 (2H, d, J = 8.4 Hz, H-5' and H-5'') and two sets of olefinic signals at δ 7.52 (2H, d, J = 16.0 Hz, H-1 and H-7), 6.40 (2H, d, J = 16.0 Hz, H-2 and H-6) were observed, suggesting the presence of two *trans*-cinnamoyl groups. In addition, the ^1H NMR spectrum showed the signals at δ 5.45 (2H, brs, H-2''' and H-2'''), δ 4.55 (4H, d, J = 6.0 Hz, H-1''' and H-1'''), δ 1.71 (6H, s, Me-4''' and Me-4''') and δ 1.68 (6H, s, Me-5''' and Me-5'''), indicating the presence of two prenyloxy groups instead of two hydroxyl groups at C-4' and C-4''. The positions of prenyloxy groups were located at C-4' and C-4'' by HMBC cross peaks between H-1'''(1''') and C-4' (4''). Key HMBC correlations of **3.4** were shown in Figure 3.6.

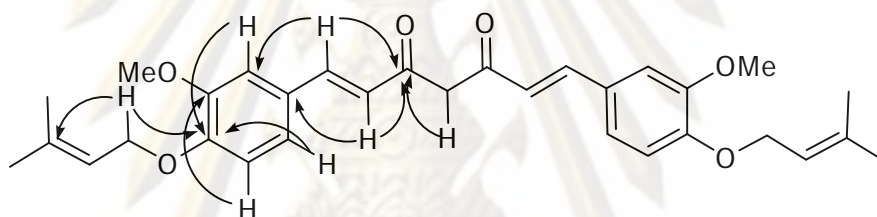


Figure 3.6 Key HMBC correlations of **3.4**

Diprenyldemethoxycurcumin **3.5** was isolated as yellow solid. The $[\text{M}+\text{H}]^+$ ion peak at m/z 475.2495 in the LC-APCIMS corresponded to the molecular formula $\text{C}_{30}\text{H}_{34}\text{O}_5$. The ^1H NMR spectrum of **3.5** was similar to that of **3.4**, except for the presence of one methoxyl signal and different aromatic systems. The signals of a disubstituted benzene at δ 7.43 (2H, d, J = 8.8 Hz, H-2' and H-6'), 6.83 (2H, d, J = 8.8 Hz, H-3' and H-5') were observed, in addition to the signals of a trisubstituted benzene. In addition, the ^1H NMR spectrum also showed the presence two prenyloxy groups at δ 5.43 (2H, dd, J = 6.8, 1.6 Hz, H-2''' and H-2'''), 4.57 (2H, d, J = 6.8 Hz, H-1'''), 4.49 (2H, d, J = 6.8 Hz, H-1'''), 1.77 (3H, s, Me-4'''), 1.74 (3H, s, Me-5''') and δ 1.73 (6H, s, Me-4''' and H-5'''). In the HMBC spectrum of **3.5**, the correlations between H-1''' / C-4' and H-1''' / C-4'' confirmed the positions of these prenyloxy groups. Key HMBC correlations of **3.5** were shown in Figure 3.7.

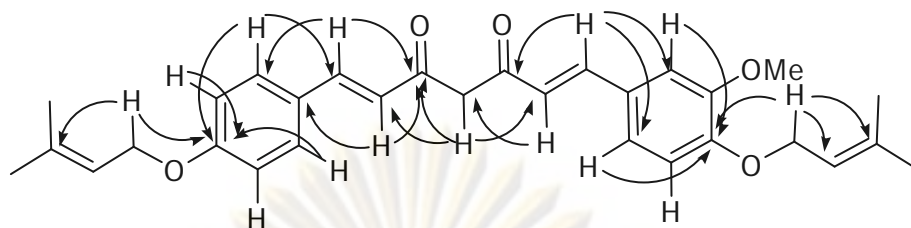


Figure 3.7 Key HMBC correlations of **3.5**

Diprenylbisdemethoxycurcumin **3.6** was obtained as yellow solid, having the molecular formula $C_{29}H_{32}O_4$ as determined by high resolution LC-APCIMS. The 1H NMR spectrum of **3.6** showed half of the signals for the molecular formula, indicating that **3.6** had a symmetrical structure. In the 1H NMR spectrum, the signals of two sets of disubstituted benzene at δ 7.37 (4H, d, $J = 8.4$ Hz, H-2', H-2'', H-6' and H-6'') and 6.78 (4H, d, $J = 8.4$ Hz, H-3', H-3'', H-5' and H-5'') were observed, but methoxy signal was not detected. In addition, the 1H NMR spectrum also showed the presence two prenyloxy groups at δ 5.38 (2H, m, H-2''' and H-2'''), 4.44 (4H, d, $J = 6.8$ Hz, H-1''' and H-1'''), 1.72 (6H, s, Me-4''' and Me-4''') and 1.67 (6H, s, H-5''' and Me-5'''). In the HMBC experiment, the correlations between H-4/C-3(5) and H-1''' (1''') / C-4' (4'') indicated that methylene group was flanked by two carbonyl groups and the two prenyloxy groups were attached at C-4' and C-4'' respectively. Key HMBC correlations of **3.6** was shown in Figure 3.8.

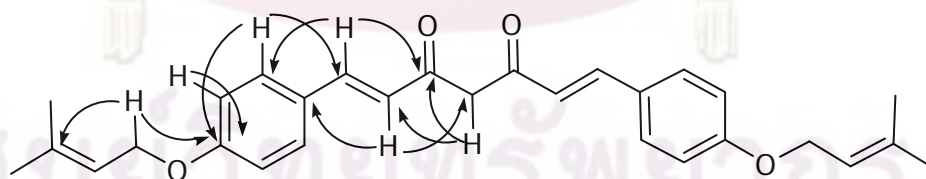
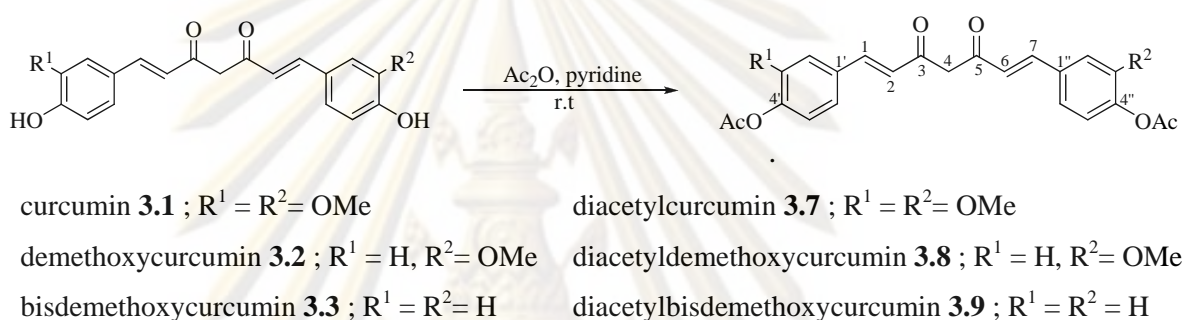


Figure 3.8 Key HMBC correlations of **3.6**

3.2.2.3 Acetylation of curcuminoids (3.1-3.3)

Curcumin (**3.1**) was acetylated using acetic anhydride in pyridine. The

mixture was stirred for 1.5 h at room temperature. After typical work up, the crude product was purified on preparative TLC developed with 1% MeOH-CH₂Cl₂ to give diacetylcurcumin **3.7** (Scheme 3.3). Similarly, demethoxycurcumin **3.2** and bisdemethoxycurcumin **3.3** were treated with the same protocol for the synthesis of **3.7** to give diacetyldemethoxycurcumin **3.8** and diacetylbisdemethoxycurcumin **3.9**, respectively. Of compounds synthesized, **3.9** is a new diacetylcurcuminoid whose structure was confirmed by HREIMS and 2D NMR.



Scheme 3.3 Acetylation of curcuminoids (**3.1-3.3**)

Structural elucidation of diacetylcurcuminoids (**3.7- 3.9**)

The ¹H NMR spectrum of **3.7** showed half of signals for the molecular formula, indicating that **3.7** had a symmetrical structure. Furthermore, the ¹H NMR spectrum showed two sets of trisubstituted benzene signals at δ 7.08 (2H, d, *J* = 8.0 Hz, H-6' and H-6''), 7.06 (2H, brs, H-2' and H-2''), 6.99 (2H, d, *J* = 8.0 Hz, H-5' and H-5'') and two sets of olefinic signals at δ 7.54 (2H, d, *J* = 16.0 Hz, H-1 and H-7), 6.48 (2H, d, *J* = 15.6 Hz, H-2 and H-6), suggesting the presence of two *trans*-cinnamoyl groups. In addition, in the ¹H NMR spectrum showed a singlet signal at δ 2.27 (6H, s, Me-2''' and Me-2''''), indicating that two hydroxyl groups in **3.1** were replaced by acetyl groups. However, the structure of **3.7** was identified on the basis of spectral data comparison with literature values [84]. Therefore, the structure of **3.7** was determined to be diacetylcurcumin.

Diacetyldemethoxycurcumin **3.8**, the ¹H NMR spectrum of **3.8** was similar to that of **3.7**, except for the presence of one methoxyl signal and different aromatic systems. The signals of a disubstituted benzene at δ 7.49 (2H, d, *J* = 8.4 Hz,

H-2' and H-6'), 7.06 (2H, d, $J = 8.4$ Hz, H-3' and H-5') were observed, in addition to the signals of a trisubstituted benzene. In addition, the ^1H NMR spectrum also showed the presence two acetyl protons at δ 2.27 (3H, s, Me-2''') and 2.24 (3H, s, Me-2'''). However, the structure of **3.8** was identified on the basis of spectral data comparison with literature values [85]. Thus, the structure of **3.8** was determined to be diacetyldemethoxycurcumin.

Diacetylbisdemethoxycurcumin **3.9** was isolated as yellow solid. Its high resolution LC-APCIMS m/z 393.1340 agreed with a molecular formula of $\text{C}_{23}\text{H}_{20}\text{O}_6$. The ^1H NMR spectrum of **3.9** showed half of the signals for the molecular formula, indicating that **3.9** had a symmetrical structure. In the ^1H NMR spectrum, the signals of two sets of disubstituted benzene at δ 7.49 (4H, d, $J = 8.4$ Hz, H-2', H-2'', H-6' and H-6'') and 7.05 (4H, d, $J = 8.4$ Hz, H-3', H-3'', H-5' and H-5'') and a pair of trans-olefinic protons at δ 7.55 (2H, d, $J = 16.0$ Hz, H-1 and H-7), 6.49 (2H, d, $J = 15.6$ Hz, H-2 and H-6) were observed. In addition, the ^1H NMR spectrum also showed the presence two acetyl groups at δ 2.25 (6H, s, Me-2''' and Me-2'''). The HMBC spectrum of **3.9**, the correlations between Me-2''' (2''') and C-1''' (1''') confirmed the presence of two acetyl groups. Key HMBC correlation of **3.9** was shown in Figure 3.9.

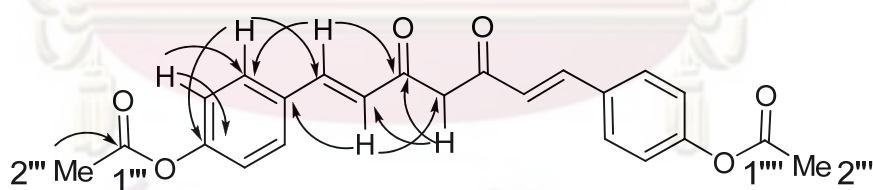


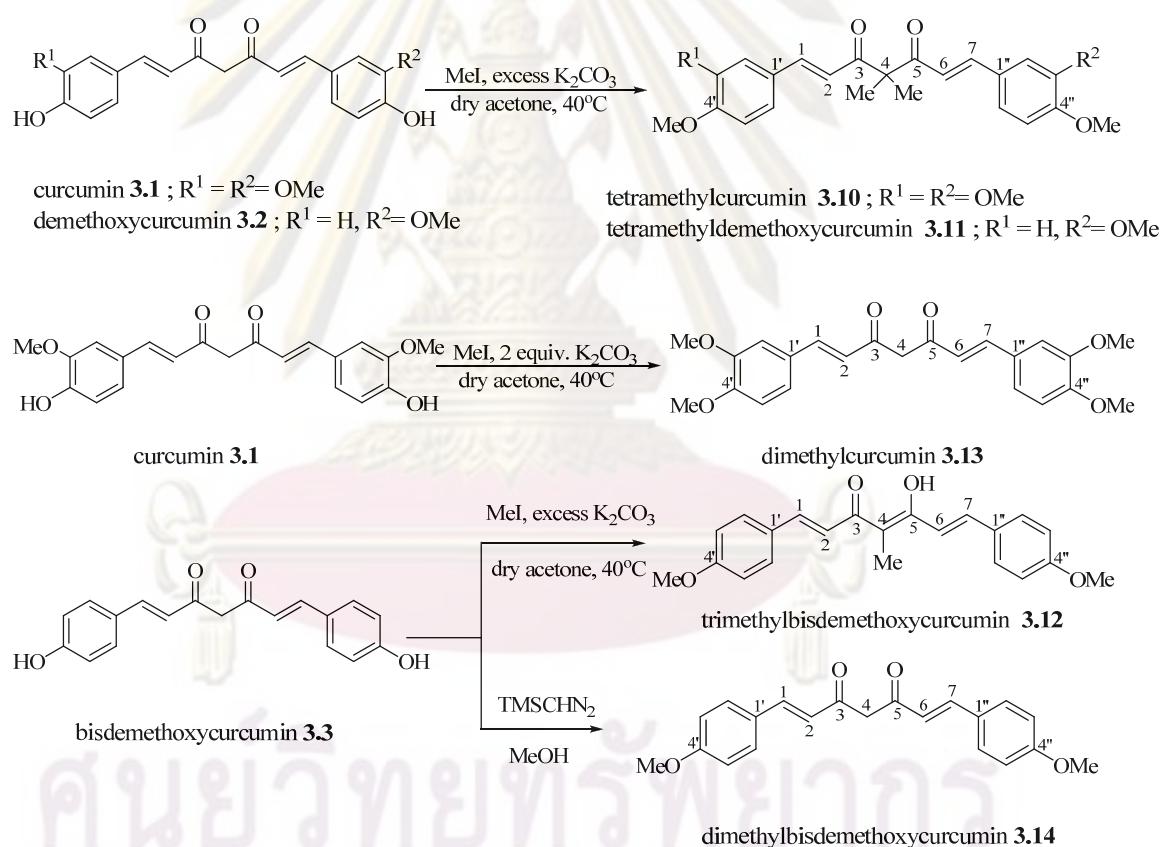
Figure 3.9 Key HMBC correlations of **3.9**

3.2.2.5 Methylation of curcuminoids (3.1-3.3)

The methylation of curcumin (**3.1**) was performed by adding methyl iodide / acetone in the presence of K_2CO_3 . The reaction mixture was refluxed at 40°C for 1.5 h. After typical work up, the crude product was purified on preparative TLC

developed with 1% MeOH-CH₂Cl₂ to give tetramethylcurcumin **3.10**. Similarly, demethoxycurcumin **3.2** and bisdemethoxycurcumin **3.3** were treated with the same protocol for the synthesis of **3.10** to give tetramethyldemethoxycurcumin **3.11** and trimethylbisdemethoxycurcumin **3.12**, respectively.

Compound **3.13** was synthesized using the same protocol for the synthesis of **3.10** and two equivalence of K₂CO₃ was used. The ¹H NMR spectrum of **3.13** was similar to that of **3.10** except the methylene group was not methylated. In addition, compound **3.14** was synthesized by using trimethylsilyldiazomethane from bisdemethoxycurcumin **3.3** (Scheme 3.4).

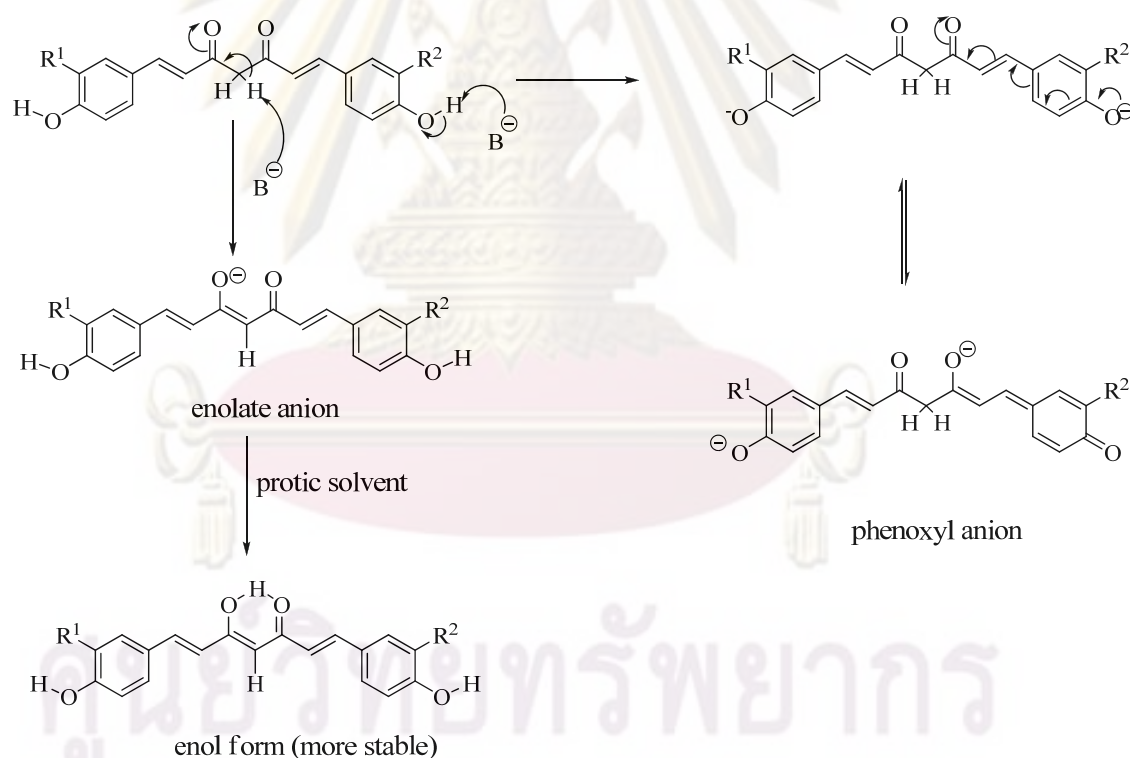


Scheme 3.4 Methylation of curcuminoids (**3.1-3.3**)

The curcuminoids have two types of acidic proton at phenolic and methylene protons, which approximate pK_a values of phenolic and methylene protons are 10.0 and 11.0, respectively [86]. Therefore, enolate and phenoxyl anions were generated in the base condition. The propose mechanism of reaction involved deprotonation of

phenolic and methylene groups to give phenoxyl and enolate anions (Scheme 3.5), respectively. In addition, the acidity of phenolic groups can be enhanced by resonance effect throughout the structure. Generally, treatment of curcuminoids with alkylating agent lead to the first alkylation at phenolic groups.

Curcumin **3.1** was methylated using methyl iodide in limited amount of base to give dimethylcurcumin **3.13**. These result revealed that hydroxyl groups were only methylated. On the other hand, curcuminoids (**3.1-3.3**) were methylated using excess amount of base to give tetramethylcurcuminoids (**3.10-3.11**) and trimethylbisdemethoxycurcumin (**3.12**). These results showed that both of hydroxyl and methylene groups were methylated. Therefore, the amount of base may be related to the alkylation reaction.



Scheme 3.5 Generation of phenoxyl and enolate anions in basic condition

Structural elucidation of tetramethylcurcuminoids (3.10-3.11), trimethylbisdemethoxycurcumin (3.12), dimethylcurcumin 3.13 and dimethylbisdemethoxycurcumin 3.14

The ^1H NMR spectrum of **3.10** showed half of signals for the molecular formula, indicating that **3.10** had a symmetrical structure. Furthermore, the ^1H NMR spectrum showed two sets of trisubstituted benzene signals at δ 7.30 (2H, d, $J = 1.6$ Hz, H-2' and H-2''), 7.21 (2H, dd, $J = 8.4, 1.6$ Hz, H-6' and H-6''), 6.95 (2H, d, $J = 8.4$ Hz, H-5' and H-5'') and two sets of olefinic signals at δ 7.59 (2H, d, $J = 15.6$ Hz, H-1 and H-7), 6.88 (2H, d, $J = 15.6$ Hz, H-2 and H-6), suggesting the presence of two *trans*-cinnamoyl groups. In addition, in the ^1H NMR spectrum showed two singlet signals at δ 3.81 (6H, s, OMe-4' and OMe-4'') and δ 1.42 (6H, s, Me-4), indicating that two hydroxyl groups and two methylene protons in **3.1** were replaced by methyl groups. However, the structure of **3.10** was identified on the basis of spectral data comparison with literature values [87]. Therefore, the structure of **3.10** was determined to be tetramethylcurcumin.

Tetramethyldemethoxycurcumin **3.11**, the ^1H NMR spectrum of **3.11** was similar to that of **3.10**, except for the presence of one methoxyl signal and different aromatic systems. The signals of a disubstituted benzene at δ 7.46 (2H, d, $J = 8.8$ Hz, H-2' and H-6'), 6.85 (2H, d, $J = 8.8$ Hz, H-3' and H-5') were observed, in addition to the signals of a trisubstituted benzene. In addition, in the ^1H NMR spectrum showed three singlet signals at δ 3.89 (3H, s, OMe-4''), δ 3.81 (3H, s, OMe-4') and δ 1.46 (6H, s, Me-4), indicating that two hydroxyl and two methylene protons in **3.1** were replaced by methyl groups. Thus, the structure of **3.11** was determined to be tetramethyldemethoxycurcumin.

Trimethylbisdemethoxycurcumin **3.12** was obtained as yellow solid. The ^1H NMR spectrum of **3.12** showed half of the signals for the molecular formula similar, indicating that it had a symmetrical structure. In ^1H NMR spectrum, two methoxy signals were absent compared with those of **3.10**, and the signals of two sets of disubstituted benzene at δ 7.45 (4H, d, $J = 8.4$ Hz, H-2', H-2'', H-6' and H-6'') and 6.84 (4H, d, $J = 8.8$ Hz, H-3', H-3'', H-5' and H-5'') were observed, instead of the signals of two trisubstituted benzene in **3.10**. In addition, the ^1H NMR spectrum also

showed the presence of one methyl group at δ 2.14 (3H, s, Me-4). The above data indicated that both hydroxyls and one methylene proton of **3.12** were methylated. This was supported by HMBC correlations between Me-4/C-3, C-5 (δ 182.0) and Me-4/C-4 (δ 106.0). Key HMBC correlations of **3.12** are shown in Figure 3.10. On the basis of NMR data, the structure of **3.12** was tentatively determined to be trimethylbisdemethoxycurcumin.

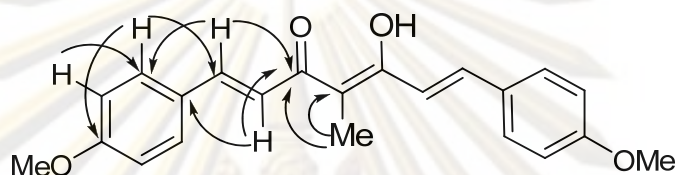


Figure 3.10 Key HMBC correlations of **3.12**

Dimethylcurcumin **3.13**, the ^1H NMR spectrum of **3.13** showed half of signals for the molecular formula, indicating that **3.13** had a symmetrical structure. Furthermore, the ^1H NMR spectrum showed two sets of trisubstituted benzene signals at δ 7.13 (2H, d, $J = 8.0$ Hz, H-6' and H-6''), 7.08 (2H, brs, H-2' and H-2''), 6.87 (2H, d, $J = 8.4$ Hz, H-5' and H-5'') and two sets of olefinic signals at δ 7.59 (2H, d, $J = 16.0$ Hz, H-1 and H-7), 6.48 (2H, d, $J = 15.6$ Hz, H-2 and H-6), suggesting the presence of two *trans*-cinnamoyl groups. In addition, in the ^1H NMR spectrum showed a singlet signal at δ 3.92 (6H, s, OMe-4' and OMe-4'') and signals of methylene groups at δ 5.82 (2H, s, H-4), indicating that only two hydroxyl groups in **3.1** were replaced by methyl groups. However, the structure of **3.13** was identified on the basis of spectral data comparison with literature values [88]. Therefore, the structure of **3.13** was determined to be dimethylcurcumin.

Dimethylbisdemethoxycurcumin **3.14**, the ^1H NMR spectrum of **3.14** showed half of the signals for the molecular formula, indicating that **3.14** had a symmetrical structure. In ^1H NMR spectrum, the signals of two sets of disubstituted benzene at δ 7.45 (4H, d, $J = 8.4$ Hz, H-2', H-2'', H-6' and H-6'') and 6.80 (4H, d, $J = 8.8$ Hz, H-3', H-3'', H-5' and H-5'') were observed, but methoxy signal was not detected. In addition, the ^1H NMR spectrum also showed the presence two methoxy

groups at δ 3.85 (6H, s, OMe-4' and OMe-4'') and signals of methylene groups at δ 5.70 (2H, s, H-4), indicating that only two hydroxyl groups in **3.3** were replaced by methyl groups. However, the structure of **3.14** was identified on the basis of spectral data comparison with literature values [77]. Therefore, the structure of **3.14** was determined to be dimethylbisdemethoxycurcumin.

3.2.3 α -Glucosidase inhibitory activity of curcuminoids and curcumin analogues

The α -glucosidase inhibitory activity of curcuminoids **3.1-3.3** and synthesized alkylcurcuminoids (**3.4-3.14**) were evaluated by colorimetric method and the results are shown in Table 3.1. Curcuminoids **3.1-3.3** showed inhibitory activities against α -glucosidase with the IC_{50} values of 0.81, 0.31 and 0.47 mM, respectively, which were comparable to that of Acarbose[®] and exhibited more potent inhibitory activity than synthesized alkylcurcuminoids (**3.4-3.14**). The results suggested that simple curcumin having at least one hydroxyl group attached to aromatic moiety possessed enhanced inhibitory effect. Interestingly, the synthesized alkylcurcuminoids (**3.4-3.14**) showed lower inhibitory activity with higher IC_{50} values than the natural curcuminoids (**3.1-3.3**). The results suggested that the introduction of alkyl groups at hydroxyl groups of curcuminoids led to the activities lower than those of curcuminoids. Therefore, the hydroxyl groups might be associated with inhibitory effect. We assumed that the hydroxyl groups of curcuminoids and curcumin analogues played a very important role on the enzyme inhibitory activity.

In addition, tetramethylcurcuminoids (**3.10-3.11**) and trimethylbisdemethoxy curcumin (**3.12**), whose C-4 was methylated, showed weak α -glucosidase inhibition with the IC_{50} values of 1.39, 0.89 and 5.27 mM, respectively. The results suggested that the methylene protons in original curcuminoids might be affect in inhibitory effect. In order to test this assumption, dimethylcurcumin **3.13** and dimethylbisdemethoxycurcumin **3.14**, whose C-4 were not methylated, were synthesized and evaluated for α -glucosidase inhibitory effect. However, **3.13** and **3.14** showed poor inhibition ($IC_{50} \geq 10.0$ mM.), thus indicating that the presence of C-4

methylene proton is not associated with blocking enzyme function. Furthermore, curcumin analogues **3.5**, **3.8** and **3.11** were asymmetrical curcuminoids which exhibited more potent inhibitory activity than the symmetrical curcuminoid congeners **3.6-3.7**, **3.9-3.10** and **3.12-3.14**.

In conclusion, curcuminoids isolated from *C. longa* showed potent α -glucosidase inhibitory activity while the synthetic alkylated curcuminoids exhibited weak inhibitory effects against α -glucosidase. The study suggested that the hydroxyl groups in curcuminoids play a very important role on the enzyme inhibitory activity.

Table 3.1 α -Glucosidase inhibitory effect of the natural curcuminoids (**3.1-3.3**) and synthesized alkylcurcuminoids (**3.4-3.14**)

Compounds	IC ₅₀ (mM)
curcumin (3.1)	0.81
demethoxycurcumin (3.2)	0.31
bisdemethoxycurcumin (3.3)	0.47
diprenylcurcumin (3.4)	0.90
diprenyldemethoxycurcumin (3.5)	0.73
diprenylbisdemethoxycurcumin (3.6)	1.30
diacetylcurcumin (3.7)	2.87
diacetyldemethoxycurcumin (3.8)	2.56
diacetylbisdemethoxycurcumin (3.9)	≥10.00
tetramethylcurcumin (3.10)	1.39
tetramethyldemethoxycurcumin (3.11)	0.89
trimethylbisdemethoxycurcumin (3.12)	5.27
dimethylcurcumin (3.13)	≥10.00
dimethylbisdemethoxycurcumin (3.14)	≥10.00
Acarbose ^{® a}	0.57

^aStandard control

3.3 Experimental

3.3.1 General experimental procedures

The NMR spectra were recorded with a Varian model Mercury+ 400 nuclear magnetic resonance spectrometer. The chemical shifts in δ (ppm) were assigned with reference to the signals of residual protons in deuterated solvents or using TMS as an internal standard in some cases. ESIMS and LC-APCIMS spectra were obtained from a VG TRIO 2000 and Bruker Daltonic Data Analysis 3.3 (microTOF) mass spectrometer, respectively. Silica gel 60 Merck cat. No. 7734 and 7729 were used for open column chromatography. Thin layer chromatography (TLC) was performed on precoated Merck silica gel 60 F₂₅₄ plates (0.25 mm thick layer).

3.3.2 Extraction and isolation

The air-dried rhizomes of *Curcuma longa* (280.0 g) were refluxed with 80% MeOH-H₂O to give the 80% MeOH-H₂O extract. The extract were partitioned with hexane. The hexane layer was evaporated under reduced pressure to yield yellow oil (21.4 g). The aqueous layer was adjusted to 50% MeOH-H₂O and partitioned with CH₂Cl₂. The CH₂Cl₂ layer was evaporated under reduced pressure to yield orange powder (42.9 g). The CH₂Cl₂ extract (20.0 g) was purified on silica gel CC using 1% MeOH-CH₂Cl₂ to afford three known major compounds, which were identified as curcumin (**3.1**), demethoxycurcumin (**3.2**) and bisdemethoxycurcumin (**3.3**) by comparison on silica gel TLC with authentic samples.

3.3.3 General procedure for the preparation of curcumin analogues

The curcumin analogues (**3.4-3.14**) were synthesized from alkylation reaction of curcumin (**3.1**), demethoxycurcumin (**3.2**) and bisdemethoxycurcumin (**3.3**), using four reagents; 3-methylallyl bromide, acetic anhydride, methyl iodide and trimethylsilyldiazomethane. The first reagent, 3-methylallyl bromide was reacted with

curcumin (**3.1**), demethoxycurcumin (**3.2**) and bisdemethoxycurcumin (**3.3**) to give diprenylcurcuminoids (**3.4**), (**3.5**) and (**3.6**), respectively. The second reagent, acetic anhydride was reacted with curcumin (**3.1**), demethoxycurcumin (**3.2**) and bisdemethoxycurcumin (**3.3**) to give diacetylcurcuminoids (**3.7**), (**3.8**) and (**3.9**), respectively. The third reagent, methyl iodide was reacted with curcumin (**3.1**), demethoxycurcumin (**3.2**) and bisdemethoxycurcumin (**3.3**) to give tetramethylcurcuminoids (**3.10**), (**3.11**) and trimethylbisdemethoxycurcumin (**3.12**), respectively. Dimethylcurcumin (**3.13**) was synthesized using the same protocol for the synthesis of **3.10** but two equivalences of anhydrous K_2CO_3 were used while dimethylbisdemethoxycurcumin (**3.14**) was synthesized using the protocol for the synthesized of **3.12** but trimethylsilyldiazomethane was used instead of methyl iodide.

3.3.3.1 Preparation of diprenylcurcuminoids (3.4-3.6)

Diprenylcurcumin (3.4). A mixture of curcumin (**3.1**, 53.5 mg, 0.15 mmol) and excess anhydrous K_2CO_3 (61.0 mg, 0.45 mmol) in dry acetone (1.5 mL) was added 3-methylallyl bromide (90.0 μ L, 0.75 mmol). The mixture was refluxed for 2 h at 40°C. The reaction mixture was extracted with CH_2Cl_2 (5 x 20 mL) and washed with 1M HCl for several times. The CH_2Cl_2 layer was dried over anhydrous Na_2SO_4 and concentrated under reduced pressure. The crude product was purified on preparative TLC developed with 1% MeOH- CH_2Cl_2 to give **3.4** (7.0 mg, 13%) as yellow solid; 1H NMR ($CDCl_3$, 400 MHz) δ 7.52 (2H, d, $J = 16.0$ Hz, H-1 and H-7), 7.04 (2H, d, $J = 8.0$ Hz, H-6' and H-6''), 7.00 (2H, brs, H-2' and H-2''), 6.80 (2H, d, $J = 8.4$ Hz, H-5' and H-5''), 6.40 (2H, d, $J = 16.0$ Hz, H-2 and H-6), 5.75 (2H, s, H-4), 5.45 (2H, brs, H-2''' and H-2'''), 4.45 (4H, d, $J = 6.0$ Hz, H-1''' and H-1'''), 3.85 (6H, s, OMe-3' and OMe-3''), 1.71 (6H, s, Me-4''' and Me-4''') and 1.68 (6H, s, Me-5''' and Me-5'''); ^{13}C NMR ($CDCl_3$, 100 MHz) δ 183.0 (C-3,5), 150.0 (C-4', 4''), 149.0 (C-3',3''), 140.0 (C-1,7), 138.0 (C-3''', 3'''), 127.0 (C-1', 1''), 122.0 (C-2, 6), 119.4 (C-2''', 2'''), 112.4 (C-5', 5''), 110.0 (C-6', 6''), 109.8 (C-2', 2''), 101.4 (C-4), 65.8 (C-1''', 1'''), 56.0 (OMe-3', 3''), 25.8 (C-4''', 4''') and 18.2 (C-5''', 5'''), LC-APCIMS m/z 505.2437 $[M+H]^+$ (calcd for $C_{31}H_{36}O_6+H$, 505.2512).

Diprenyldemethoxycurcumin (3.5). A mixture of demethoxycurcumin (**3.2**, 60.7 mg, 0.18 mmol) and excess anhydrous K_2CO_3 (75.0 mg, 0.54 mmol) in dry acetone (1.8 mL) was added 3-methylallyl bromide (110.0 μ L, 0.90 mmol). The mixture was refluxed for 2 h at 40°C. The reaction mixture was extracted with CH_2Cl_2 (5 x 20 mL) and washed with 1M HCl for several times. The CH_2Cl_2 layer was dried over anhydrous Na_2SO_4 and concentrated under reduced pressure. The crude product was purified on preparative TLC developed with 1% MeOH- CH_2Cl_2 to give **3.5** (6.8 mg, 12%) as yellow solid; 1H NMR (acetone- d_6 , 400 MHz) δ 7.64 (1H, d, J = 15.6 Hz, H-1), 7.62 (1H, d, J = 15.6 Hz, H-7), 7.43 (2H, d, J = 8.8 Hz, H-2' and H-6'), 7.06 (1H, dd, J = 8.4, 1.6 Hz, H-5''), 6.96 (1H, d, J = 1.6 Hz, H-2''), 6.83 (2H, d, J = 8.8 Hz, H-3' and H-5'), 6.78 (1H, d, J = 8.4 Hz, H-6''), 6.63 (1H, d, J = 15.6 Hz, H-2), 6.61 (1H, d, J = 15.6 Hz, H-6), 5.74 (2H, s, H-4), 5.43 (2H, dd, J = 6.8, 1.6 Hz, H-2''' and H-2'''), 4.57 (2H, d, J = 6.8 Hz, H-1'''), 4.49 (2H, d, J = 6.4 Hz, H-1'''), 3.85 (3H, s, OMe-3''), 1.77 (3H, s, Me-4'''), 1.74 (3H, s, Me-5''') and 1.73 (6H, s, Me-4'''' and Me-5'''') ; ^{13}C NMR ($CDCl_3$, 100 MHz) δ 183.0 (C-3, 5), 160.05 (C-4'), 150.5 (C-4''), 149.5 (C-3''), 140.0 (C-1, 7), 139.0 (C-3'''), 138.5 (C-3'''), 129.8 (C-2', 6'), 129.0 (C-1''), 123.0 (C-2, 6), 119.5 (C-2'''), 119.2 (C-2'''), 115.0 (C-3', 5'), 112.6 (C-5''), 110.0 (C- 6''), 101.6 (C-4), 65.8 (C-1'''), 65.0 (C-1'''), 56.0 (OMe-3''), 26.0 (C-4''', 4''') and 18.3 (C-5''', 5'''), LC-APCIMS m/z 475.2495 $[M+H]^+$ (calcd for $C_{30}H_{35}O_5+H$, 475.2406).

Diprenylbisdemethoxycurcumin (3.6). A mixture of bisdemethoxycurcumin (**3.3**, 55.6 mg, 0.18 mmol) and excess anhydrous K_2CO_3 (75.0 mg, 0.54 mmol) in dry acetone (1.8 mL) was added 3-methylallyl bromide (110.0 μ L, 0.90 mmol). The mixture was refluxed for 2 h at 40°C. The reaction mixture was extracted with CH_2Cl_2 (5 x 20 mL) and washed with 1M HCl for several times. The CH_2Cl_2 layer was dried over anhydrous Na_2SO_4 and concentrated under reduced pressure. The crude product was purified on preparative TLC developed with 1% MeOH- CH_2Cl_2 to give **3.6** (8.8 mg, 16%) as yellow solid; 1H NMR ($CDCl_3$, 400 MHz) δ 7.58 (2H, d, J = 15.6 Hz, H-1 and H-7), 7.34 (4H, d, J = 8.4 Hz, H-2', H-2'', H-6' and H-6''), 6.78 (4H, d, J = 8.4 Hz, H-3', H-3'', H-5' and H-5''), 6.58 (2H, d, J = 15.6 Hz, H-2 and H-6), 5.75 (2H, s,

H-4), 5.38 (2H, brs, H-2''' and H-2'''), 4.44 (4H, d, $J = 6.8$ Hz, H-1''' and H-1'''), 1.72 (6H, s, Me-4''' and Me-4''') and 1.67 (6H, s, Me-5''' and Me-5''') ; ^{13}C NMR (CDCl_3 , 100 MHz) δ 183.0 (C-3, 5), 160.0 (C-4', 4''), 140.0 (C-1, 7), 139.0 (C-3''', 3'''), 129.8 (C-2', 6', 2'', 6''), 127.0 (C-1', 1''), 121.8 (C-2, 6), 119.5 (C-2''', 2'''), 115.0 (C-3', 5', 3'', 5''), 101.2 (C-4), 66.0 (C-1''', 1'''), 25.8 (C-4''', 4''') and 18.2 (C-5''', 5'''), LC-APCIMS m/z 445.2376 $[\text{M}+\text{H}]^+$ (calcd for $\text{C}_{29}\text{H}_{32}\text{O}_4+\text{H}$, 445.2301).

3.3.3.2 Preparation of diacetylcurcuminoids (3.7-3.9)

Diacetylcurcumin (3.7). To a solution of curcumin (**3.1**, 50.6 mg, 0.14 mmol) in pyridine (1.5 mL) was added acetic anhydride (65.0 μL , 0.70 mmol). The mixture was stirred for 1.5 h at room temperature. The reaction mixture was extracted with CH_2Cl_2 (5 x 20 mL) and washed with 1M HCl for several times. The CH_2Cl_2 layer was dried over anhydrous Na_2SO_4 and concentrated under reduced pressure. The crude product was purified on preparative TLC developed with 1% MeOH- CH_2Cl_2 to give **3.7** (3.1 mg, 6%) as yellow solid; ^1H NMR (CDCl_3 , 400 MHz) δ 7.54 (2H, d, $J = 16.0$ Hz, H-1 and H-7), 7.08 (2H, d, $J = 8.0$ Hz, H-6' and H-6''), 7.06 (2H, brs, H-2' and H-2''), 6.99 (2H, d, $J = 8.0$ Hz, H-5' and H-5''), 6.48 (2H, d, $J = 15.6$ Hz, H-2 and H-6), 5.79 (2H, s, H-4), 3.82 (6H, s, OMe-3' and OMe-3'') and 2.27 (6H, s, OAc-4' and OAc-4'').

Diacetyldemethoxycurcumin (3.8). To a solution of demethoxycurcumin (**3.2**, 52.4 mg, 0.16 mmol) in pyridine (1.6 mL) was added acetic anhydride (75.0 μL , 0.80 mmol). The mixture was stirred for 1.5 h at room temperature. The reaction mixture was extracted with CH_2Cl_2 (5 x 20 mL) and washed with 1M HCl for several times. The CH_2Cl_2 layer was dried over anhydrous Na_2SO_4 and concentrated under reduced pressure. The crude product was purified on preparative TLC developed with 1% MeOH- CH_2Cl_2 to give **3.8** (2.3 mg, 5%) as yellow solid; ^1H NMR (CDCl_3 , 400 MHz) δ 7.56 (1H, d, $J = 16.0$ Hz, H-1), 7.54 (1H, d, $J = 16.0$ Hz, H-7), 7.49 (2H, d, $J = 8.4$ Hz, H-2' and H-6'), 7.08 (2H, brd, $J = 8.4$ Hz, H-2'' and H-6''), 7.06 (2H, d, $J = 8.4$ Hz, H-3' and H-5'), 6.99 (1H, d, $J = 8.0$ Hz, H-5''), 6.49 (1H, d, $J = 16.0$ Hz, H-2),

6.48 (1H, d, $J = 15.6$ Hz, H-6), 5.78 (2H, s, H-4), 3.82 (3H, s, OMe-3''), 2.27 (3H, s, OAc-4') and 2.24 (3H, s, OAc-4'').

Diacetylbisdemethoxycurcumin (3.9). To a solution of bisdemethoxycurcumin (**3.3**, 52.9 mg, 0.17 mmol) in pyridine (1.8 mL) was added acetic anhydride (82.0 μ L, 0.85 mmol). The mixture was stirred for 1.5 h at room temperature. The reaction mixture was extracted with CH_2Cl_2 (5 x 20 mL) and washed with 1M HCl for several times. The CH_2Cl_2 layer was dried over anhydrous Na_2SO_4 and concentrated under reduced pressure. The crude product was purified on preparative TLC developed with 1% MeOH- CH_2Cl_2 to give **3.9** (25.0 mg, 47%) as yellow solid; ^1H NMR (CDCl_3 , 400 MHz) δ 7.55 (2H, d, $J = 16.0$ Hz, H-1 and H-7), 7.49 (4H, d, $J = 8.4$ Hz, H-2' , H-2'', H-6' and H-6''), 7.05 (4H, d, $J = 8.4$ Hz, H-3', H-3'', H-5' and H-5''), 6.49 (2H, d, $J = 15.6$ Hz, H-2 and H-6), 5.76 (2H, s, H-4) and 2.25 (6H, s, OAc-4' and OAc-4'') ; ^{13}C NMR (CDCl_3 , 100 MHz) δ 183.0 (C-3, 5), 169.0 (C-1''', 1''''), 152.0 (C-4', 4''), 140.0 (C-1, 7), 133.0 (C-2', 6', 2'', 6''), 129.0 (C-1', 1''), 124.5 (C-2, 6), 122.0 (C-3', 5', 3'', 5''), 102.0 (C-4) and 21.0 (C-2''', 2''''), LC-APCIMS m/z 393.1340 $[\text{M}+\text{H}]^+$ (calcd for $\text{C}_{23}\text{H}_{20}\text{O}_6+\text{H}$, 393.1260).

3.3.3.3 Preparation of tetramethylcurcuminoids (3.10-3.11), trimethylbisdemethoxycurcumin (3.12), dimethylcurcumin (3.13) and dimethyldebismethoxycurcumin (3.14)

Tetramethylcurcumin (3.10). A mixture of curcumin (**3.1**, 51.5 mg, 0.14 mmol), excess anhydrous K_2CO_3 (58.0 mg, 0.42 mmol) in dry acetone (1.5 mL) was added methyl iodide (140.0 μ L, 0.70 mmol). The mixture was refluxed for 1.5 h at 40°C. The reaction mixture was extracted with CH_2Cl_2 (5 x 20 mL) and washed with 1M HCl for several times. The CH_2Cl_2 layer was dried over anhydrous Na_2SO_4 and concentrated under reduced pressure. The crude product was purified on preparative TLC developed with 1% MeOH- CH_2Cl_2 to give **3.10** (22.0 mg, 43%) as yellow solid; ^1H NMR (CDCl_3 , 400 MHz) δ 7.59 (2H, d, $J = 15.6$ Hz, H-1 and H-7), 7.30 (2H, d, $J = 1.6$ Hz, H-2' and H-2''), 7.21 (2H, dd, $J = 8.4, 1.6$ Hz, H-6' and H-6''), 6.95 (2H, d,

$J = 8.4$ Hz, H-5' and H-5''), 6.88 (2H, d, $J = 15.6$ Hz, H-2 and H-6), 3.83 (6H, s, OMe-3' and OMe-3''), 3.81 (6H, s, OMe-4' and OMe-4'') and 1.42 (6H, s, Me-4).

Tetramethyldemethoxycurcumin (3.11). A mixture of demethoxycurcumin (**3.2**, 52.1 mg, 0.15 mmol), excess anhydrous K_2CO_3 (64.0 mg, 0.45 mmol) in dry acetone (1.6 mL) was added methyl iodide (190.0 μ L, 0.75 mmol). The mixture was refluxed for 1.5 h at 40°C. The reaction mixture was extracted with CH_2Cl_2 (5 x 20 mL) and washed with 1M HCl for several times. The CH_2Cl_2 layer was dried over anhydrous Na_2SO_4 and concentrated under reduced pressure. The crude product was purified on preparative TLC developed with 1% MeOH- CH_2Cl_2 to give **3.11** (5.3 mg, 10%) as yellow solid; 1H NMR ($CDCl_3$, 400 MHz) δ 7.67 (1H, d, $J = 15.6$ Hz, H-1), 7.65 (1H, d, $J = 15.6$ Hz, H-7), 7.46 (2H, d, $J = 8.8$ Hz, H-2' and H-6'), 7.10 (1H, dd, $J = 8.4, 1.6$ Hz, H-6''), 6.99 (1H, dd, $J = 1.6$ Hz, H-2''), 6.85 (2H, d, $J = 8.8$ Hz, H-3' and H-5'), 6.82 (1H, d, $J = 8.4$ Hz, H-5''), 6.64 (1H, d, $J = 15.6$ Hz, H-2), 6.61 (1H, d, $J = 15.6$ Hz, H-6), 3.89 (6H, s, OMe-3'' and OMe-4''), 3.81 (3H, s, OMe-4') and 1.46 (6H, s, Me-4).

Trimethylbisdemethoxycurcumin (3.12). A mixture of bisdemethoxycurcumin (**3.3**, 50.9 mg, 0.17 mmol) and excess anhydrous K_2CO_3 (69.0 mg, 0.51 mmol) in dry acetone (1.7 mL) was added methyl iodide (200.0 μ L, 0.85 mmol). The mixture was refluxed for 1.5 h at 40°C. The reaction mixture was extracted with CH_2Cl_2 (5 x 20 mL) and washed with 1M HCl for several times. The CH_2Cl_2 layer was dried over anhydrous Na_2SO_4 and concentrated under reduced pressure. The crude product was purified on preparative TLC developed with 1% MeOH- CH_2Cl_2 to give **3.12** (1.8 mg, 4%) as yellow solid; 1H NMR ($CDCl_3$, 400 MHz) δ 7.65 (2H, d, $J = 15.6$ Hz, H-1 and H-7), 7.45 (4H, d, $J = 8.4$ Hz, H-2', H-2'', H-6' and H-6''), 6.84 (4H, d, $J = 8.8$ Hz, H-3', H-3'', H-5' and H-5''), 6.62 (2H, d, $J = 15.6$ Hz, H-2 and H-6), 3.80 (6H, s, OMe-4' and OMe-4'') and 2.14 (3H, s, Me-4); ^{13}C NMR ($CDCl_3$, 100 MHz) δ 182.0 (C-3, 5), 161.5 (C-4', 4''), 140.8 (C-1, 7), 129.6 (C-2', 6', 2'', 6''), 129.0 (C-1', 1''), 118.4 (C-2, 6), 114.2 (C-3', 5', 3'', 5''), 106.0 (C-4), 55.1 (OMe-4' and OMe-4'') and 12.0 (Me-4).

Dimethylcurcumin (3.13). A mixture of curcumin (**3.1**, 24.2 mg, 0.07 mmol), excess anhydrous K_2CO_3 (18.0 mg, 0.21 mmol) in dry acetone (1.5 mL) was added methyl iodide (50.0 μ L, 0.35 mmol). The mixture was refluxed for 1.5 h at 40°C. The reaction mixture was extracted with CH_2Cl_2 (5 x 20 mL) and washed with 1M HCl for several times. The CH_2Cl_2 layer was dried over anhydrous Na_2SO_4 and concentrated under reduced pressure. The crude product was purified on preparative TLC developed with 1% MeOH- CH_2Cl_2 to give **3.13** (5.5 mg, 22.7%) as yellow solid; 1H NMR ($CDCl_3$, 400 MHz) δ 7.59 (2H, d, $J = 16.0$ Hz, H-1 and H-7), 7.13 (2H, brd, $J = 8.0$ Hz, H-6' and H-6''), 7.08 (2H, d, $J = 1.2$ Hz, H-2' and H-2''), 6.87 (2H, d, $J = 8.4$ Hz, H-5' and H-5''), 6.48 (2H, d, $J = 15.6$ Hz, H-2 and H-6), 5.82 (2H, s, H-4), 3.93 (6H, s, OMe-3' and OMe-3'') and 3.92 (6H, s, OMe-4' and OMe-4'').

Dimethylbisdemethoxycurcumin (3.14). Bisdemethoxycurcumin (**3.3**, 20.0 mg, 0.06 mmol) dissolved in MeOH (3 mL) was added dropwise 2.0 M trimethylsilyldiazomethane in hexane until yellow solution persisted. The mixture was stirred at room temperature for 1.5 h. After the reaction mixture was evaporated to dryness, the residue was purified on preparative TLC developed with 100% CH_2Cl_2 to afford **3.14** (5.0 mg, 25.0%) as yellow solid; 1H NMR ($CDCl_3$, 400 MHz) δ 7.60 (2H, d, $J = 15.6$ Hz, H-1 and H-7), 7.45 (4H, d, $J = 8.4$ Hz, H-2', H-2'', H-6' and H-6''), 6.80 (4H, d, $J = 8.8$ Hz, H-3', H-3'', H-5' and H-5''), 6.40 (2H, d, $J = 15.6$ Hz, H-2 and H-6) 5.70 (2H, s, H-4) and 3.85 (6H, s, OMe-4' and OMe-4'').

3.3.4 α -Glucosidase inhibitory assay

3.3.4.1 α -Glucosidase inhibitory assay methods

The α -glucosidase inhibitory activity was performed using colorimetric method with a slight modification [89]. The α -glucosidase activity was determined by measuring the product *p*-nitrophenol released from *p*-nitrophenyl- α -D-glucopyranoside at UV 405 nm using microplate reader (Figure 3.11).

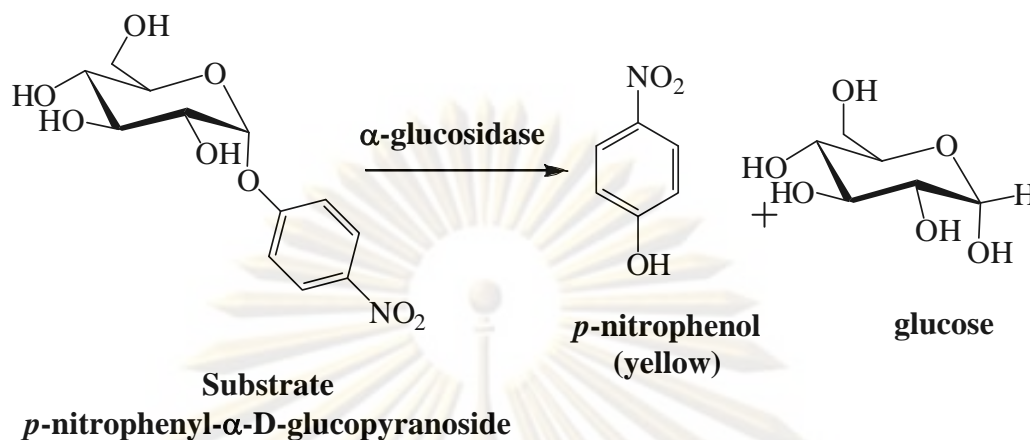


Figure 3.11 Hydrolysis of *p*-nitrophenyl- α -D-glucopyranoside by α -glucosidase

3.3.4.2 Chemical and equipment

The α -glucosidase (EC 3.2.1.20) from Baker's yeast and *p*-nitrophenyl α -D-glucopyranoside (pNPG) were purchased from Sigma-Aldrich (St. Louis, MO, USA). The substrate solution *p*-nitrophenyl- α -D-glucopyranoside was prepared in 0.1M phosphate buffer and adjusted to pH 6.9, to simulate a model of intestinal fluid. Yeast glucosidase was dissolved in 0.1M phosphate buffer (pH 6.9) to yield 57 U/mL stock-solution, which was further diluted with 0.1M phosphate buffer to get the concentration of 1 U/mL. Acarbose (Glucobay[®] 50 N 1; Bayer Vital, Leverkusen, Germany) as a synthetic inhibitor of α -glucosidase was obtained from a local pharmacy. Bio-Rad microplate reader model 3550 UV was used to measure the absorbance at 405 nm of enzyme reaction.

3.3.4.3 Procedures

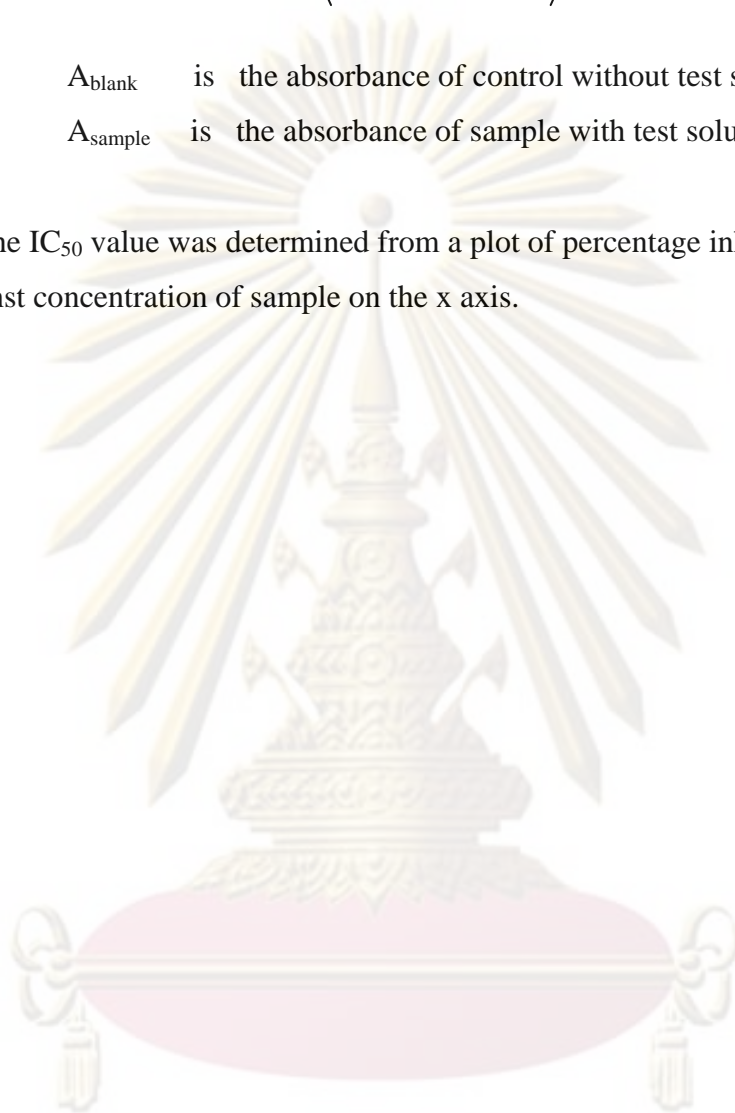
In the 96-well plate, 10 μ L of test compounds dissolved in DMSO were incubated for 10 min with 50 μ L of yeast α -glucosidase enzyme (1 U/mL). After 10 min of incubation, 50 μ L of substrate (pNPG) was added into a microplate. The reaction was terminated by adding 1M Na₂CO₃. The increment in absorption at 405 nm due to the hydrolysis of pNPG by α -glucosidase enzyme was measured. Percent inhibition was calculated according to the equation shown below [90].

$$\% \text{ inhibition} = \left(\frac{A_{\text{blank}} - A_{\text{sample}}}{A_{\text{blank}}} \right) \times 100$$

A_{blank} is the absorbance of control without test solution

A_{sample} is the absorbance of sample with test solution

The IC_{50} value was determined from a plot of percentage inhibition on the y axis against concentration of sample on the x axis.



ศูนย์วิทยทรัพยากร
จุฬาลงกรณ์มหาวิทยาลัย

CHAPTER IV

CONCLUSION

4.1 Bioactive compounds from the lianas of *Gnetum macrostachyum*

In summary, the isolation of the acetone crude extract from the lianas of *Gnetum macrostachyum* led to the isolation of two new compounds; 5,7,2'-trihydroxy-5'-methoxyflavone (**1.1**) and stilbenoid tetramer (**3.10**), along with eight known compounds ; 5,7,4'-trihydroxy-3'-methoxyflavanone (**1.2**), resveratrol (**1.3**), 3-methoxyresveratrol (**1.4**), shegansu B (**1.5**), gnetulin (**1.6**), gnetuhainin C (**1.7**), parvifolol B (**1.8**) and pallidol (**1.9**).

The structure of flavanoids and its derivatives and stibinoids isolated from the lianas of *G. macrostachyum* were summarized in Figure 4.1

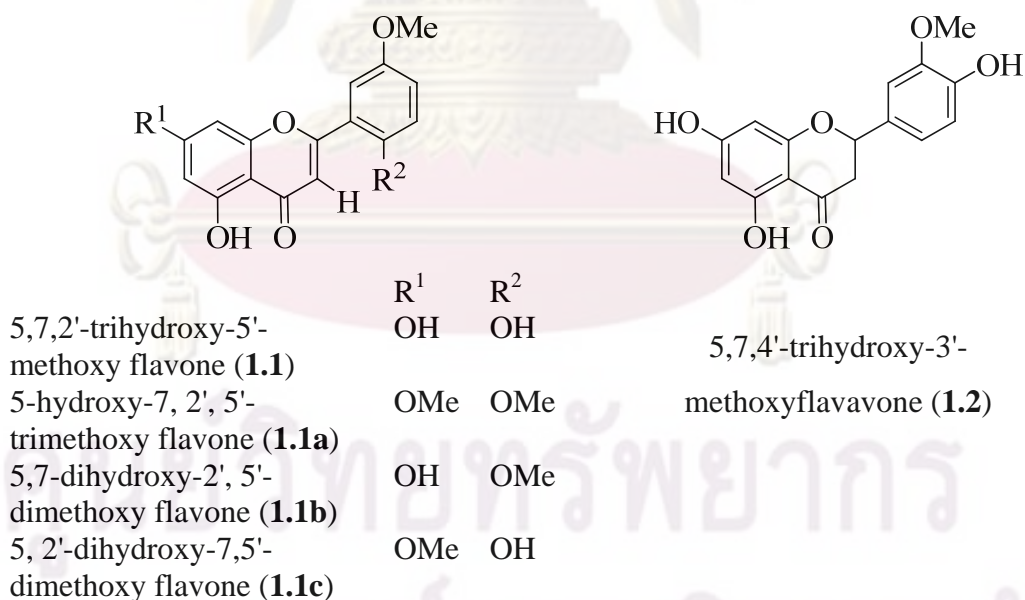


Figure 4.1 The isolated flavanoids and its derivatives and stibinoids from *Gnetum macrostachyum* lianas

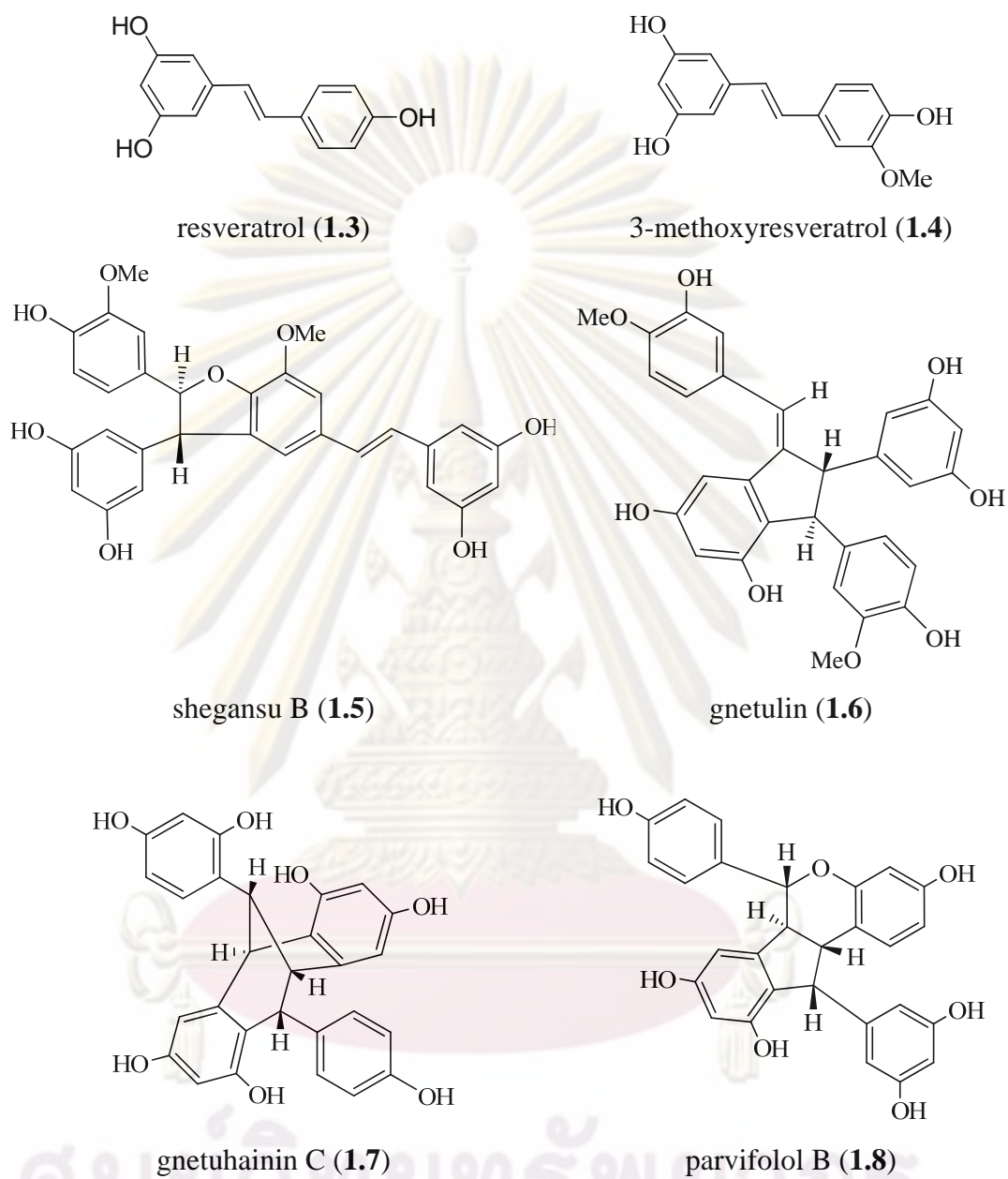


Figure 4.1 The isolated flavanoids and its derivatives and stibinoids from *Gnetum macrostachyum* lianas (cont.)

จุฬาลงกรณ์มหาวิทยาลัย

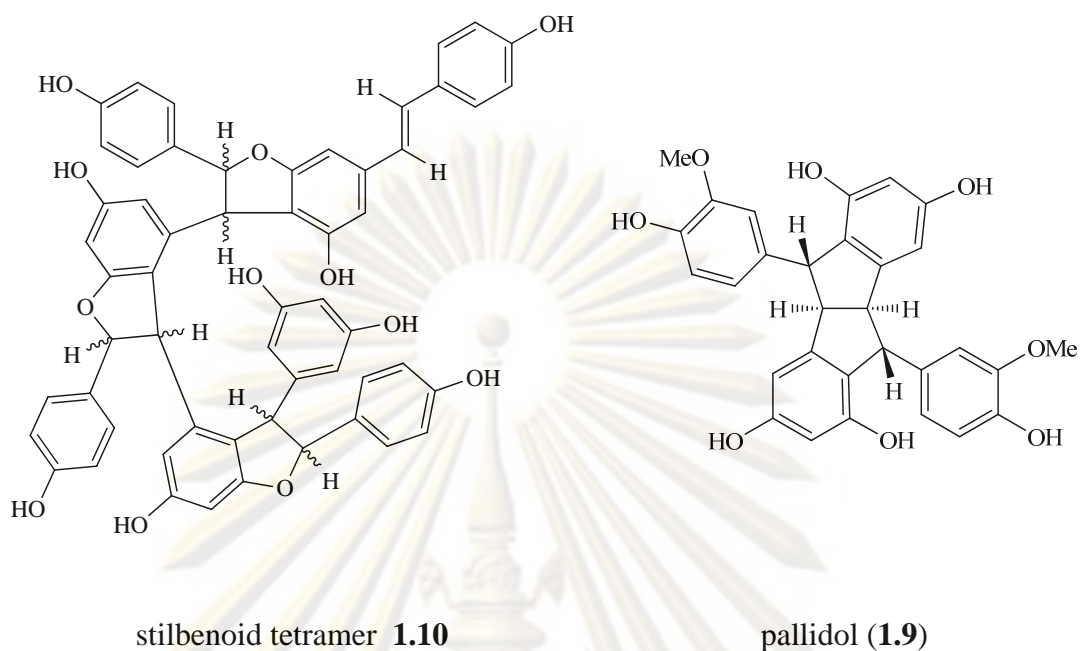
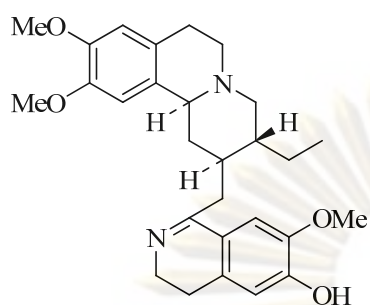


Figure 4.1 The isolated flavanoids and its derivatives and stibinoids from *Gnetum macrostachyum* lianas (cont.)

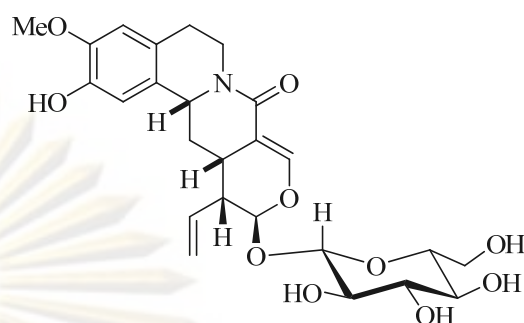
The all isolated compounds except tetramer **1.10** were tested for radical scavenging on DPPH. The results indicated that gnetulin (**1.6**) was the most effective compound in antioxidant activity with IC_{50} values of 0.21 mM. In addition, resveratrol (**1.3**), 3-methoxyresveratrol (**1.4**) and pallidol (**1.9**) were also found to be active in antioxidant activity with IC_{50} values of 0.40, 0.30 and 0.53 mM, respectively.

4.2 Bioactive compounds from the roots of *Alangium salviifolium*

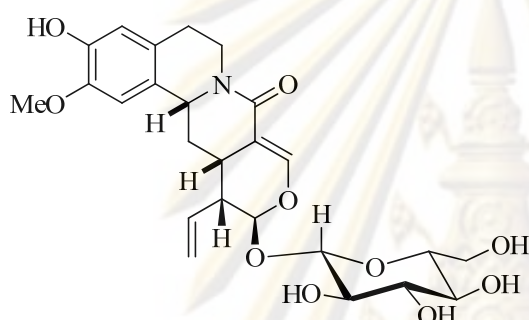
In this investigation, the chromatographic separation from the butanolic and water crude extracts of the roots of *Alangium salviifolium* led to the isolation of seven known alkaloids, psychotrine (**2.1**), alangiside (**2.2**), 3-*O*-demethyl-2-*O*-methylalangiside (**2.3**), alangicine (**2.4**), demethylalangiside (**2.5**), 1', 2'-dehydrotubulosine (**2.6**) and demethylpsychotrine (**2.7**). The structures of all isolated compounds from the roots of *A. salviifolium* were characterized by spectroscopic methods as well as comparison with the previous literature data and summarized in Figure 4.2.



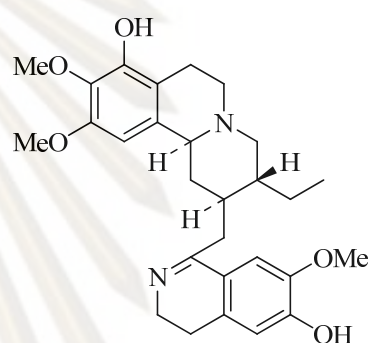
psychotrine (2.1)



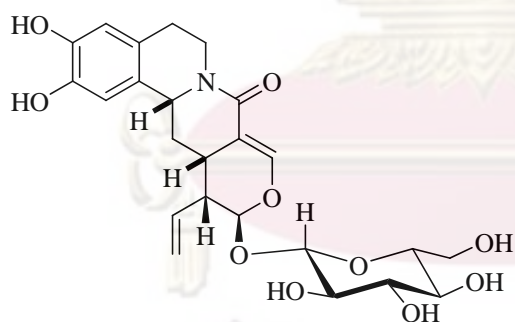
alangiside (2.2)



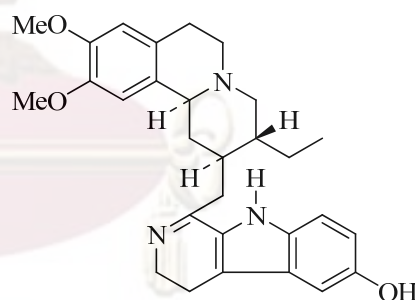
3-O-demethyl-2-O-methylalangiside (2.3)



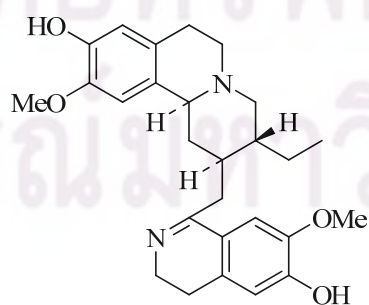
alangicine (2.4)



demethylalangiside (2.5)



1', 2'-dehydrotubulosine (2.6)



demethylpsychotrine (2.7)

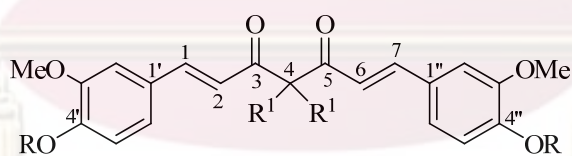
Figure 4.2 The isolated compounds from *Alangium salviifolium* roots

The evaluation for cytotoxicity against KB and HeLa cell lines showed that compound **2.1** has highest cytotoxicity against both KB and HeLa cell lines with IC₅₀ value 1.00 and 0.70 µg/ml, respectively.

The future work may involve the synthesis of isolated compounds for increasing quantity and biological activity that could be developed into new drugs. Novel active compounds will afford the target for future synthesis and structure activity relationship studies as well. This will lead to better understanding on the interaction between active compounds and diseases.

4.3 Bioactive compounds from the rhizomes of *Curcuma longa*

The isolation of CH₂Cl₂ extract from the rhizomes of *Curcuma longa* afforded three major known compounds; curcumin (**3.1**), demethoxycurcumin (**3.2**) and bisdemethoxycurcumin (**3.3**). Curcuminoids were modified by alkylation to afford ten curcumin analogues, which included four new compounds; **3.4-3.6, 3.9** and seven known analogues **3.7, 3.8, 3.10-3.14**. The structures of all compounds are summarized in Figure 4.3.



curcumin **3.1** ; R, R¹= H

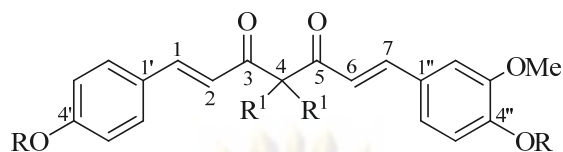
diprenylcurcumin **3.4** ; R= C₅H₉, R¹= H

diacetylcurcumin **3.7** ; R= Ac, R¹= H

tetramethylcurcumin **3.10** ; R= Me, R¹= Me

dimethylcurcumin **3.13** ; R= Me, R¹= H

Figure 4.3 The structures of curcuminoids and curcumin analogues

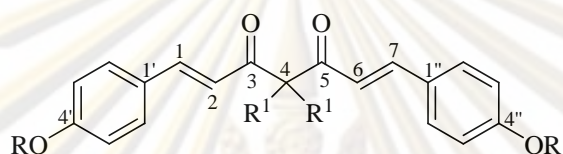


demethoxycurcumin **3.2** ; $R = R^1 = H$

diprenyldemethoxycurcumin **3.5** ; $R = C_5H_9$, $R^1 = H$

diacetyldemethoxycurcumin **3.8** ; $R = Ac$, $R^1 = H$

tetramethyldemethoxycurcumin **3.11** ; $R = Me$, $R^1 = Me$

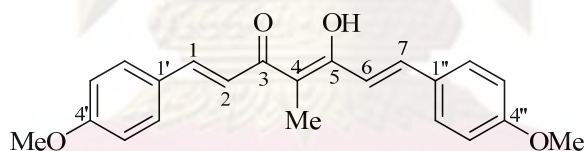


bisdemethoxycurcumin **3.3** ; $R = R^1 = H$

diprenylbisdemethoxycurcumin **3.6** ; $R = C_5H_9$, $R^1 = H$

diacetyl bisdemethoxycurcumin **3.9** ; $R = Ac$, $R^1 = H$

dimethylbisdemethoxycurcumin **3.14** ; $R = Me$, $R^1 = H$



trimethylbisdemethoxycurcumin **3.12** ; $R = Me$, $R^1 = Me$

Figure 4.3 The structures of curcuminoids and curcumin analogues (cont.)

The α -glucosidase inhibitory activity of curcuminoids **3.1-3.3** and curcumin analogues **3.4-3.14** were evaluated by colorimetric method. Curcuminoids **3.1-3.3** showed inhibitory activities against α -glucosidase with the IC_{50} values of 0.81, 0.31 and 0.47 mM, respectively, which were comparable to that of Acarbose[®] and exhibited more potent inhibitory activity than synthesized alkylcurcuminoids (**3.4-3.14**). Interestingly, the synthesized alkylcurcuminoids (**3.4-3.14**) showed lower inhibitory activity with higher IC_{50} values than the natural curcuminoids (**3.1-3.3**).

The results suggested that simple curcumin having at least one hydroxyl group attached to aromatic moiety possessed enhanced inhibitory effect whereas, the introduction of alkyl groups at hydroxyl groups of curcuminoids led to the activities lower than those of the natural curcuminoids. We assumed that the hydroxyl groups of curcuminoids and curcumin analogues played very an important role on the enzyme inhibitory activity.

In addition, tetramethylcurcuminoids (**3.10-3.11**) and trimethylbisdemethoxy curcumin (**3.12**), whose C-4 was methylated, showed weak α -glucosidase inhibition with the IC_{50} values of 1.39, 0.89 and 5.27 mM, respectively. The results suggested that the methylene protons in original curcuminoids might be affect in inhibitory effect. In order to test this assumption, dimethylcurcumin **3.13** and dimethylbisdemethoxycurcumin **3.14**, whose C-4 were not methylated, were synthesized and evaluated for α -glucosidase inhibitory effect. However, **3.13** and **3.14** showed poor inhibition ($IC_{50} \geq 10.0$ mM.), thus indicating that the presence of C-4 methylene proton is not associated with blocking enzyme function. Furthermore, curcumin analogues **3.5**, **3.8** and **3.11** were asymmetrical curcuminoids which exhibited more potent inhibitory activity than the symmetrical curcuminoid congeners **3.6-3.7**, **3.9-3.10** and **3.12-3.14**.

In conclusion, curcuminoids isolated from *C. longa* were found as potent α -glucosidase inhibitors while the synthetic alkylated curcuminoids exhibited weak inhibitory effects against α -glucosidase. The study suggested that the hydroxyl groups in curcuminoids play a very important role on the enzyme inhibitory activity.

REFERENCES

- [1] Ito, T.; Tanaka, T.; Iinuma, M.; Iliya, I.; Nakaya, K.I.; Ali, Z.; Takahashi, Y.; Sawa, R.; Shirataki, Y.; Murata, J. and Darnaedi, D. New resveratrol oligomers in the stem bark of *Vatica pauciflora*. *Tetrahedron* 59 (2003) : 5347-5363.
- [2] Ge, H. M.; Huang, B.; Tan, S.H.; Shi, D.H.; Song, Y.C. and Tan, R.X. Bioactive oligostilbenoids from the stem bark of *Hopea exalata*. *J. Nat. Prod.* 69 (2006) : 1800-1802.
- [3] Huang, K.S.; Lin, M.; Yu, L. N. and Hong, M. Four novel oligostilbenes from the roots of *Vitis amurensis*. *Tetrahedron* 56 (2000) : 1321-1329.
- [4] Huang, K.S.; Lin, M. and Cheng, G.F. Anti-inflammatory tetramers of resveratrol from the roots of *Vitis amurensis* and the conformations of the seven-membered ring in some oligostilbenes. *Phytochemistry* 58 (2001) : 357-362.
- [5] Yamada, M.; Hayashi, K.I.; Hayashi, H.; Ikeda, S.; Hoshino, T.; Tsutsui, K.; Iinuma, M. and Nozaki, H. Stilbenoids of *Kobresia nepalensis* (Cyperaceae) exhibiting DNA topoisomerase II inhibition. *Phytochemistry* 67 (2006) : 307-313.
- [6] Lins, A. P.; Ribeiro, M. N. D. S.; Gottlieb, O. R. and Gottlieb, H. E. Gnetins: resveratrol oligomers from Gnetum species. *J. Nat. Prod.* 45 (1982) : 754-761.
- [7] Tanaka, T.; Iliya, I.; Ito, T.; Furusawa, M.; Nakaya, K.I.; Iinuma, M.; Shirataki, Y.; Matsuura, N.; Ubukata, M.; Murata, J.; Simozono, F. and Hirai, K. Stilbenoids in lianas of *Gnetum parvifolium*. *Chem. Pharm. Bull.* 49 (2001) : 858-862.
- [8] Huang, K.S.; Wang, Y.H.; Li, R.L. and Lin, M. Five new stilbene dimers from the lianas of *Gnetum hainanense*. *J. Nat. Prod.* 63 (2000a) : 86-89.
- [9] Lin, M.; Li, J.B.; Wu, B. and Zheng, Q.T. A stilbene derivative from *Gnetum parvifolium*. *Phytochemistry* 30 (1991) : 4201-4203.
- [10] Iliya, I.; Tanaka, T.; Iinuma, M.; Ali, Z.; Furusawa, M.; Nakaya, K.I.; Shirataki, Y.; Murata, J. and Danaedi, D. Stilbene derivatives from two species of Gnetaceae. *Chem. Pharm. Bull.* 50 (2002) : 796-801.

- [11] Luo, H.F.; Zhang, L.P. and Hu, C.Q. Five novel oligostilbenenes from the roots of *Caragana sinica*. *Tetrahedron* 57 (2001) : 4849-4854.
- [12] Farag, S.F.; Takaya, Y. and Niwa, M. Stilbene glucosides from the bulbs of *Iris tingitana*. *Phytochemistry Letters* (2009), DOI : 10.1016/j.phytol.2009.05.001.
- [13] Kawazoe, K.; Shimogai, N.; Takaishi, Y.; Rao, K.S. and Imakura, Y. Four stilbene from *Salacia lehmbachii*. *Phytochemistry* 44 (1997) : 1569-1573.
- [14] Sarker, S.D.; Whiting, P. and Dinan, L. Identification and ecdysteroid antagonist activity of three resveratrol trimers (Suffruticosols A, B and C) from *Paeonia suffruticosa*. *Tetrahedron* 55 (1999) : 513-524.
- [15] Syah, Y.M.; Achmad, S.A.; Ghisalberti, E.L.; Hakim, E.H.; Iman, M.Z.N.; Makmur, L. and Mujahiddin, D. Andalasin A, a new stilbene dimer from *Morus macrourea*. *Fitoterapia* 71 (2000) : 630-635.
- [16] Huang, K.S.; Li, R. L.; Wang, Y. H. and Lin, M. Three new stilbene trimers from the lianas of *Gnetum hainanense*. *Planta Med.* 67 (2001) : 61-64.
- [17] Ito, T.; Akao, Y.; Tanaka, T.; Iinuma, M. and Nozawa, Y. Vaticanol C, A novel resveratrol tetramer, inhibits cell growth through induction of apoptosis in colon cancer cell lines. *Biol. Pharm. Bull.* 25 (2002) : 147-148.
- [18] Kulanthaivel, P., Janzen, W.P., Ballas, L.M., Jiang, J.B., Hu, C.Q., Darges, J.W., Seldin, J.C., Cofield, D.J., Adams, L.M. Naturally occurring protein kinase inhibitors; II. Isolation of oligomeric stilbenes from *Caragana sinica*. *Planta Med.* 61 (1995) : 41-44.
- [19] Dai, J.R., Hallock, Y.F., Cardellina, II, J.H., Boyd, M.R., HIV Inhibitory and cytotoxic oligostilbenes from the leaves of *Hopeamalibato*. *J. Nat. Prod.* 61 (1998) : 351-353.
- [20] Ducrot, P.H., Kollmann, A., Balla, A.E., Majira, A., Kerhoas, L., Delorne, R., Einhorn, J., Cyphostemmins A-B, two new antifungal oligostilbenes from *Cyphostemma crotalarioides* (Vitaceae). *Tetrahedron Lett.* 39 (1998) : 9655-9658.
- [21] Cichewicz, R.H., Kouzi, S.A., Hamann, M.T. Dimerization of resveratrol by the grapevine pathogen *Botrytis cinerea*. *J. Nat. Prod.* 63 (2000) : 29-33.
- [22] Huang, K.S., Lin, M., Yu, L.N. and Kong, M. Four novel oligostilbenes from the roots of *Vitis amnrensis*. *Tetrahedron* 56 (2000) : 1321-1329.

- [23] Sotheeswaran, S. and Pasupathy, V. Distribution of resveratrol oligomers in plants. *Phytochemistry* 32 (1993) : 1083-1092.
- [24] Holscher, D. and Schneider, B. A resveratrol dimer from *Anigozanthos preissii* and *Musa Cavendish*. *Phytochemistry* 43 (1996) : 471-473.
- [25] Li, X.M.; Huang, K.S.; Lin, M. and Zhou, L.X. Studies on formic acid-catalyzed dimerization of isorhapontigenin and of resveratrol to tetralins. *Tetrahedron* 59 (2003) : 4405-4413.
- [26] Itoh, T.; Tanaka, T.; Iinuma, M.; Nakaya, K.I.; Takahashi, Y.; Sawa, R.; Murata, J. and Darnaedi, D. Three new resveratrol oligomers from the stem bark of *Vatica pauciflora*. *J. Nat. Prod.* 67 (2004) : 932-937.
- [27] Ito, T.; Tanaka, T.; Iinuma, M.; Nakaya, K.I.; Takahashi, Y.; Sawa, R.; Naganawa, H. and Chelladurai, V. Two new oligostilbenes with dihydrobenzofuran from the stem bark of *Vateria indica*. *Tetrahedron* 59 (2003) : 1255-1264.
- [28] Prakash, S.; Khan, M.A.; Khan, K.Z. and Zaman, A. Stilbenes of *Gnetum ula*. *Phytochemistry* 24 (1985) : 622-624.
- [29] Siddiqui, Z.S.; Rahman, M.; Khan, M.A. and Zaman, A. Gnetulin, a dimer of 3', 4, 5'-trihydroxystilbene from *Gnetum ula*. *Tetrahedron* 49 (1993) : 10393-10396.
- [30] Boralle, N.; Gottlieb, H.E.; Gottlieb, O.R.; Kubitzki, K.; Lopes, L.M.X.; Yoshida, M. and Young, M.C.M. Oligostilbenoids from *Gnetum venosum*. *Phytochemistry* 34 (1993) : 1403-1407.
- [31] Ali, Z.; Tanaka, T.; Iliya, I.; Iinuma, M.; Furusawa, M.; Ito, T.; Nakaya, K.I.; Murata, J. and Darnaedi, D. Phenolic Constituents of *Gnetum klossii*. *J. Nat. Prod.* 66 (2003) : 558-560.
- [32] Iliya, I.; Ali, Z.; Tanaka, T.; Iinuma, M.; Furusawa, M.; Nakaya, K.I.; Jin Murata, J. and Darnaedi, D. Stilbenoids from the stem of *Gnetum latifolium* (Gnetaceae). *Phytochemistry* 61 (2002) : 959-961.
- [33] Iliya, I.; Ali, Z.; Tanaka, T.; Iinuma, M.; Furusawa, M.; Nakaya, K.I.; Murata, J.; Darnaedi, D.; Matsuura, N. and Ubukata, M. Stilbene derivatives from *Gnetum gnemon* Linn. *Phytochemistry* 62 (2003) : 601-606.

- [34] Iliya, I.; Ali, Z.; Tanaka, T.; Inuma, M.; Furasawa, M.; Nakaya, K.I.; Shirataki, Y.; Murata, J.; Danaedi, D.; Matsuura N. and Ubukata, M. Three new trimeric stilbenes from *Gnetum gnemon*. *Chem. Pharm. Bull.* 51 (2003) : 85-88.
- [35] Yao, C.S. and Lin, M. Bioactive stilbene dimmers from *Gnetum cleistostachyum*. *Natural Product Research* 19 (2005) : 443-448.
- [36] Huang, K.S.; Wang, Y.H.; Li, R.L. and Lin, M. Stilbene dimers from the lianas of *Gnetum hainanense*. *Phytochemistry* 54 (2000b) : 875-881.
- [37] Xianga, W.; Jianga, B.; Lib, X.M.; Zhanga, H.J.; Zhaoa, Q.S.; Lia, S.H.; and Sun, H.D. Constituents of *Gnetum montanum*. *Fitoterapia* 73 (2002) : 40-42.
- [38] Li, X.M.; Lin, M.; Wang, Y.H. and Liu, X. Four New stilbenoids from the lianas of *Gnetum montanum f. megalocarpum*. *Planta. Med.* 70 (2004) : 160-165.
- [39] Li, X.M.; Wang, Y.H. and Lin, M. Stilbenoids from the lianas of *Gnetum pendulum*. *Phytochemistry* 58 (2001) : 591-594.
- [40] Smitinand, T.; Larsen, K. *Flora of Thailand* 2 (1975) : 207.
- [41] เต็ม สมิตินันท์. *ข้อพรรณไม้แห่งประเทศไทย (ชื่อวิทยาศาสตร์-ชื่อพื้นเมือง)*. ครั้งที่ 2 พันธุ์พืชมลพิษซึ่ง : กรุงเทพฯ 2523, 166.
- [42] Garo, E.; Maillard, M.; Antus, S.; Mavi, S. And Hostettmann, K. Five Flavans from *Mariscus psilostachys*. *Phytochemistry* 43 (1996) : 1265-1269.
- [43] Khan, M.A.; Nabi, S.G.; Prakash, S. and Zaman, A. Pallidol, A resveratrol dimer from *Cissus pallida*. *Phytochemistry* 25 (1986) : 1945-1948.
- [44] Panzella, L.; De Lucia, M.; Amalfitano, C.; Pezzella, A.; Evidente, A.; Napolitano, A. and D'Ischia, M. Acid-Promoted Reaction of the Stilbene Antioxidant Resveratrol with Nitrite Ions : Mild Phenolic Oxidation at the 4'-Hydroxystyryl Sector Triggering Nitration, Dimerization and Aldehyde-Forming Routes *Journal of Organic Chemistry* 71 (2006) : 4246-4254.
- [45] Miliauskas, G.; Venskutonis, P. R. and Beek, T. A. V. Screening of radical scavenging activity of some medicinal and aromatic plant extracts. *Food Chemistry*. 85 (2004) : 231-237.
- [46] Rao, K.N. and Venkatachalam, S.R. Dihydrofolate reductase and cell growth activity inhibition by the β -carboline-benzoquinolizidine plant alkaloid deoxytubulosine from *Alangium lamarckii*: Its potential as an antimicrobial

- and anticancer agent. *Bioorganic & Medicinal Chemistry* 7 (1999) : 1105-1110.
- [47] Ma, W.W.; Anderson, J.E.; Mckenzie, A.T.; Byrn, S.R. and Mclaughlin, J.L. Tubulosine: an antitumor constituent of *Pogonopus speciosus*. *J. Nat. Prod.* 53 (1990) : 1009-1014.
- [48] Murugan, V.; Shareef, H.; Sarma, G.V.S.R.; Ramanathan, M. and Suresh, B. Anti-fertility activity of the stem bark of *Alangium salviifolium* (Linn.f) wang in wistar female rats. *Indian Journal of Phamacology* 32 (2000) : 388-389.
- [49] Mosaddik, M.A.; Kabir, K.E. and Hassan, P. Antibacterial activity of *Alangium salviifolium* flowers. *Fitoterapia* 71 (2000) : 447-449.
- [50] De-Eknamkul, W.; Suttipanta, N. and Kutchan, T.M. Purification and characterization of deacetylpecoside synthase from *Alangium lamarckii* Thw. *Phytochemistry* 55 (2000) : 177-181.
- [51] Jain, S.; Sinha, A. and Bhakuni, D.S. The biosynthesis of β -carboline and quinolizidine alkaloids of *Alangium lamarckii*. *Phytochemistry* 60 (2002) : 853-859.
- [52] Pakrashi, S.C. and Ali, E. Newer alkaloids from *Alangium lamarckii* Thw. *Tetrahedron Letters* 23 (1967) : 2143-2146.
- [53] Itoh, A.; Tanahashi, T. and Nagakura, N. Isolation of two unusual Tetrahydroisoquinoline-monoterpene glucosides from *Alangium lamarckii* as possible intermediates in the non-enzymatic formation of Alangimarine and Alangiside. *Heterocycles* 48 (1998) : 499-505.
- [54] Itoh, A.; Tanahashi, T. and Nagakura, N. Acylated tetrahydroisoquinoline-monoterpene glucosides from *Alangium lamarckii*. *Phytochemistry* 41 (1996) : 651-656.
- [55] Itoh, A.; Tanahashi, T.; Tabata, M.; Shikata, M.; Kakite, M.; Nagai, M. And Nagakura, N. Tetrahydroisoquinoline-monoterpene and iridoid glycosides from *Alangium lamarckii*. *Phytochemistry* 56 (2001) : 623-630.
- [56] Tanahashi, T.; Kobayashi, C.; Itoh, A.; Nagakura, N.; Inoue, K.; Kuwajima, H. and Wu, H.X. A Tetrahydroisoquinoline-monoterpene glucoside and an iridoid glucoside from *Alangium kurzii*. *Chem. Pharm. Bull.* 48 (2000) : 414-419.

- [57] Itoh, A.; Tanahashi, T.; Ikejima, S.; Inoue, M.; Nagakura, N.; Inoue, K.; Kuwajima, H. and Wu, H.X. Five phenolic glycosides from *Alangium Chinense*. *J. Nat. Prod.* 63 (2000) : 95-98.
- [58] Sakurai, N.; Nakagawa-Goto, K.; Ito, J.; Sakurai, Y.; Nakanishi, Y.; Bastow, K.F.; Cragg, G. and Lee, K.H. Cytotoxic *Alangium* alkaloids from *Alangium longiflorum*. *Phytochemistry* 67 (2006) : 894-897.
- [59] Anjum, A.; Haque, M.E.; Rahman, M.M. and Sarker, S.D. Antibacterial compounds from the flowers of *Alangium salviifolium*. *Fitoterapia* 73 (2002) : 526-528.
- [60] Worapan Sitthithaworn, Alkaloids from roots and leaves of *Alangium salviifolium* wang. Subsp *hexa petalum* wang. Master's Thesis, Department of Pharmacognosy, Faculty of Pharmacology, Chulalongkorn University, 1995.
- [61] Fujii, T.; Yamada, K.; Minami, S.; Yoshifuji, S. and Ohba, M. Quinolizidines. VIII. Structure and synthesis of the *Alangium* Alkaloid Alangicine: Syntheses of (±)- and (+)- Alangicines. *Chem. Pharm. Bull.* 31 (1983) : 2583-2592.
- [62] Budzikiewicz, H.; Pakrashi, S.C. and Vorbruggen, H. Die isolierung von Emetin, Cephaelin und Psychotrin aus *Alangium lamarckii* und die identifizierung von Almarckine mit N-methylcephaelin. *Tetrahedron* 20 (1964) : 399-408.
- [63] Shoeb, A.; Raj, K.; Kapil, R.S. and Popli, S.P. Alangiside, the monoterpenoids alkaloidal glycoside from *Alangium lamarckii* Thw. *J. Chem. Soc. Perkin Trans I* (1975) : 1245-1248.
- [64] Itoh, A.; Tanahashi, T. and Nagakura, N. Five tetrahydroisoquinoline-monoterpene glycosides with a disaccharide moiety from *Alangium lamarckii*. *Phytochemistry* 46 (1997) : 1225-1229.
- [65] Itoh, A.; Tanahashi, T.; Nagakura, N. and Nayeshiro, H. Tetrahydroisoquinoline-monoterpene glucosides from *Alangium lamarckii* and *Cephaelis ipecacuanha*. *Phytochemistry* 36 (1994) : 383-387.
- [66] Fujii, T.; Yamada, K. and Yoshifuji, S. Structure and stereochemistry of Alangicine: synthesis of (±)-Alangicine. *Tetrahedron Letters* 29 (1976) : 2553-2556.

- [67] Itoh, A.; Tanahashi, T. and Nagakura, N. Six tetrahydroisoquinoline-monoterpene glucosides from *Cephaelis ipecacuanha*. *Phytochemistry* 30 (1991) : 3117-3123.
- [68] Itoh, A.; Ikuta, Y.; Tanahashi, T. and Nagakura, N. Two alangium alkaloids from *Alangium lamarckii*. *J. Nat. Prod.* 63 (2000) : 723-725.
- [69] Ito, A.; Lee, Y.H.; Chai, H.B.; Gupta, M.P.; Farnsworth, N.R.; Cordell, G.A.; Pezzuto, J.M. and Kinghorn, A.D. 1', 2', 3', 4'-Tetrahydrotubulosine, a cytotoxic alkaloid from *Pogonopus speciosus*. *J. Nat. Prod.* 62 (1999) : 1346-1348.
- [70] Sakurai, N.; Nakagawa-Goto, K.; Ito, J.; Sakurai, Y.; Nakanishi, Y.; Bastow, K.F.; Cragg, G. and Lee, K.H. Cytotoxic *Alangium* alkaloids from *Alangium longiflorum*. *Phytochemistry* 67 (2006) : 894-897.
- [71] Weber, W.M.; Hunsaker, L.A.; Abcouwer, S.F.; Deck, L.M. and Vander Jagt, D.L. Anti-oxidant activities of curcumin and related enones. *Bioorganic & Medicinal Chemistry* 13 (2005) : 3811-3820.
- [72] Youssef, K.M.; EI-Sherbeny, M.A.; EI-Shafie, F.S; Farag, H.A.; AI-Deeb, O.A. and Awadalla, S.A. A. Synthesis of curcumin analogues as potential antioxidant, cancer chemopreventive agents. *Arch. Pharm.Med. Chem.* 337 (2004) : 42-54.
- [73] Wang, X.; Jiang, Y.; Wang, Y.W.; Huang, M.T.; Ho, C.T. and Huang, Q. Enhancing anti-inflammation activity of curcumin through O/W nanoemulsions. *Food Chemistry* 108 (2008) : 419-424.
- [74] Nurфина, A.; Reksohadiprodjo, M.; Timmerman, H.; Jenie, U.; Sugiyanto, D. and Goot, H.V.D. Synthesis of some symmetrical curcumin derivatives and their anti-inflammatory activity. *Eur. J. Med. Chem.* 32 (1997) : 321-328.
- [75] Ishida, J.; Ohtsu, H.; Tachibana, Y.; Nakanishi, Y.; Bastow, K.F.; Nagai, M.; Wang, H.K.; Itokawa, H. and Lee, K.H. Antitumor agents. Part 214: Synthesis and evaluation of curcumin analogues as cytotoxic agents. *Bioorganic & Medicinal Chemistry* 10 (2002) : 3481-3487.
- [76] Qiu, X.; Liu, Z.; Shao, W.Y.; Liu, X.; Jing, D.P.; Yu, Y.J.; An, L.K.; Huang, S.L.; Bu, X.Z.; Huang, Z.S. and Gu, L.Q. Synthesis and evaluation of

- curcumin analogues as potential thioredoxin reductase inhibitors. *Bioorganic & Medicinal Chemistry* 16 (2008) : 8035-8041.
- [77] Mazumder, A.; Neamati, N.; Sunder, S.; Schulz, J.; Pertz, H.; Eich, E. and Pommier, Y. Curcumin analogs with altered potencies against HIV-1 Integrase as probes for biochemical mechanisms of drug action. *J. Med. Chem.* 40 (1997) : 3057-3063.
- [78] Vajragupta, O.; Boonchoong, P.; Morris, G.M. and Olson, A.J. Active site binding modes of curcumin in HIV-1 protease and integrase. *Bioorganic & Medicinal Chemistry Letters* 15 (2005) : 3364-3368.
- [79] Woo, H.B.; Shin, W.S.; Lee, S. and Ahn, C.M. Synthesis of novel curcumin mimics with asymmetrical units and their anti-angiogenic activity. *Bioorganic & Medicinal Chemistry Letters* 15 (2005) : 3782-3786.
- [80] Narayannasamy, A.; Namasivayam, N. and Radha, K. Effect of turmeric on the enzymes of glucose metabolism in diabetic rats. *Journal of Herbs, Spices & Medicinal Plants* 10 (2002) : 75-84.
- [81] Nishiyama, T.; Mae, T.; Kishida, H.; Tsukagawa, M.; Mimaki, Y.; Kuroda, M.; Sashida, Y.; Takahashi, K.; Kawada, T.; Nakagawa, K. and Kitahara, M. Curcuminoids and sesquiterpenoids in turmeric (*Curcuma longa* L.) Suppress an increase in blood glucose level in type 2 diabetic KK-A^y mice. *J. Agric. Food Chem.* 53 (2005) : 959-963.
- [82] Du, Z.Y.; Liu, R.R.; Shao, W.Y.; Mao, X.P.; Ma, L.; Gu, L.Q.; Huang, Z.S. and Chan, A. α -Glucosidase inhibition of natural curcuminoids and curcumin analogs. *European Journal of Medicinal Chemistry* 41 (2006) : 213-218.
- [83] Hermel, A.P.; Mathur, R. *Davidson's Diabetes Mellitus : Diagnosis and treatment*. 5th ed. Saunders: Philadelphia, 2004.
- [84] Matthes, H.W.D.; Luu, B. and Ourisson, G. Cytotoxic components of *Zingiber Zerumbet*, *Curcuma Zedoaria* and *C. Domestica*. *Phytochemistry* 19 (1980): 2643-2650.
- [85] Ali, M.; Bagati, A. and Gupta, J. Synthesis and anti-inflammatory activity of some curcumin analogues. *Indian Journal of Chemistry sect. B. : Organic Chemistry, including medical chemistry* 54 (1995) : 884-888.

- [86] Grossman, R.B. *The Art of Writing Reasonable Organic Reaction Mechanism*. 2th ed. Springer-verlag: New York, 2003.
- [87] Roughley, P.J. and Whiting, D.A. Experiments in the biosynthesis of curcumin. *Journal of the Chemical Society, Perkin Transaction 1* (1973) : 2379-2388.
- [88] Mishra, S.; Karmodiya, K.; Surolia, N. and Surolia, A. Synthesis and exploration of novel curcumin analogues as anti-malarial agents. *Bioorganic & Medicinal Chemistry* 16 (2008) : 2894-2902.
- [89] Pullela, S.V.; Tiwari, A.K.; Vanka, U.S.; Vummenthula, A.; Tatipaka, H.B.; Dasari, K.R.; Khan, I.A.; Janaswamy, M.R. HPLC assisted chemobiological standardization of α -glucosidase-I enzyme inhibitory constituents from *Piper longum* Linn-An Indian medicinal plant. *J. Ethnopharmacol.* 108(2006) : 445–449.
- [90] Ogawa, S.; Asada, M.; Ooki, Y.; Mori, M.; Itoh, M.; Korenaga, T. Design and synthesis of glycosidase inhibitor 5-amino-1,2,3,4-cyclohexanetetrol derivatives from (-)-vibo-quercitol. *Bioorg. Med. Chem.* 13(2005) : 4306-4314.

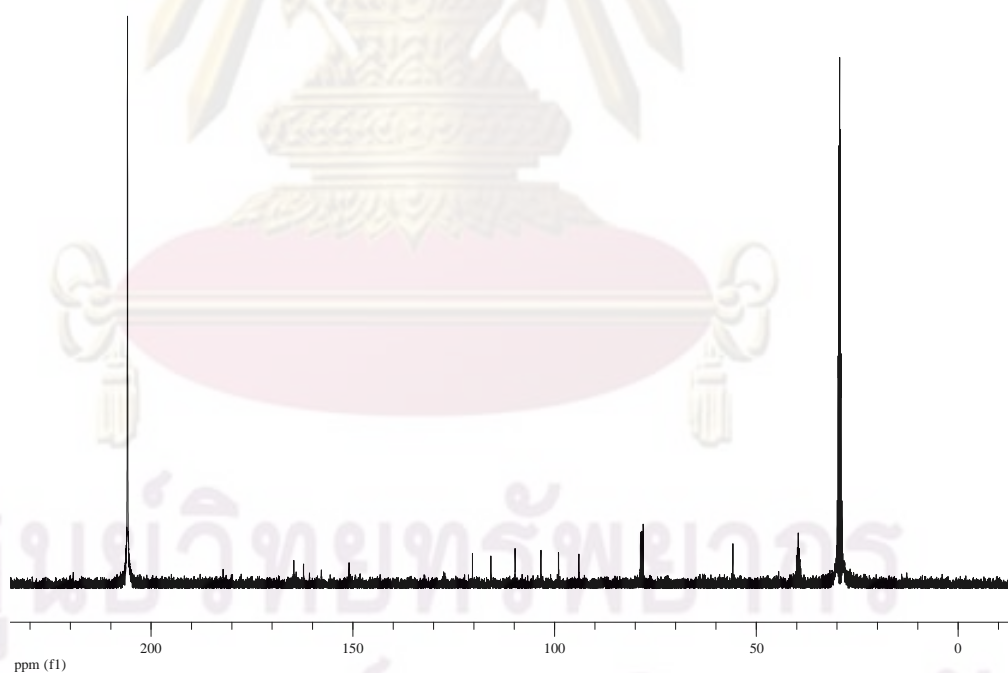
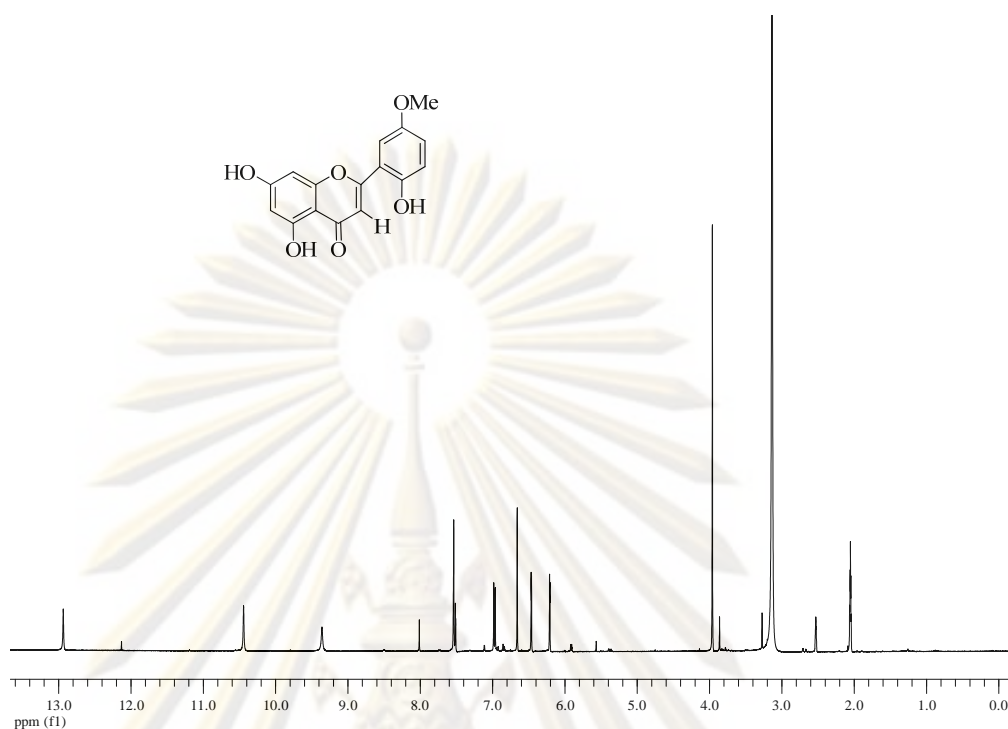


ศูนย์วิทยทรัพยากร
จุฬาลงกรณ์มหาวิทยาลัย



APPENDIX

ศูนย์วิทยทรัพยากร
จุฬาลงกรณ์มหาวิทยาลัย



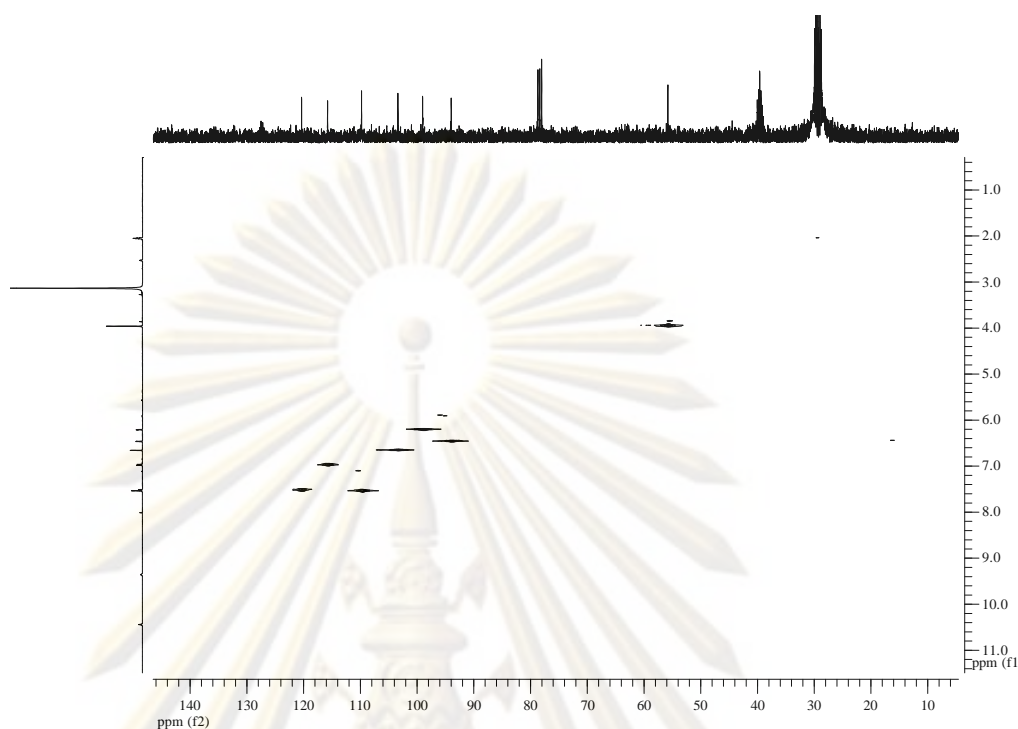


Figure A-1.3 HSQC spectrum (acetone- d_6) of **1.1**.

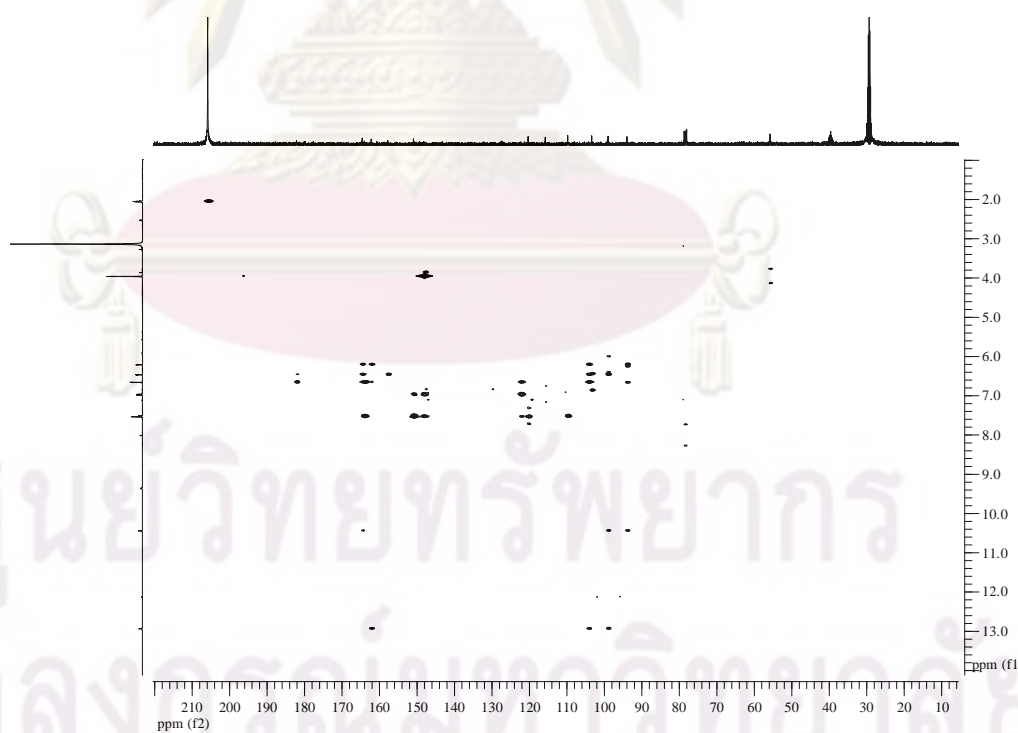


Figure A-1.4 HMBC spectrum (acetone- d_6) of **1.1**.

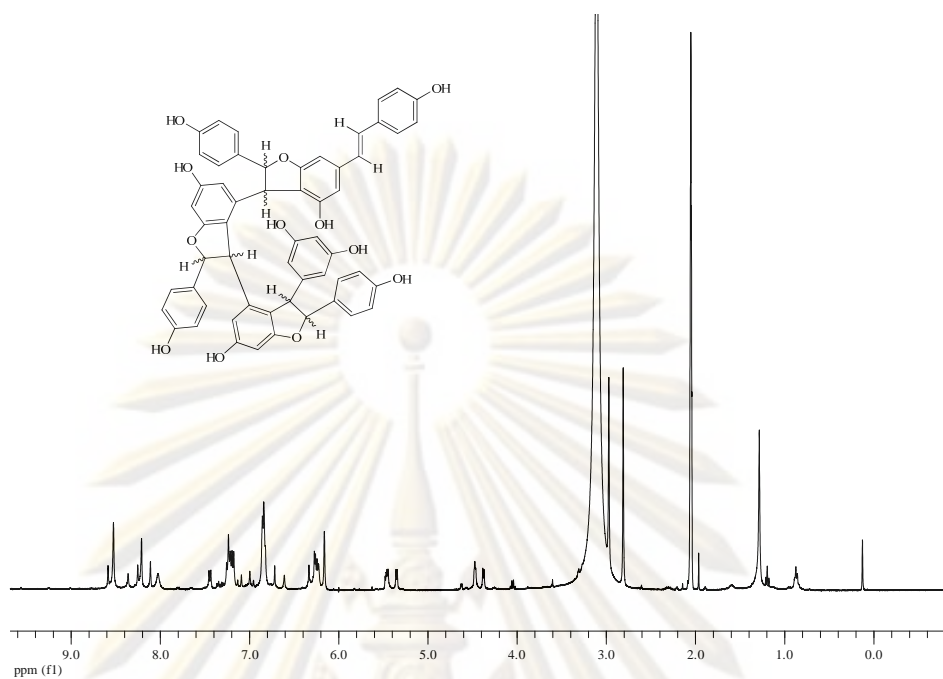


Figure A-1.5 ^1H NMR spectrum (acetone- d_6) of **1.10**.

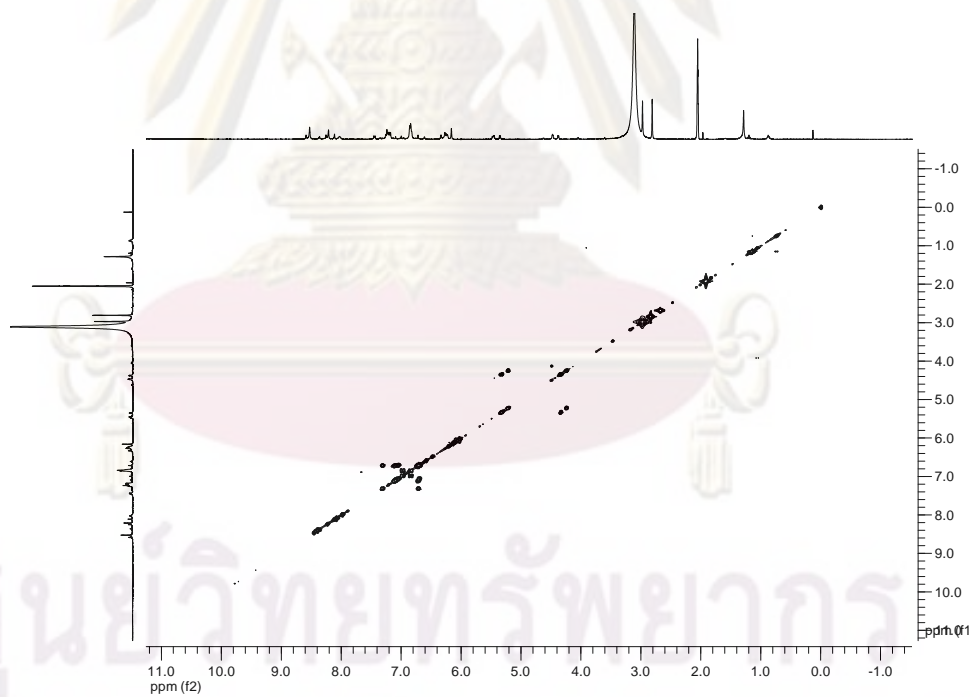


Figure A-1.6 COSY spectrum (acetone- d_6) of **1.10**.

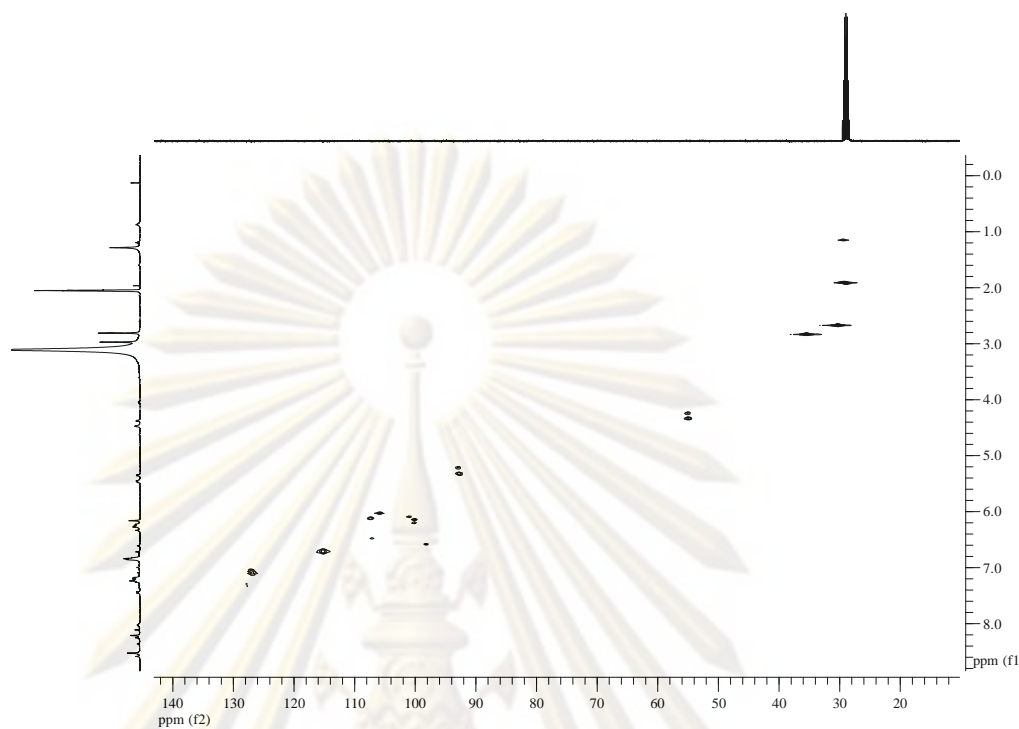


Figure A-1.7 HMQC spectrum (acetone- d_6) of **1.10**.



Figure A-1.8 HMBC spectrum (acetone- d_6) of **1.10**.

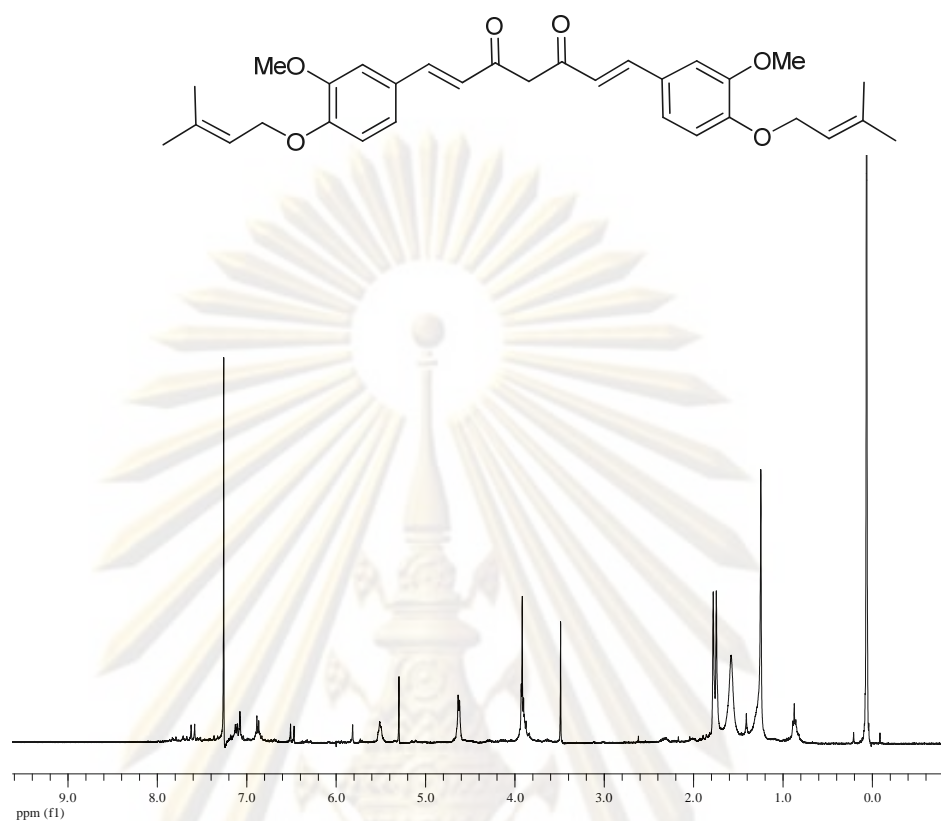


Figure A-1.9 ^1H NMR spectrum (CDCl_3) of 3.4.

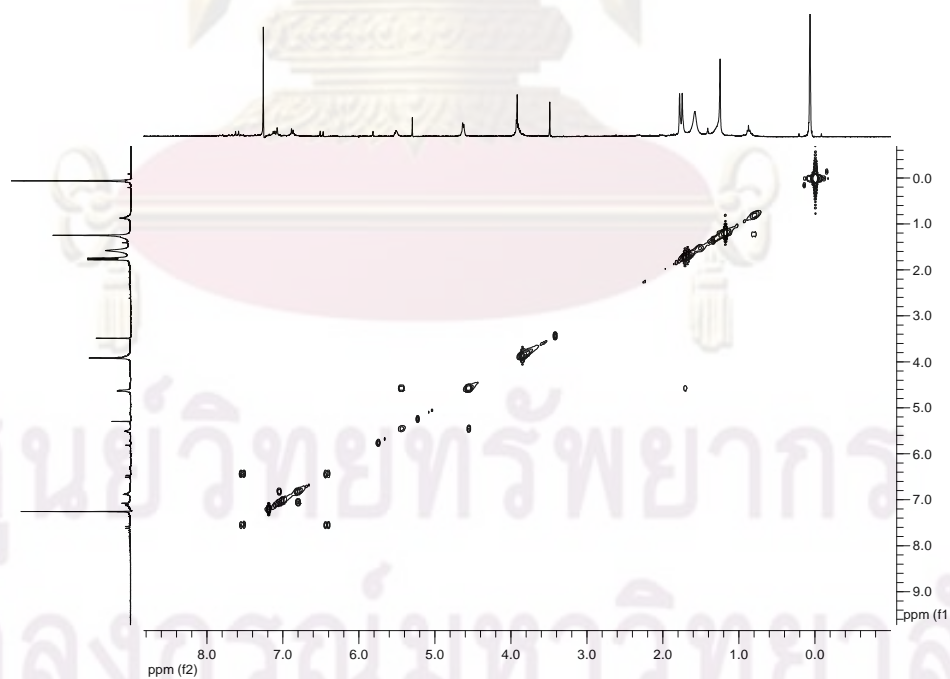


Figure A-1.10 COSY spectrum (CDCl_3) of 3.4.

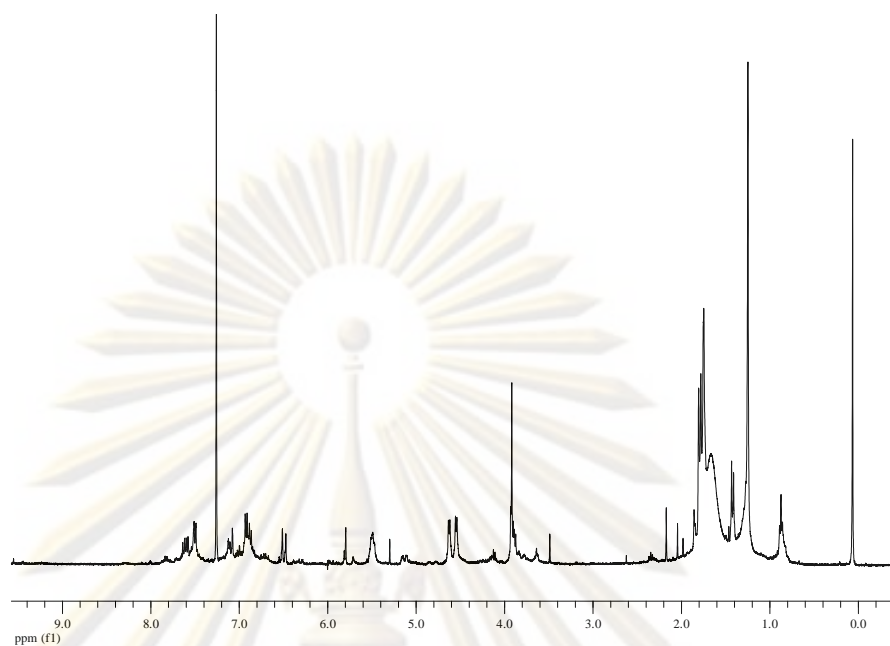


Figure A-1.13 ^1H NMR spectrum (CDCl_3) of **3.5**.

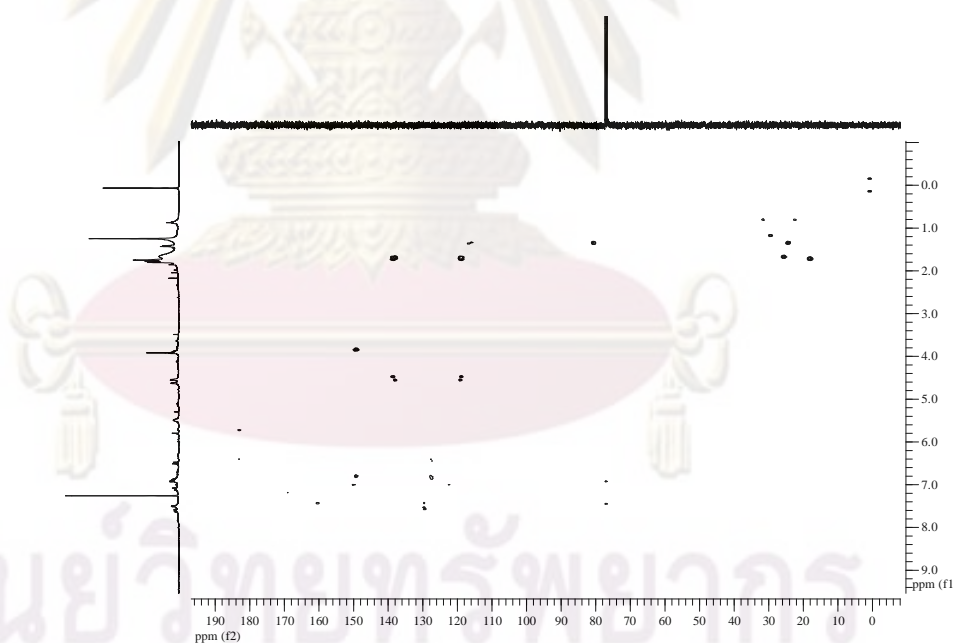
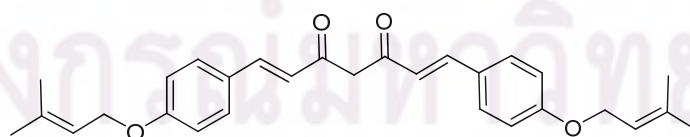


Figure A-1.14 HMBC spectrum (CDCl_3) of **3.5**.



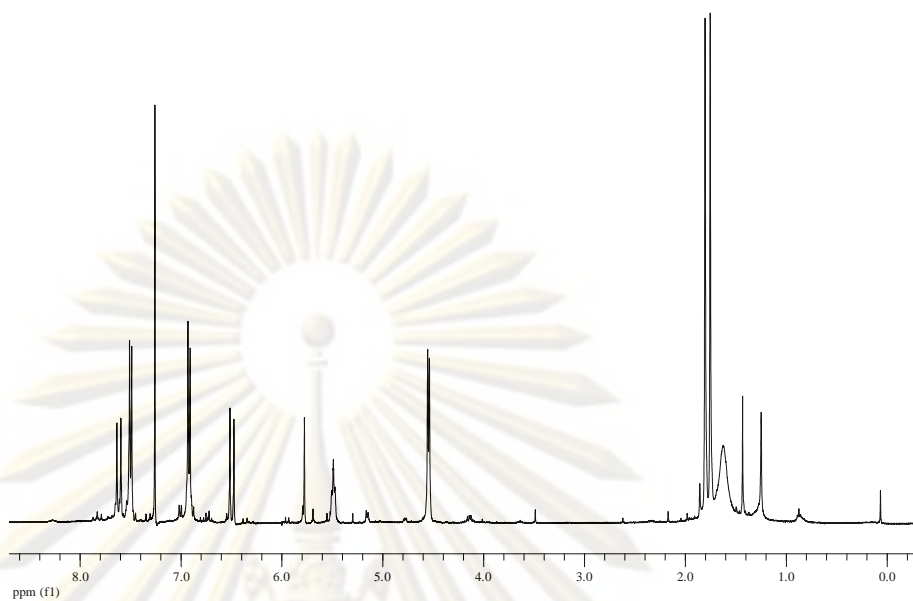


Figure A-1.15 ^1H NMR spectrum (CDCl_3) of **3.6**.

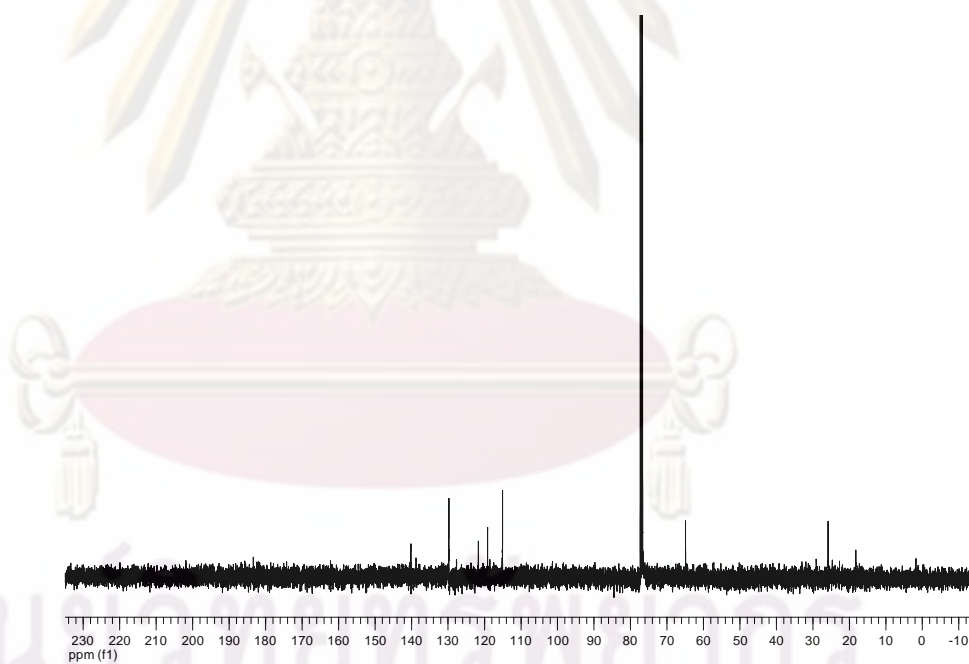


Figure A-1.16 ^{13}C NMR spectrum (CDCl_3) of **3.6**.

ศูนย์วิจัยทรัพยากรทดแทน
จุฬาลงกรณ์มหาวิทยาลัย

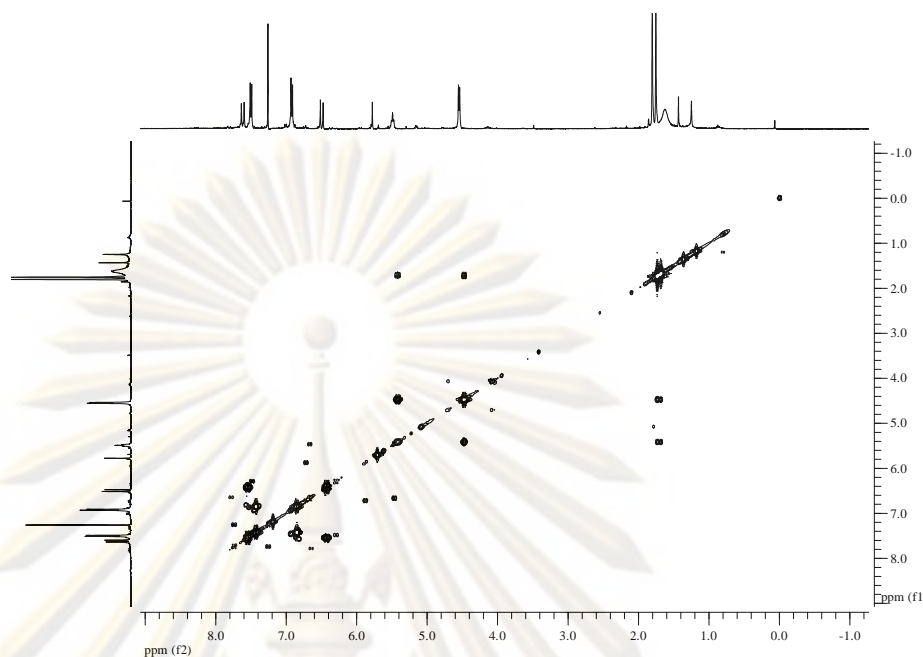


Figure A-1.17 COSY spectrum (CDCl_3) of **3.6**.

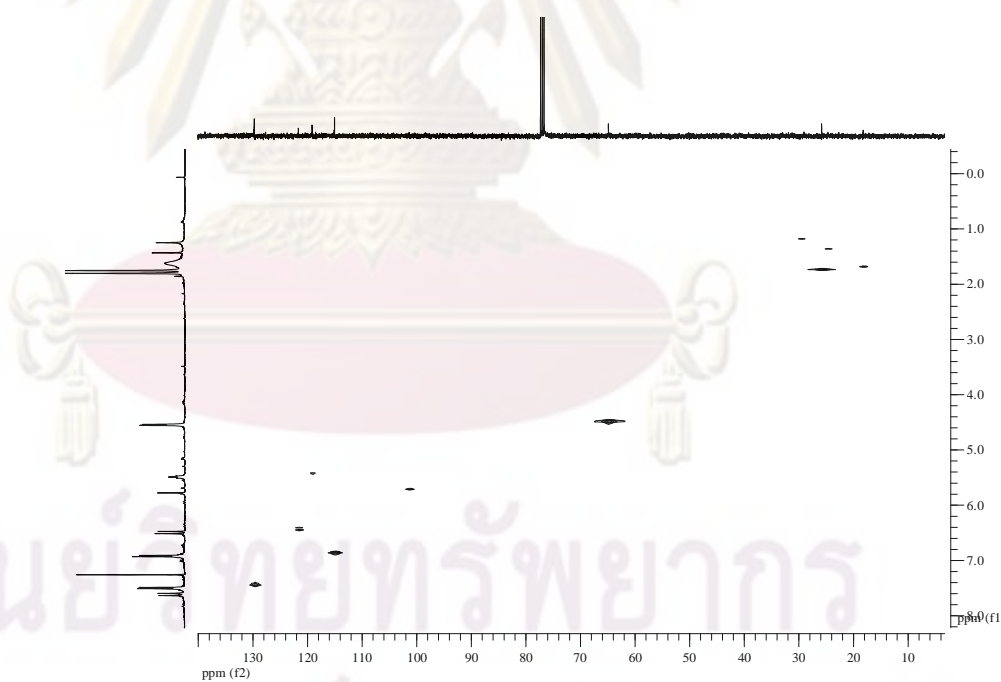


Figure A-1.18 HMBC spectrum (CDCl_3) of **3.6**.

ศูนย์วิจัยเภสัชวิทยา
จุฬาลงกรณ์มหาวิทยาลัย

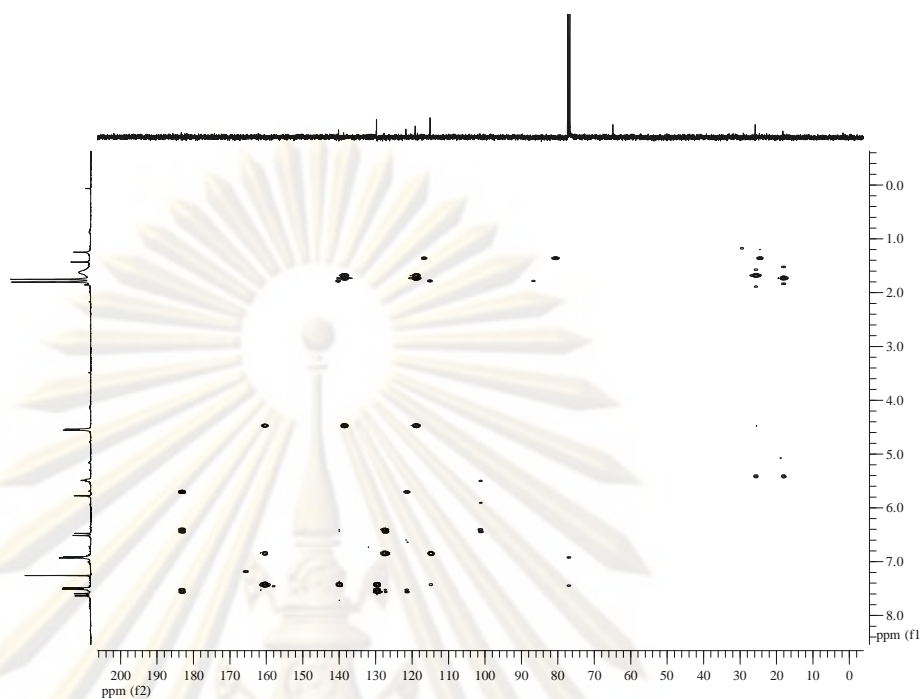


Figure A-1.19 HMBC spectrum (CDCl_3) of **3.6**.

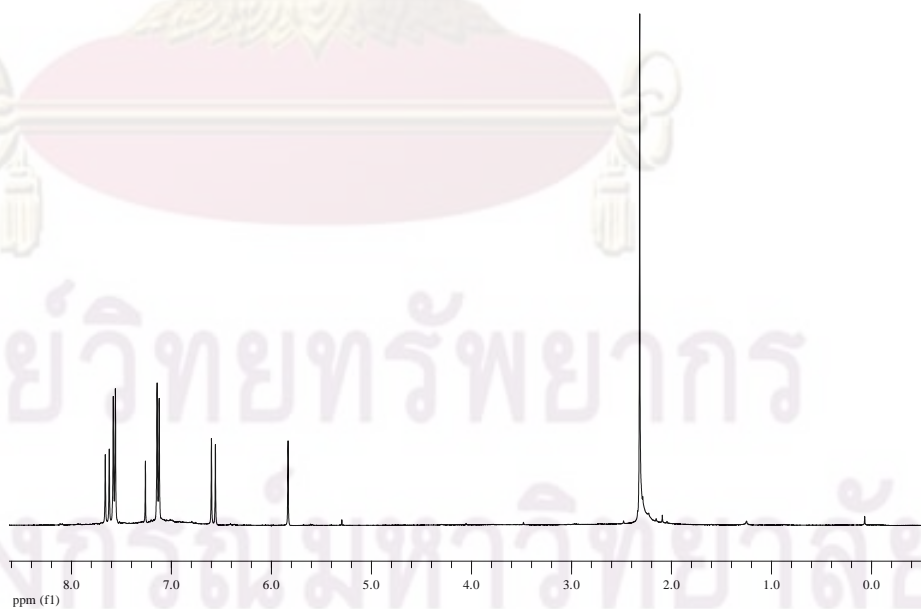
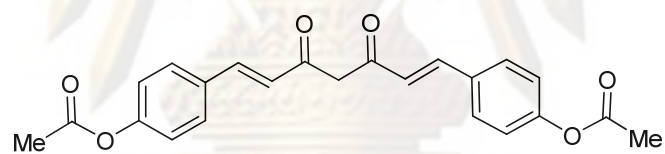


Figure A-1.20 ^1H NMR spectrum (CDCl_3) of **3.9**.

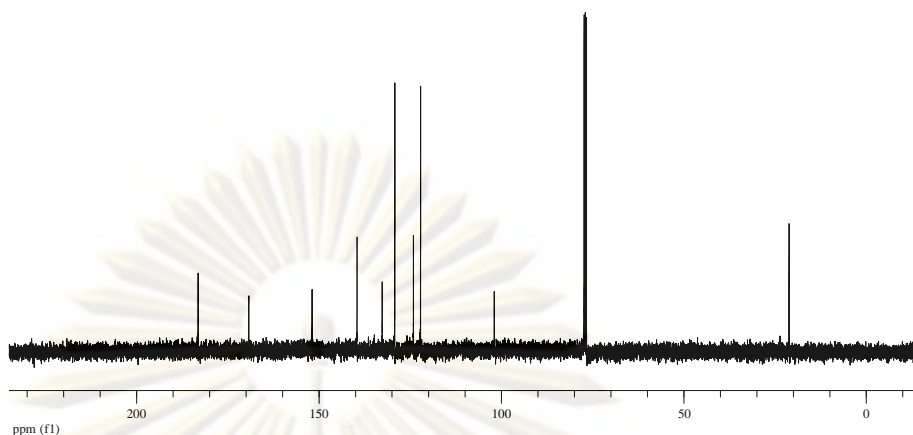


Figure A-1.21 ^{13}C NMR spectrum (CDCl_3) of **3.9**.

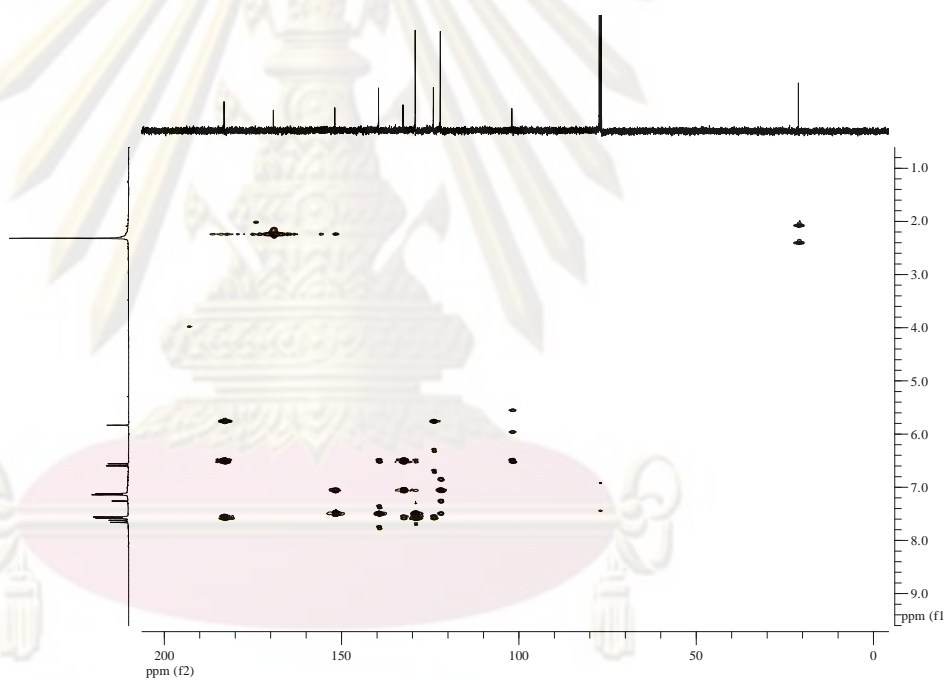
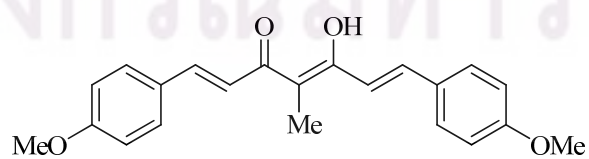


Figure A-1.22 HMBC spectrum (CDCl_3) of **3.9**.



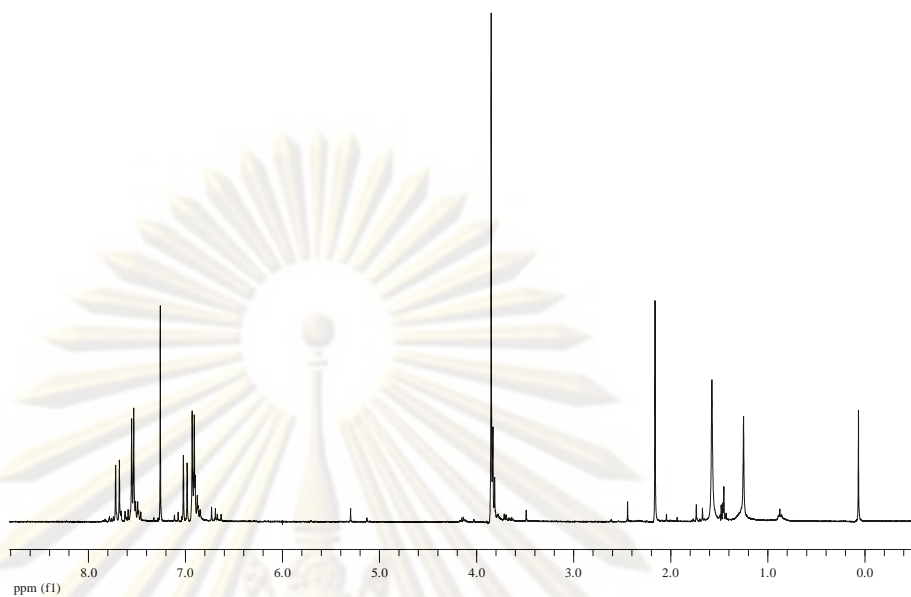


Figure A-1.23 ^1H NMR spectrum (CDCl_3) of **3.12**.

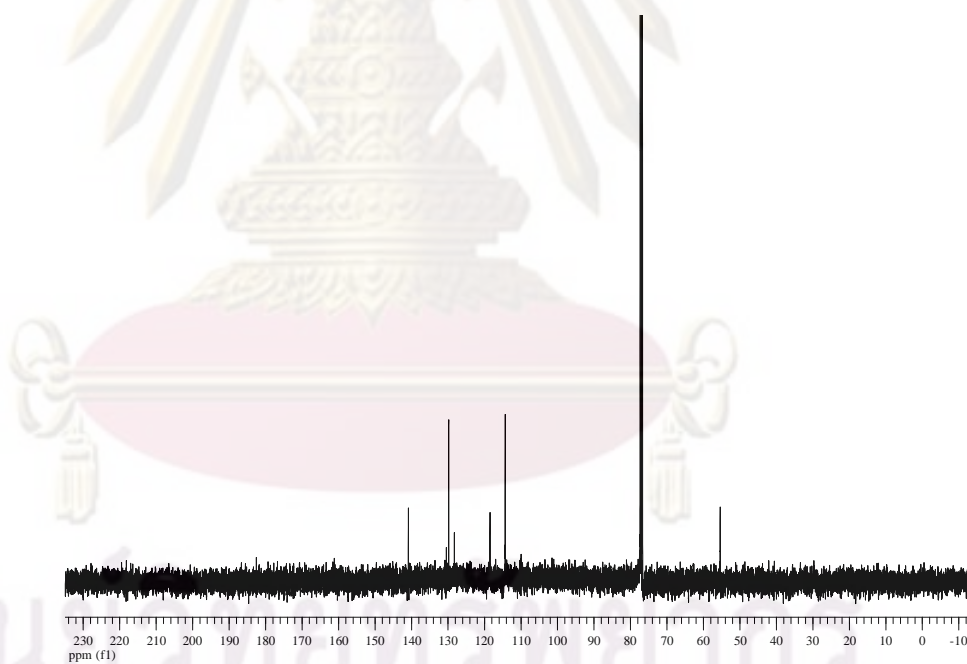


Figure A-1.24 ^{13}C NMR spectrum (CDCl_3) of **3.12**.

ศูนย์วิจัยทางเภสัชศาสตร์
จุฬาลงกรณ์มหาวิทยาลัย

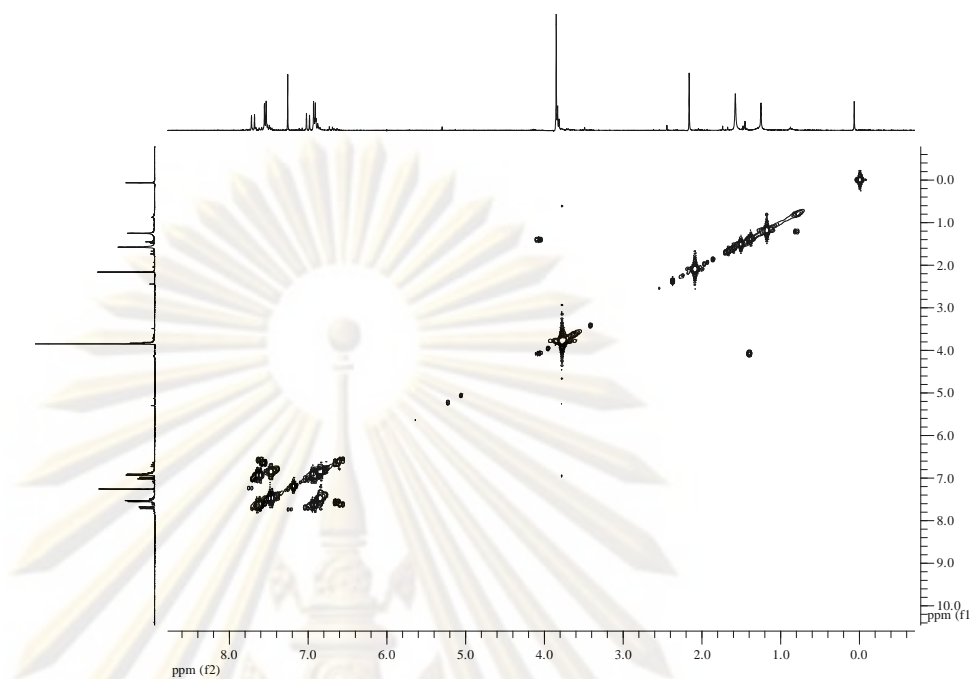


Figure A-1.25 COSY spectrum (CDCl_3) of **3.12**.

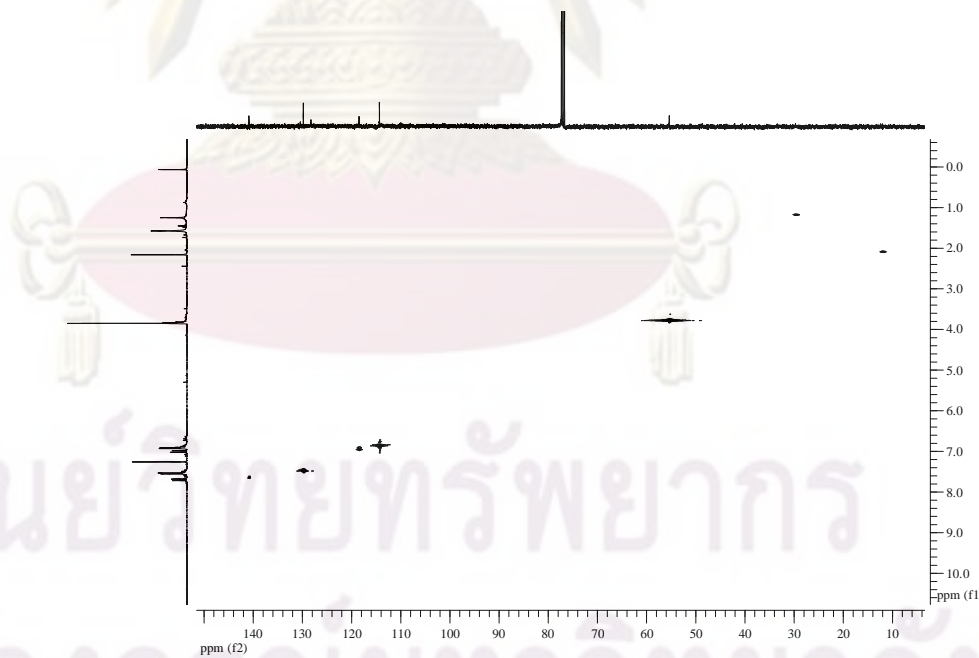


Figure A-1.26 HMQC spectrum (CDCl_3) of **3.12**.

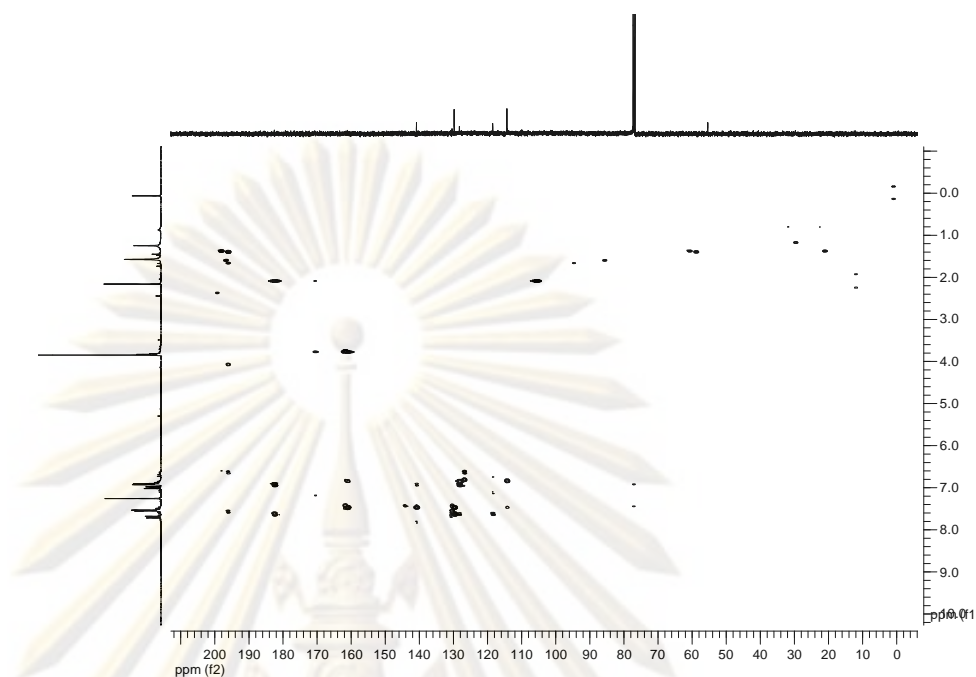


Figure A-1.27 HMBC spectrum (CDCl_3) of **3.12**.

ศูนย์วิทยทรัพยากร
จุฬาลงกรณ์มหาวิทยาลัย

VITA

Miss Suwannee Saisin was born on February 12, 1970 in Bangkok, Thailand. She graduated with Bachelor Degree of Science, majoring Chemistry from Faculty of Science, Ramkhamheang University, in 1990 and graduated with Master Degree of Science, majoring Organic Chemistry from Faculty of Science, Mahidol University, in 2000. During her studies towards the Doctoral's degree in Department of Chemistry, she received a financial support for her Doctoral program from Huachiew Chalermprakiet University and a research grant for her dissertation from Graduate School, Chulalongkorn University.

Her present address is 66/61 Moo 5, K.C. Romkao village Tambon Minburi, Amphoe Minburi, Bangkok, Thailand, 10510, Tel: 02-9150474.



ศูนย์วิทยทรัพยากร
จุฬาลงกรณ์มหาวิทยาลัย